ABSTRACT

HO, TRICIA CHRISTINE. Defining the Mannitol Dehydrogenase (MTD) Interactome during Unconventional Protein Secretion. (Under the direction of Dr. Michael B. Goshe and Dr. John D. Williamson).

Although Golgi-dependent secretion was long believed to be the sole protein secretory pathway in cells, unconventional, non-Golgi secretion has been more recently confirmed to occur in both animals and plants. Specific mechanisms for such unconventional secretion, however, were transformed to express celery mannitol dehydrogenase (MTD), a protein have yet to be completely elucidated. To characterize these mechanisms *Arabidopsis thaliana* cells known to be secreted by unconventional/leaderless means, to identify components of its secretory interactome/complex. Using *in vivo* formaldehyde crosslinking to preserve protein interactions triggered by the endogenous pathogen response signal salicylic acid (SA), the MTD-interacting complex was "captured" using co-immunoprecipitation, and quantitative liquid chromatography-tandem mass spectrometry (LC/MS/MS) to identify proteins potentially involved in MTD secretion. After implementing statistical analysis with appropriate controls, 30 candidate proteins of high confidence were identified that were not only crosslinked to MTD, but also displayed significant increases/decreases in response to SA. Many of these proteins (e.g. chaperones, AAA-ATPases and their regulators, as well as proteases and kinases) have been implicated in various trafficking pathways, including exocytosis and autophagy. The developed methodology and its application to MTD secretion provided insight into the early mechanisms of leaderless protein export and forms the basis for future biochemical studies.

Defining the Mannitol Dehydrogenase (MTD) Interactome during Unconventional Protein Secretion

by
Tricia Christine Ho

A thesis submitted to the Graduate Faculty of
North Carolina State University
in partial fulfillment of the
requirements for the Degree of
Master of Science

Biochemistry

Raleigh, North Carolina

2016

APPROVED BY:

Dr. Michael B. Goshe
Co-Chair of Advisory Committee

Dr. John D. Williamson
Co-Chair of Advisory Committee

Dr. James A. Knopp

Dr. Paul Wollenzien

BIOGRAPHY

Tricia Christine Ho was born in Columbia, Maryland. She attended the University of Virginia and obtained her Bachelor of Science in Biology in 2011. After working in an environmental laboratory for 2 years, she began her graduate studies in the Biochemistry Master of Science Program at North Carolina State University and will graduate in 2016. Currently, she is contemplating the new direction she will take in her life and career.

TABLE OF CONTENTS

LIST OF TABLES

LIST OF FIGURES

CHAPTER 1

Mapping a Protein's Journey: The Highways and Byways of Protein Trafficking

Protein trafficking is required for almost all cellular processes, making it a crucial part of cell function and survival. Cell maintenance, metabolism, secretion, defense, and response to stimuli are only a few of an extensive list of processes that involve protein trafficking. In animals for instance, neurotransmitters secreted into the synaptic cleft are recognized by receptors on the postsynaptic target that could be involved in the control of many pathways and systems (Hyman, 2005). If neurotransmitters are packaged and secreted inefficiently, or not at all, a number of processes would be affected. In both plants and animals, environmental signals can trigger events that require protein trafficking. For example, a plant senses it is under pathogen attack via receptors on the cell surface, targeting transport of specific transcription factors into the nucleus and triggering expression of required defense proteins. Once defense proteins are made, they must be directed toward the point of pathogen attack. Not only is accurate and timely protein trafficking required for cell survival, but often for survival of the organism as a whole.

Trafficking of proteins that are initially co-translated into the lumen of the endoplasmic reticulum (ER) can be divided into two major classes: Golgi-dependent trafficking (classical) and Golgi-independent trafficking (nonclassical), often referred to as conventional and unconventional protein secretion/trafficking, respectively. Other proteins, such as mitochondrial and chloroplast proteins, are initially translated in the cytosol and then transported directly into their respective organelles independent of the ER/Golgi apparatus. Classical, Golgi-mediated secretion largely restricts secretory responses to regulation by activation of gene expression. This is, or can be, relatively slow, because not only does it require gene activation and production of a new protein, it also requires trafficking through the entire Golgi pathway prior to secretion. To enter the Golgi stacks, proteins must first be recognized by the presence of a signal sequence and inserted into the ER lumen. After insertion into the ER, some proteins with signal sequences bypass the Golgi and utilize an unconventional/nonclassical secretion pathway. There are also proteins that undergo constitutive or stress/stimulus-regulated “leaderless” secretion (Nickel, 2011).

1.1 Conventional, Golgi-Dependent Secretion

1.1.1 Protein Insertion into the ER

Transport and localization of proteins begins as early as translation, where signal sequences often are responsible for targeting proteins to specific cellular compartments or the plasma membrane (PM). In prokaryotes, secretory and membrane proteins are targeted directly to the PM by a 20 to 30 amino acid, N-terminal signal sequence. Secreted proteins can be delivered to the PM by a post-translational or co-translational mechanism (Cross et al., 2009). In eukaryotes, an analogous signal sequence first targets nascent proteins to the ER for later sorting via the Golgi (Luirink and Sinning, 2004). Signal sequences in prokaryotes and eukaryotes have the same general structure consisting of three domains: an N (N-terminal) domain, an H (hydrophobic) domain, and a C (C-terminal) domain (Hegde and Bernstein, 2006). While the basic and slightly polar natures of the N and C domains, respectively, are present in all signal peptides, it is the hydrophobic H domain that appears to be essential for binding the signal recognition machinery (Gierasch, 1989; von Heijne, 1990). Of the 3 domains, the N domain is the most variable in length and composition, ranging from 1-5 residues. It does, however, typically have a net positive charge. The H domain, ranging from 7-15 residues, can contain Pro, Gly, Ser, or Thr residues, but is generally rich in Leu, Ala, Met, Val, Ile, Phe, and Trp residues. The C domain, ranging from 3-7 residues, has a higher polarity than those in the N domain and determines the cleavage site.

As soon as the signal sequence emerges from the exit tunnel of the ribosomal complex during translation (Halic and Beckmann, 2005; Hegde and Bernstein, 2006), the signal recognition particle (SRP) binds and triggers a pause in translation (Stroud and Walter, 1999). Both the SRP and the SRP receptor (SR) must then each bind their own GTP molecule before the SRP/ribosome-nascent chain (RNC) complex can bind to the SR on the target ER membrane (Luirink and Sinning, 2004; Halic and Beckmann, 2005). At this point the RNC is transferred to the translocon, an integral membrane protein-conducting channel, and the signal peptide enters the channel (Halic and Beckmann, 2005). GTP hydrolysis then drives SRP/SR dissociation and allows translation to proceed into the lumen of the ER (Luirink and Sinning, 2004; Halic and Beckmann, 2005).

1.1.2 Trafficking from the ER to the Final Destination via the Golgi/TGN

In eukaryotic cells, once newly synthesized proteins enter the lumen of the ER, resident lumenal proteins catalyze or mediate modification and folding. Upon leaving the ER, proteins then pass through the vesicular-tubular clusters (VTCs) or intermediate compartment (IC) (more recently termed the ER-Golgi intermediate compartment [ERGIC]) (Duden, 2003), followed by transport through a series of stacked, membrane-bounded Golgi compartments (*cis*-, *medial*-, and *trans*-), or cisternae, where further modification occurs. Each Golgi compartment also has its own set of resident protein processing enzymes. The *trans*-Golgi face gives rise to the *trans*-Golgi network (TGN), where mature proteins are packaged into vesicles for secretion or transport to other cellular compartments **(Figure 1.1)**. This is the longest route from the ER, with proteins passing through all of these compartments before reaching their final destination, the extracellular space or a specific organelle. There are a variety of coated and non-coated vesicles specific to each segment of anterograde (i.e. transport from the ER to the Golgi) and retrograde transport (i.e. transport from the Golgi to the ER). As described later, some protein trafficking can be Golgi-independent, and therefore, much more rapid.

Figure 1.1 Trafficking of Proteins from the TGN
There are a number of pathways a protein can take from the TGN as well as a variety of final destinations. A majority of the classical transport pathways transit the TGN. From the TGN, proteins can be targeted directly to the PM **(1)** or secreted via secretory granule formation **(2)**. Alternately, DVs formed at the TGN first deliver cargo to the MVB then to the PSV **(3)**, or CCVs formed at the TGN can also deliver cargo to MVBs/LEs/PVCs. Both pathways eventually lead to the lysosome. CCVs can also deliver cargo directly to the LV (Golgi-dependent) **(4)**. PACs can originate from either the TGN (Golgi-dependent) or directly from the ER (Golgi-independent) to transport cargo to the PSV **(5, 6)**. Proteins can be directly taken to the LV from the ER bodies (not shown) that originate from the ER (Golgi-independent) **(7)**. Some of these pathways **(3** and **4)** are connected to the endocytic pathway **(8)**, where proteins endocytosed at the PM form EEs before fusing with/into MVBs, also called LEs. Mitochondrial **(9)** and chloroplastic **(10)** proteins are translated in the cytosol and delivered directly to their respective organelles without passing through the ER-Golgi.

(Details for each pathway can be found in the text).
[a] found only in plant cells

CCV, clathrin-coated vesicle; DV, dense vesicle; EE, early endosome; ER, endoplasmic reticulum; ERES, ER export sites; ERGIC, ER-Golgi intermediate compartment; ISG, immature secretory granule; LE, late endosome; LV, lytic vacuole; MSG, mature secretory granule; MVB, multivesicular bodies; PAC, precursor-accumulating compartments; PSV, protein storage vacuole; PVC, prevacuolar compartment; SV, secretory vesicle; TGN, *trans*-Golgi network

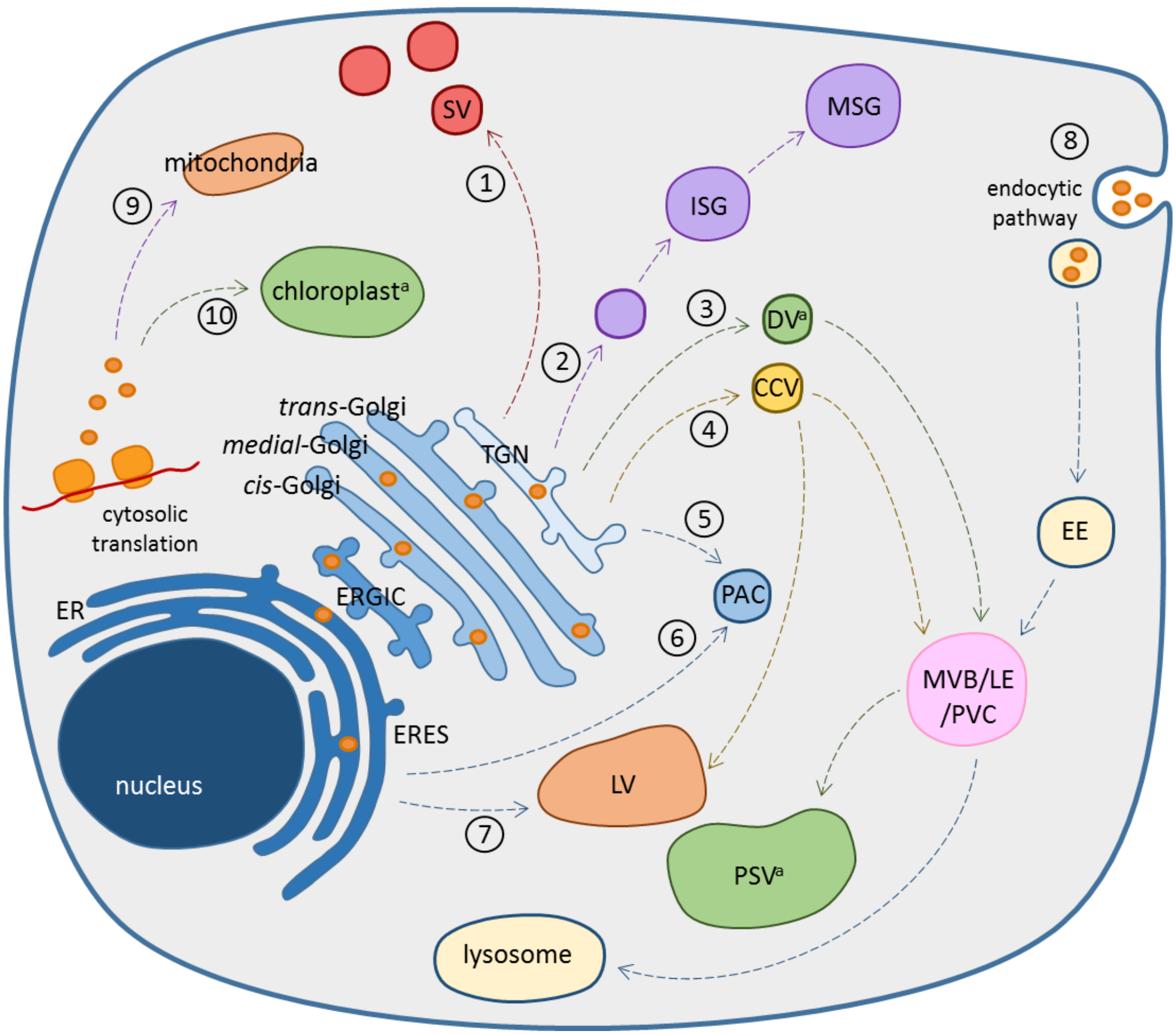
SV
MSG
ISG
mitochondria
chloroplast[a]
endocytic pathway
DV[a]
CCV
trans-Golgi
medial-Golgi
cis-Golgi
TGN
cytosolic translation
PAC
EE
ER
ERGIC
MVB/LE /PVC
ERES
nucleus
LV
PSV[a]
lysosome
1
2
3
4
5
6
7
8
9
10

1.1.2.1 ER to the Golgi

As translation continues, the signal sequence is fully extruded into the ER, where it is then removed by a membrane-bound signal sequence peptidase complex (SPC) (Braakman and Hebert, 2013). Once translation is complete, proteins are processed, folded, and then either retained in the ER (as discussed below) or packaged and directed to the Golgi. Proteins exit the ER at ER export sites (ERES), or the transitional ER (tER), membrane domains where vesicles containing proteins targeted for secretion begin to form (Watson and Stephens, 2005). COPII proteins (coat proteins), including Sar1p, Sec23/24p, and Sec13/31p, mediate vesicle formation for anterograde transport of proteins from the ER to the Golgi (Duden, 2003). Before reaching the Golgi, the COPII coat dissociates, resulting in naked vesicles that then fuse to form the VTCs/ERGIC (Duden, 2003; De Matteis and Luini, 2008). Proteins in the ERGIC can then either continue on to the Golgi or undergo retrograde transport (i.e. be transported back to the ER); both options are thought to involve formation of COPI-coated vesicles (Szul and Sztul, 2011). COPI proteins mediate the formation of vesicles in a manner similar to COPII vesicle formation, both of which are described below.

There are currently two models that describe cargo vesicle transport from the ER to the Golgi: the transport complex model and the stable compartment model (Brandizzi and Barlowe, 2013). In the transport complex model, ERGIC compartments track on microtubules from ERES to the Golgi. The stable compartment model proposes that ERES-Golgi transport is a two-step process: the first being a microtubule-independent, short-range transport from ER to ERGIC, followed by microtubule-dependent, long-range transport from ERGIC to the Golgi. In both models, dynein and kinesin motors are thought to be responsible for anterograde and retrograde transport, respectively, along microtubules. In mammalian cells, COPII-coated vesicles are known to be associated with microtubules that span the region between the ER and the *cis*-Golgi. COPII vesicles interact briefly with microtubules before the Sec13/31 complexes are depolymerized. The Sec23/Sec24 complexes, however, remain on the vesicle and interact with the

TRAPPI (transport protein particle I) tethering complex, located on the ERGIC, and resulting in a partially microtubule-independent transport. In plant cells, however, the ER and Golgi are in much closer proximity, and are thought to be stabilized in the correct orientation for vesicular exchange by a matrix of tubular connections or tethering factors. Thus, ER to Golgi transport does not rely on microtubule transport, and additionally, plants lack an identifiable ERGIC (Hwang and Robinson, 2009). In addition, the role of COPII-coated vesicles in this process in plants is itself under debate (Brandizzi and Barlowe, 2013). The precise mechanism whereby cargo vesicles reach the *cis*-Golgi from ERGIC is still unclear. From ERGIC, COPI-coated vesicles are responsible for anterograde transport to the *cis*-Golgi (Brandizzi and Barlowe, 2013). ER and Golgi resident proteins, such as those comprising the trafficking machinery itself, are recycled from the *trans*- to the *cis*-Golgi compartments via retrograde COPI-coated vesicles in both plant and mammalian cells (Nakano and Luini, 2010).

1.1.2.2 Maturation through the Golgi

Proteins destined for secretion or further transport move through the Golgi stack from the *cis*- to the *medial*- and then to the *trans*-Golgi face, before moving on into the TGN (De Matteis and Luini, 2008) **(Figure 1.2)**. Proteins entering the TGN are segregated from resident proteins and undergo modifications and processing as they mature through the various Golgi compartments. Four models have been proposed for Golgi trafficking in animal cells, differing primarily with regard to the mechanism by which cisternae transition from the *cis*- to the *trans*-Golgi (Moremen et al., 2012). The two classic models are the cisternal maturation model and the vesicular transport model. The cisternal maturation model proposes that cisternae undergo translocation as they mature, with processing enzymes being delivered to each compartment and with mature vesicles eventually budding off at the TGN. Transport vesicles enriched with processing enzymes have been identified, however, leading to the proposal of the modified cisternal maturation model, in which processing enzymes undergo retrograde transport to earlier Golgi cisternae. The vesicular transport model, in contrast, describes cisternae as stable or fixed, and that processing enzymes constantly undergo anterograde/retrograde transport. These models, however, appear to be inconsistent with more recent data suggesting that new proteins can quickly access all the different stages of the Golgi cisternae. This observation gave rise to the rapid partitioning model, which proposes that specific lipid composition regulates the polarity of the Golgi and the distribution of resident proteins, either involved in transport or localization of resident proteins, respectively. This model is supported by the observation that the membrane composition of the *cis*-Golgi more closely resembles the ER membrane, being enriched in glycerophospholipids (GPLs) (Patterson et al., 2008). The membrane of the *trans*-Golgi, however, is enriched in sphingolipids (SLs) and is thus more similar to the PM (Patterson et al., 2008). Cargo proteins and resident proteins are believed to have affinity for either SL or GPL domains, respectively, which then retain specific proteins using thermodynamic partitioning (Patterson et al., 2008).

1.1.2.3 Exit from the TGN

When a protein reaches the TGN, there are several exit routes it can take: 1) transport to the PM for secretion, 2) continued transport through recycling, early, or late endosomes, or 3) through “specialized” compartments (De Matteis and Luini, 2008) **(Figure 1.1)**. Proteins leaving the TGN for endosomes are found in clathrin-coated vesicles (CCVs). These are formed by Arf1 (ADP-ribosylation factor 1) and the adaptor protein (AP) complex recruitment of clathrin triskelions, composed of three heavy and three light chains (Campelo and Malhotra, 2012; Robinson and Pimpl, 2014). At the TGN, clathrin can be recruited by AP1 or AP3 complexes (Robinson and Pimpl, 2014). Although endosomes are derived from the PM, they can still fuse with vesicles from the TGN and all the cargo transported together to lysosomes or vacuoles for degradation (Huotari and Helenius, 2011). Secretory proteins leaving through “specialized” compartments, however, such as secretory granules containing hormones or neurotransmitters, are not transported in coated vesicles (Kienzle and von Blume, 2014). The low pH of the lumen promotes aggregation of secretory cargo molecules, separating them from the other soluble proteins (Robinson and Pimpl, 2014). These clusters interact with specific lipid domains in the TGN, causing budding and formation of immature secretory granules (ISGs) that develop into mature secretory granules (MSGs) (Robinson and Pimpl, 2014). Proteins destined for the apical/basolateral membranes also leave the TGN through lipid domain-mediated budding, although the sorting mechanisms for these proteins are currently unclear (Kienzle and von Blume, 2014). Lastly, vacuolar-targeted proteins also exit the TGN via CCVs, forming multivesicular bodies (MVBs) (Robinson and Pimpl, 2014), more details of which are discussed below.

1.1.3 Protein Modifications in the ER and Golgi

Protein processing and post-translational modifications (PTMs) that are essential for folding and protein maturation can occur as early as co-translation into the ER and continue through arrival at the TGN **(Figure 1.2)**. Glycosylation, for instance, can occur as soon a suitable glycosylation site (sequon), is far enough into lumen of the ER (Braakman and Bulleid, 2011) to be accessible to a membrane integral oligosaccharyltransferase (OST) that is proximal to the translocon. OSTs covalently transfer preassembled glycans to the asparagine (Asn) residue within the sequon via an amide linkage (Moremen et al., 2012). The consensus sequence for a standard N-glycosylation sequon is Asn-X-Ser/Thr, where X can be any amino acid except for proline, and is the most common glycosylation consensus in nascent polypeptides (Moremen et al., 2012). Simultaneously, protein disulfide isomerases (PDIs) and prolylpeptidyl *cis-trans* isomerases (PPIases) can catalyze the formation of disulfide bonds and proline-isomerization, respectively, in the elongating polypeptide (Braakman and Hebert, 2013). These processing events are crucial for the proper folding of the growing protein and later act as signals for additional modifications in the Golgi, especially O-glycosylation (Stanley, 2011; Braakman and Hebert, 2013). O-glycosylation, the most prevalent protein modification in the Golgi, involves the addition of sugar residues onto Ser or Thr via a glycosidic linkage that occurs once a protein reaches the *cis*-Golgi (Moremen et al., 2012). As summarized in Moremen et al. (2012), several different glycosyltransferases catalyze various O-glycosylation reactions, each targeting a specific consensus sequence containing Ser or Thr. The branched glycan modifications themselves can then be modified many times before the protein arrives at the TGN. Glycosyltransferases catalyze the transfer of sugars, glycosidases (glycoside hydrolases) remove sugars, and epimerases and sulfotransferases modify the sugars on the target protein (Stanley, 2011). These enzymes are found in *cis*-, *medial*-, *trans*-Golgi compartments, or in the TGN, and although they may be transported to neighboring compartments, they are eventually recycled back to their original Golgi compartment as resident proteins (Stanley, 2011).

1.1.4 Export and Retention Signals

Resident proteins in both the ER and Golgi that assist in processing newly synthesized proteins must be recycled back to their original compartments. This is mediated by retention signals, amino acids in the proteins that allow them to be identified and returned to the ER/Golgi **(Figure 1.2)**. Most ER-synthesized, transmembrane proteins contain ER export signals. The most common export sequences contain di-acidic (D/EXD/E), di-hydrophobic (FF, YY, LL, FY), and aromatic motifs, that allow direct binding of Sec24 through the membrane of the budding vesicle (Gillon et al., 2012). Soluble ER-synthesized proteins, however, lack the ability to bind Sec24, and require transmembrane cargo receptors that bind both Sec24 and the soluble protein itself (Gillon et al., 2012). Cargo receptors also require export and retention signals so they can undergo anterograde transport during packaging of the soluble proteins as well as retrograde transport to allow recycling (Gillon et al., 2012). Resident ER and Golgi proteins also must be recycled at the end of the transport process (Gao et al., 2014). To initiate this process, COPI recognizes resident membrane proteins via various retention signals. These include a C-terminal di-lysine motif, a hydrophobic motif, or an N-terminal arginine motif to target proteins to the ER, and C-terminal KXD/E to target proteins back to the Golgi (Gao et al., 2014). Resident ER lumenal proteins are identified via a different retention signal, K/HDEL (lysine/histidine-aspartic acid-glutamic acid-leucine), and undergo retrograde transport from the Golgi by binding the transmembrane K/HDEL receptor (Capitani and Sallese, 2009; Yamamoto et al., 2001; Cancino et al., 2013).

Figure 1.2 Trafficking from the ER to the TGN
Nascent polypeptides enter the ER lumen cotranslationally, and undergo initial modification, such as N-glycosylation by oligosaccharyltransferases (OSTs) and processing by PDIs and PPIases **(1)**. Anterograde transport from the endoplasmic reticulum (ER) to the ER-Golgi intermediate compartment (ERGIC) occurs via coat protein complex II (COPII)-coated vesicles **(2a)**. Recruitment of the COPII complex involves Sec12, Sar1, Sec13/31p, and Sec23/24p. Proteins bound for the ERGIC are have export signals: D/EXD/E, FF, YY, LL, FY, or aromatic motifs. Retrograde transport from ERGIC to the ER occurs via COPI-coated vesicles **(2b)**. Recruitment and disassembly of the COPI complex involves Arf1, a guanine nucleotide exchange factor (GEF), and a GTPase activating protein (GAP). Resident ER proteins are recognized by K/HDEL, diLys, hydrophobic, or N-terminal Arg motifs. Cargo proteins undergo anterograde transport in COPI-coated vesicles to the Golgi; retrograde transport also uses COPI-coated vesicles to return to the ERGIC and ER **(3)**. Proteins are modified and processed as they mature and transit the Golgi stack **(4)**. O-glycosylation is the most common modification; branched glycans can also be modified by glycotransferases (GTs), glycosidases (GHs), epimerases, and sulfotransferases (SULTs). Resident Golgi proteins, with KXD/E motifs, undergo retrograde transport to the *cis*-Golgi via COPI-coated vesicles. Proteins arriving at the TGN have several ways of being transported to their final destination **(5)**. Resident Golgi proteins are returned to the *cis*-Golgi via retrograde transport.

***** Two models describe transport from ERGIC to Golgi: the transport complex model and the stable compartment model.
****** Four models describe maturation through Golgi: the cisternal maturation model, the vehicular transport model, the modified cisternal maturation model, and the rapid partition model.
Details concerning each step can be found in text.

ER, endoplasmic reticulum; ERES, ER export sites; ERGIC, ER-Golgi intermediate compartment; GAP, GTPase activating protein; GEF, guanine nucleotide exchange factor; GH, glycosidase; GT, glycotransferase; OST, oligosaccharyltransferase; PDI, protein disulfide isomerase; PPIase, prolylpeptidyl *cis-trans* isomerases; SULT, sulfotransferases

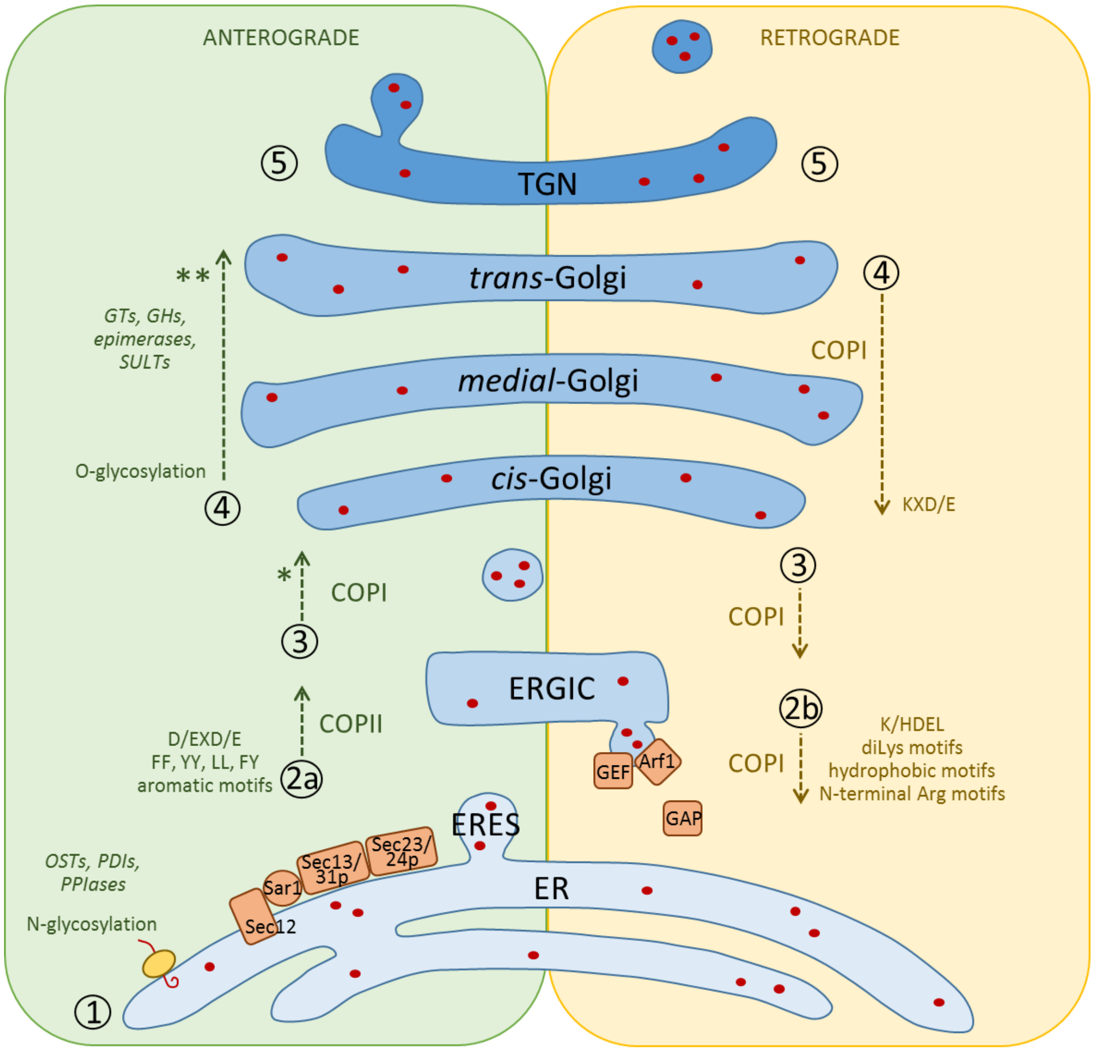

ANTEROGRADE
RETROGRADE
5
5
TGN
trans-Golgi
4
**
GTs, GHs, epimerases, SULTs
COPI
medial-Golgi
O-glycosylation
cis-Golgi
4
KXD/E
3
*
COPI
3
COPI
ERGIC
COPII
2b
K/HDEL
diLys motifs
hydrophobic motifs
N-terminal Arg motifs
D/EXD/E
FF, YY, LL, FY
aromatic motifs
2a
GEF
Arf1
COPI
GAP
ERES
Sec23/24p
Sec13/31p
Sar1
OSTs, PDIs, PPIases
ER
Sec12
N-glycosylation
1

1.2 Intracellular Vesicular Trafficking

1.2.1 Endosomal Trafficking Pathways

Endosomes in eukaryotic cells are involved in a number of cellular trafficking pathways, including protein transport to the lysosome/vacuole for degradation or in returning integral membrane proteins to the PM **(Figure 1.3)**. Vesicles forming at the PM and blebbing into the cytoplasm, classified as either clathrin-independent or clathrin-dependent endocytosis (Conner and Schmid, 2003; Doherty and McMahon, 2009), deliver cargo to the early endosome (EE) for sorting (Grant and Donaldson, 2009). From the EE, the cargo can take several routes: to lysosomes/vacuoles via late endosomes, directly to the TGN, or back to the PM via recycling endosomes (Grant and Donaldson, 2009). In the recycling pathway, EEs/recycling endosomes are responsible both for returning recycled membrane proteins to the PM and for returning cargo receptors to the TGN (Reyes et al., 2011). From the EE, proteins that must be returned to the PM are first routed to the juxtanuclear endocytic recycling compartment (ERC), from which recycling endosomes are then formed (Grant and Donaldson, 2009). Clathrin-dependent cargo can also be returned to the PM using a rapid recycling pathway from the EEs (Grant and Donaldson, 2009). Membrane proteins bound for lysosomal or vacuolar degradation are sorted in the late endosomes (LEs), also called MVBs or prevacuolar compartments, prior to transport into endosomal intraluminal vesicles (ILVs) (Reyes et al., 2011). LE's also transport newly synthesized lysosomal and vacuolar proteins to their respective organelles (Reyes et al., 2011). Certain proteins are known to associate with specific types of vesicles depending on its cargo and destination; for example, Rab5 is found on early endosomes and Rab11 is found on recycling endosomes (Grant and Donaldson, 2009).

Figure 1.3 Endosomal Trafficking Pathways

Vesicles formed at the PM, both clathrin-dependent and -independent, deliver cargo to the EEs for sorting. From the EE, they can be transported to the lysosome, vacuole, or TGN **(1)** via MVBs/LEs/PVCs or directly to the TGN **(2)**. Proteins returned to the PM can undergo rapid or slow recycling. Rapid recycling **(3)** involves direct transport of cargo proteins to the PM, while in slow recycling **(4)**, proteins are first targeted to the ERC, where they are returned to the PM in recycling endosomes. ILVs in the MVB can also be secreted into the extracellular space **(5)** after MVB fusion with the PM. To initiate the MVB pathway (grey box) **(6)**, ESCRT-0 (green) binds ubiquitinated proteins and PtdIns3P on endosomal membranes, resulting in recruitment of ESCRT-1 (purple). ESCRT-1, which interacts with both ESCRT-0 and proteins modified with ubiquitin (brown circle), recruits ESCRT-II (yellow). ESCRT-II interacts with ESCRT-I, ubiquitinated proteins, and PtdIns3P (blue circle) on the endosomal membrane. Vps25, a subunit of ESCRT-II, is the nucleation point where Vps20, a subunit of ESCRT-III (orange), initiates assembly of the filamentous ESCRT-III complex by triggering oligomerization of Snf7 (orange triangle), another ESCRT-III subunit. Oligomerization terminates when Vps24 (ESCRT-III) (orange square) binds to the last Snf7, completing vesicle formation. ESCRT-III recruits deubiquitinases that deubiquitinate the cargo proteins. Vps2 (ESCRT-III) and accessory proteins recruit the Vps4 complex (cream), which disassembles ESCRT-III via ATP hydrolysis, terminating cargo sorting and vesicle formation.

ATP, adenosine triphosphate; EE, early endosome; ERC, endocytic recycling compartment; ESCRT, endosomal sorting complexes required for transport; ILV, intraluminal vesicles; LE, late endosomes; MVB, multivesicular body; PM, plasma membrane; PtdIns3P, phosphatidylinositol 3 phosphate; TGN, *trans*-Golgi network; Vps, vacuolar protein sorting

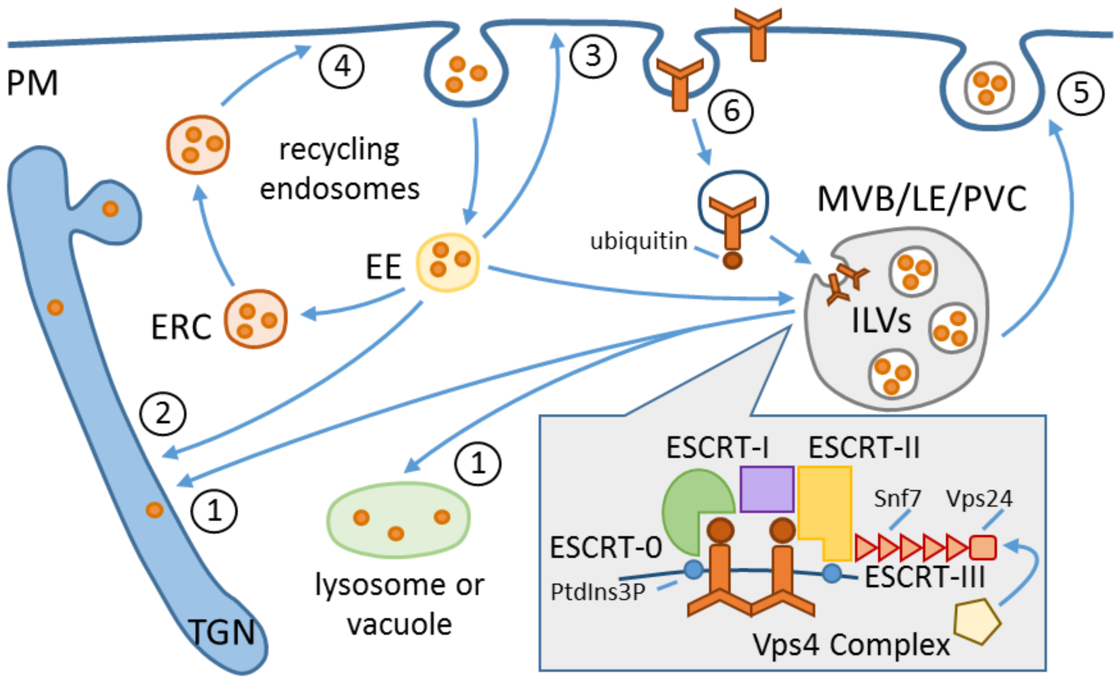
PM
4
3
6
5
recycling
endosomes
MVB/LE/PVC
ubiquitin
EE
ERC
ILVs
2
1
1
ESCRT-I
ESCRT-II
Snf7
Vps24
ESCRT-0
PtdIns3P
ESCRT-III
lysosome or
vacuole
TGN
Vps4 Complex

1.2.2 Vesicle Formation

Proteins are transported within the cell in various types of vesicles. COPI and COPII proteins are key players in vesicular protein transport, interacting with and sorting specific cargo proteins. Vesicle formation can also occur via the MVB pathway, mediated by ESCRT (endosomal sorting complexes required for transport) complexes, or via autophagosome formation during autophagy.

1.2.2.1 COPI, COPII

As previously mentioned, the COPII proteins, Sar1p, Sec23/24p, and Sec13/31p, are responsible for membrane deformation and vesicle budding at the ER. Sec12, an integral ER membrane protein, acts as a guanine nucleotide exchange factor (GEF) for Sar1, a small GTPase (Lee et al., 2004). Sar1-GTP binds to the ER membrane and recruits Sec23/24p, a heterodimeric protein complex that interacts with cargo protein sorting signals (Lee et al., 2004). The Sar1-Sec23/24p complex then recruits Sec13/31p, another heterodimer, which leads to polymerization of COPII complexes. The subsequent deformation and budding of the membrane that is then triggered leads to formation of the COPII vesicle (Lee et al., 2004). Disassociation of COPII proteins from the vesicle is triggered by hydrolysis of Sar1p-GTP, catalyzed by Sec23p, a GTPase activating protein (GAP) (Duden, 2003). COPI-coated vesicles are involved in retrograde transport and form much like COPII vesicles. To form COPI vesicles, ADP ribosylation factor (ARF) GEF, a membrane-associated protein, binds to and mediates GTP exchange on Arf1, resulting in the recruitment of preassembled cytosolic coatomer complexes consisting of seven subunits (Lee et al., 2004). This polymerization of coatomers causes membrane deformation, followed by vesicle budding and disassembly of COPI proteins with an ARF GAP-assisted hydrolysis of Arf1-GTP (Lee et al., 2004).

1.2.2.2 MVB and the ESCRT Pathway

Although the ESCRT complexes are involved in a number of cellular processes (e.g. cytokinesis and HIV [human immunodeficiency virus] budding), this section will focus mainly on their role in the MVB pathway as described by Schmidt and Teis (2012) **(Figure 1.3)**. ESCRT protein complexes assemble at the cytosolic membrane, rather than at the lumenal membrane, of the MVB and are crucial to the formation and budding of vesicles from the MVB membrane into the MVB lumen. There are five ESCRT complexes, listed in the order in which they assemble: ESCRT-0 ESCRT-I, ESCRT-II, ESCRT-III, and the Vps4 complex (vacuolar protein sorting). Protists and plants lack ESCRT-0, which is found only in fungi and animals. ESCRT-III and the Vps4 complex are highly conserved and found in all eukaryotic organisms as well as a few prokaryotes. While both cytokinesis and HIV budding require only three ESCRT complexes, the MVB pathway utilizes all five. This pathway is the best described in yeast, but is also present in higher organisms.

The ESCRT-0 complex, a Vps27/Hse1 (vacuolar protein sorting HSE1) heterodimer (also called HRS/STAM1/2 [hepatocyte growth factor-regulated tyrosine kinase substrate/signal transducing adaptor molecule1/2] in humans) (Henne et al., 2011), binds phosphatidylinositol 3 phosphate (PtdIns3P) and ubiquitinated proteins on endosomal membranes to initiate the MVB pathway. Once bound to the endosome and cargo, ESCRT-0 recruits ESCRT-I. Although the MVB pathway exists in protists and plants, they are assumed to use a different complex to recruit ESCRT-I (Schmidt and Teis, 2012). ESCRT-I, a heterotetramer of Vps23/Vps28/Vps37 (Tsg101/hVps28/Vps37[A-C] in humans) and Mvb12 (hMvb12[A,B] in humans) (Henne et al., 2011) or UBAP1 (ubiquitin-associated protein), interacts with both ESCRT-0 and ubiquitinated proteins (Schmidt and Teis, 2012). ESCRT-I recruits ESCRT-II, another heterotetramer composed of Vps36/Vps22 and two Vps25 subunits (Eap45/Eap30 and Eap20, respectively, in humans) (Henne et al., 2011), which interacts with ESCRT-I, ubiquitinated proteins, and the endosomal membrane via PtdIns3P (Schmidt and Teis, 2012). ESCRT-III is composed of four core subunits, Vps20/Snf7/Vps24/Vps2 (CHMP6/CHMP4[A-

C]/CHMP3/CHMP2[A,B] in humans) (Henne et al., 2011), and accessory components. Vps25 (ESCRT-II) is the nucleation point where Vps20 (ESCRT-III) initiates assembly of the filamentous ESCRT-III complex by triggering oligomerization of Snf7. The binding of Vps24 to the last Snf7 protomer terminates oligomerization, and results in recruitment and binding of Vps2. ESCRT-III recruits deubiquitinases, resulting in deubiquitination of cargo and recycling of ubiquitin prior to MVB vesicle formation. Vps2, along with ESCRT-III accessory proteins, recruits the Vps4 complex, composed of Vps4 (an AAA [ATPase associated with various cellular activities]-ATPase) and Vta1 (Henne et al., 2011; Schmidt and Teis, 2012). The Vps4 forms a homododecamer, two hexameric rings stacked together with a central pore, and is activated by Vta1 binding (Schmidt and Teis, 2012). After Vps4 disassembles ESCRT-III via ATP hydrolysis, the Vps4 complex dissociates and becomes inactive once again.

There are two models that describe ESCRT-III-mediated vesicle maturation: the Snf7 oligomerization model and the dome model (Henne et al., 2011) (not shown). The Snf7 oligomerization model proposes that the tension of ESCRT-III rings cause the membrane to deform, resulting in an inverted, elongated tube. Membrane deformation allows the Snf7 rings to readjust to a preferred diameter, followed by capping of Vps24/Vps2 (Lenz et al., 2009). The dome model proposes that ESCRT-III rings define an area of the membrane, which is then capped by a Vps24/Vps2 protein hemisphere consisting of multiple subunits protruding into the neck of the budding vesicle (Fabrikant et al., 2009).

1.2.3 Vesicle Fusion

After coat proteins (COPI, COPII, and clathrins) are removed from transiting vesicles, the resulting naked vesicles approach their acceptor/destination compartments and tethering occurs. Tethering is mediated by Rab GTPases, tethering proteins, and SNAREs (soluble NSF [N-ethyl-maeleimide sensitive fusion attachment] protein receptor) in a highly conserved mechanism that is reviewed in detail by Chen and Scheller (2001). Vesicle/donor SNAREs (v-SNAREs) and target/acceptor SNAREs (t-SNAREs) interact to initiate membrane fusion, followed by release of the vesicle cargo into the target compartment (Brandizzi and Barlowe, 2013).

The exocyst, a highly conserved complex of eight subunits: Sec3, Sec5, Sec6, Sec8, Sec10, Sec15, Exo70, and Exo84, mediates vesicle tethering to the PM, assisting in a number of cellular processes (TerBush et al., 1996; Hsu et al., 1996; Guo et al., 1999; Heider and Munson, 2012). The exocyst is a member of the CATCHR (Complex Associated with Tethering Containing Helical Rods) family; with all eight subunits having conserved helical bundles that form similar rod-like structures (Heider and Munson, 2012).

1.2.4 Autophagy

Long-lived proteins that require periodic replacement, damaged organelles, and invasive pathogens all undergo a cellular recycling process collectively called autophagy, involving the formation of additional subcellular membranes (as opposed to vesicle budding from existing membranes) and cargo sequestration (Levine and Klionsky, 2004; He and Klionsky, 2009). There are 32 autophagy-related (ATG) proteins identified to date in yeast that function at various steps in autophagy (He and Klionsky, 2009). ATG proteins are involved in initiation of the formation of the phagophore, the site where damaged components are sequestered and which later develops into the autophagosome (He and Klionsky, 2009). Once formed, the double-membrane delimited autophagosomes deliver cargo to the lysosome in eukaryotic cells or to the vacuole in yeast and plant cells (He and Klionsky, 2009). He and Klionsky (2009) describe autophagy as being divided into distinct steps: induction, cargo recognition/selection, vesicle formation, autophagosome/vacuole fusion, and cargo degradation.

1.2.4.1 Induction of Autophagosome Formation

The Ser/Thr kinase TOR (target of rapamycin), negatively regulates Atg1, another Ser/Thr kinase, under nutrient-rich conditions. During starvation or in the presence of rapamycin, however, Atg1 is derepressed and forms a scaffold with Atg13 and Atg17, causing recruitment of additional Atg proteins and initiation of autophagosome formation. In mammalian cells, Unc-51-like kinase 1 (ULK1) and Unc-51-like kinase 2 (ULK2), homologs of Atg1, and FIP200 (focal adhesion kinase family-interacting protein of 200 kDa, the homolog of yeast Atg17) form a complex during starvation that localizes to the phagophore (Hara et al., 2008; Jung et al., 2009).

1.2.4.2 Cargo Recognition/Selection

Autophagy has been shown to be a substrate specific process in yeast, mammalian, and plant cells, although bulk cytosol can undergo random autophagy (He and Klionsky, 2009; Liu and Bassham, 2012). Receptor proteins, such as the Atg proteins, recognize and interact with cargo proteins to recruit additional factors and initiate formation of the phagophore. In yeast, prApe1 (precursor form of aminopeptidase I) is delivered to the vacuole via the Cvt (cytoplasm-to-vacuole targeting) pathway where mature Ape1 is generated. Atg19 recognizes and interacts with a vacuolar targeting signal on prApe1, which recruits Atg8, a key protein of the autophagosome-forming machinery (Scott et al., 2001; Shintani et al., 2002). In mammals, p62/sequestosome 1 (SQSTM1) (Bjørkøy et al., 2005; Pohl and Jentsch, 2009) or Ref(2)P (“Refractory to sigma P”) (the Drosophila p62 homolog) (Nezis et al., 2008) binds to ubiquitin and LC3 (microtubule-associated protein 1 light chain 3), a homolog of Atg8 (Pankiv et al., 2007; Kim et al., 2008), to link ubiquitinated cargo and the autophagy machinery.

1.2.4.3 Autophagosome Formation

As indicated above, autophagosomes are assembled at the phagophore assembly site (PAS) by addition of new membranes, as opposed to vesicle budding from existing membranes. In yeast, assembly of the new phagophore membrane requires the class III phosphatidylinositol 3 kinase (PtdIns3K) complex, which consists of PtdIns3K Vps34 (vacuolar protein sorting 34), myristoylated Ser/Thr kinase Vps15, Atg14, and Atg6/Vps30 (Liang et al., 1999; Kihara et al., 2001; Itakura et al., 2008; Sun et al., 2008). In mammalian cells, Bcl-2 (B-cell lymphoma/leukemia-2) regulates Beclin 1, the homolog of yeast Atg6/Vps30, by binding and sequestering it during nutrient-rich conditions, but dissociating from it during starvation to trigger autophagosome formation (Kang et al., 2011). Atg proteins bind to PtdIns3P (phosphatidylinositol 3 phosphate), which is produced by the PtdIns3K complex (Nice et al., 2002; Stromhaug et al., 2004; Obara et al., 2008). Two ubiquitin-like (Ubl) conjugation systems (Atg12-Atg5-Atg16 and Atg8-phosphatidylethanolamine [PE]) are then recruited to the phagophore by the PtdIns3K complex and Atg proteins, including Atg9, an integral membrane protein needed for final autophagosome formation (Suzuki et al., 2001; Suzuki et al., 2007).

1.2.4.4 Fusion and Degradation

Once the autophagosome is formed, Atg proteins dissociate, Atg4 cleaves Atg8 from phosphatidylethanolamine (PE), releasing the autophagosome into the cytosol (Kirisako et al., 2000). The uncoating mechanism for the remaining Atg proteins is unknown. Release of the autophagosome into the cytosol allows it to fuse with the lysosome, and initiates cargo degradation. The machinery involved in homotypic vacuole membrane fusion (fusion between membranes with the same composition) also mediates autophagosome-lysosome fusion in both mammalian and yeast cells (Jäger et al., 2004; Tanaka et al., 2000; Klionsky, 2005). Once fusion is complete, lysosomal/vacuolar hydrolases degrade the cargo (Tanida, 2011) and the resulting molecules are recycled to the cytosol.

1.3 Intracellular Protein Targeting/Transport

1.3.1 Targeting/Transport to Proteasomes

Lemus and Goder (2014) describe the ER-associated protein degradation (ERAD) pathway, which is conserved in all eukaryotes. This pathway targets misfolded proteins within the ER lumen to the cytosol, a process known as relocation. In yeast, there are three ERAD pathways that recognize misfolded proteins. The protein domain that is misfolded dictates which ERAD pathway is used to transport the protein to the cytosol, with the ERAD-L, ERAD-M, and ERAD-C pathways recognizing proteins with misfolding in their ER lumenal, transmembrane, or cytoplasmic domains, respectively. These three pathways have also been identified in mammalian cells, although the preference for specific substrates does not appear to be as strong as in yeast. ERAD substrates (misfolded regions) are targeted to ER membrane-embedded E3 ligases that assist in ubiquitination of the substrate as it emerges into the cytosol. The precise mechanisms for substrate recognition and retrotranslocation have not yet been identified; however, polyubiquitination in the cytosol is known to target the misfolded protein to the 26S proteasome for degradation in eukaryotic cells.

1.3.2 Targeting/Transport to Mitochondria and Chloroplasts

Although mitochondria and chloroplasts themselves contain small, prokaryotic-like genomes called, mtDNA/mDNA or ctDNA/cpDNA, respectively, the majority of mitochondrial and chloroplastic proteins are encoded by the nuclear genome. Translation of nuclear-encoded mitochondrial and chloroplastic proteins occurs in the cytosol as described by Neupert and Herrmann (2007) and Soll and Schleiff (2004), respectively. Most of these proteins remain unfolded, supported by chaperones in a conformation that is later, post-translationally, transported across the organellar membrane. Cytosolic chaperones prevent degradation and aggregation of these translated, but as yet unfolded, organellar preproteins or precursors (Becker et al., 2012). These precursor proteins contain cleavable presequences, commonly referred to as transit sequences, which direct them to specific locations within the organelle, much as secretory protein signal sequences target proteins to the ER. This presequence is usually located at the N-terminus, but internal sequences are observed as well, particularly in mitochondrial preproteins. Both mitochondria and chloroplasts have outer (OM) and inner membranes (IM), and therefore require two translocases for protein import into the inner matrix or stroma, respectively **(Figure 1.4)**. The outer mitochondrial membrane translocase (TOM complex, consisting of Tom40, Tom70, Tom22, and Tom20) and the inner mitochondrial membrane translocase (TIM23 or TIM22 complex) are responsible for importing the majority of proteins into the mitochondrial matrix (Becker et al., 2012). Tom40, Tim23, and Tim22 are the channel proteins that make up the TOM, TIM23 (consisting of Tim23, Tim17, Tim21, and Tim50), and TIM22 complexes (consisting of Tim22, Tim18, and Tim54), respectively (Becker et al., 2012). In chloroplasts, the main translocases are known as the TOC and TIC complexes, which also have associated channel proteins (Soll and Schleiff, 2004). The TOC complex consists of 2 receptors (Toc159 and Toc34), a channel (Toc75), and peripheral components (Toc64) (Lee et al., 2013; Flores-Pérez and Jarvis, 2013). The TIC complex is composed of multiple subunits, including, among others, Tic110, Tic62, Tic55, and Tic40; however, the subunits that form the actual channel have not been identified. The complexes mentioned above might contain additional subunits or accessory proteins, but only representative/main subunits are listed **(Figure 1.4)**.

1.3.2.1 Protein Import into Mitochondria

Five pathways have been described for mitochondrial protein import, three only recently (see Becker et al. 2012) **(Figure 1.4a)**. The two classical routes are the presequence pathway and the carrier pathway. The presequence pathway involves preproteins with positively charged, N-terminal presequences that target the preprotein to the TOM complex, where, after membrane transit, they are cleaved by the mitochondrial processing peptidase (MPP) in the matrix. In one case (the presequence pathway), preproteins with hydrophobic presequences are inserted into the IM, after which transit sequences are cleaved by an IM peptidase (IMP) in the inner membrane space (IMS), located between the OM and IM. The carrier pathway in contrast, targets hydrophobic preproteins that lack N-terminal presequences, but have internal presequences, that interact with cytosolic chaperones, Hsp70 and Hsp90 (heat shock proteins) (Neupert and Herrmann, 2007). The TOM complex recognizes the carrier precursor-chaperone complex and transports the precursor through the Tom40 channel into the IMS. In the IMS, cleavable precursor proteins cross the IM via the TIM23 complex, and hydrophobic carrier precursors are inserted into the IM via the TIM22 complex. Three newly described import pathways are applied to more specific types of proteins but also involve the TOM complex. The β-barrel pathway (SAM) imports β-barrel protein precursors that are inserted into the OM with help from the SAM (sorting and assembly machinery) complex (Sam50, Sam35, and Sam 37); the mitochondrial intermembrane space assembly pathway (MIA) imports cysteine-rich IMS proteins, which are folded by Mia40; and finally the α-helical insertion (Mim1) pathway is responsible for transporting OM proteins with multiple transmembrane α-helices via the Mim1 complex.

1.3.2.2 Protein Import into Chloroplasts

Known mechanisms of protein import into chloroplasts are outlined by Flores-Pérez and Jarvis (2013). N-terminal transit sequences in chloroplastic precursor proteins vary in length, but are generally rich in hydroxylated residues, resulting in a net positive charge. Several cytosolic chaperones are able to bind these transit sequences and direct the precursor protein to the corresponding TOC and TIC complexes mediating outer and inner membrane transit, respectively (Lee et al., 2013) **(Figure 1.4b)**. 14-3-3 proteins and Hsp70 have been shown to bind certain transit sequences and target them to Toc34. Hsp70 can also target precursors to Toc159 or transport non-photosynthetic plastid precursors to Toc132 without the aid of 14-3-3 proteins. It is, however, unknown if other cytosolic factors are needed for either mechanism (Lee et al., 2013). Hsp90 binds several different transit sequences and targets the precursor protein to the peripheral channel protein Toc64 (Lee et al., 2013). Lastly, ankyrin repeat-containing protein 2 (AKR2), in conjunction with Hsp17.8, escorts OM proteins to the Toc75 channel protein. The ankyrin repeat is a common structural motif in proteins, consisting of a helix-loop-helix-β-hairpin fold that mediates protein-protein interactions (Mosavi et al., 2004). Once precursors destined for the stroma cross the OM through their respective channels, they interact with Tic22, a subunit of the TIC complex in the intermembrane space (IMS) that guides proteins across the IM via the TIC channel. When the N-terminal transit peptide emerges into the stroma, it is cleaved by the stromal processing peptidase (SPP) and the emergent protein is then folded with the assistance of chaperones/chaperonins, such as Hsp70, Cpn60/10, and cpSRP43.

Lumenal thylakoid proteins are transported using the cpSec and the cpTat pathway, while integral membrane proteins on the thylakoid are transported using the spontaneous pathway and the cpSRP pathway, as described by Schünemann (2007). Lumenal proteins contain a bipartite transit sequence that allows them to first traverse the envelope membrane into the stroma where the envelope transit sequence is cleaved. The remaining transit sequence is required for transport across the thylakoid membrane by one of the two pathways mentioned above. The cpSRP (chloroplast signal recognition particle) pathway seems to be used exclusively for members of the light-harvesting chlorophyll binding proteins (LHCPs). A transit sequence targets the LHCPs into the stroma and is cleaved off; LHCPs then bind to the cpSRP to form a transit complex responsible for LHCP integration. Some thylakoid membrane proteins insert into the membrane without energy or assistance from other proteins in the spontaneous insertion pathway. These proteins also contain a bipartite sequence that first targets them into the stroma and then to the thylakoid membrane.

1.3.3 Targeting/Transport to Vacuoles

The vacuole is the most prominent feature in most plant cells and can occupy up to 90% of the cell volume (Zhang et al., 2014). It was initially accepted that there was but a single type of vacuole that functioned in storage of proteins and pigments, and controlled cell osmotic potential by regulated transport of small ions. Although not universally accepted, the work of Paris et al. (1996) and others, suggested there are two types of vacuoles in plants, a protein storage vacuole (PSV) and lytic vacuole (LV). Having a function complementary to that of the 26S proteasome, LVs, analogous to lysosomes in animal cells, are responsible for storage and degradation of certain classes of unwanted materials (Xiang et al., 2013). In addition, it was initially believed that transport to vacuoles occurred only through a Golgi-dependent mechanism. However, Golgi-independent vacuolar targeting was suggested when it was observed that transport of wheat seed storage proteins was not associated with Golgi complexes (Levanony et al., 1992). Subsequently, it was discovered that protein targeting to both of types vacuoles can occur via either Golgi-dependent or Golgi-independent mechanisms as reviewed by Xiang et al. (2013). Both mechanisms require targeting signals called vacuolar sorting determinants (VSDs), as well as vacuolar membrane receptors that recognize and bind the VSDs. Three classes of VSDs have been identified: sequence-specific, C-terminal, and protein structure-dependent VSDs. Two families of membrane receptors have also been described: the vacuolar sorting receptor (VSR) and the receptor membrane ring-H2 (RMR).

1.3.3.1 Golgi-Dependent Vacuolar Trafficking

Two variants of the traditional Golgi-dependent trafficking pathway to the PSV have been identified (see Xiang et al., 2013) **(Figure 1.4c)**. In the first, trafficking of storage proteins diverges from the classical protein secretory pathway at the *cis*-Golgi, where dense vesicles (DVs), unique to plants, are formed. The TGN releases the mature DVs, which fuse first into multivesicular bodies (MVBs) and then into the storage vacuole. In the second, precursor-accumulating compartments (PACs) can also form at the TGN and deliver cargo to the PSV. In Golgi-dependent sorting into LVs, VSRs recognize the C-terminal vacuolar-sorting signal (VSS) on cargo proteins (Richter et al., 2009). In turn, the TGN-associated AP1 complex recognizes the cytosolic tail of VSRs via a tyrosine motif (YMPL), allowing CCV formation and transport into LVs (Richter et al., 2009). The formation of vesicles at the TGN that are bound for the LV can also be mediated by the AP3 complex.

1.3.3.2 Golgi-Independent Vacuolar Trafficking

Golgi-independent transport can also occur via PACs that form when cargo proteins using this pathway aggregate (Xiang et al., 2013; Michaeli et al., 2014) **(Figure 1.4c)**. These PACs, however, originate from the ER membrane, in a RMR-mediated process, and fuse directly with the storage vacuole (Xiang et al., 2013). RMRs as described above are transmembrane proteins that function as receptors for protein sorting by binding to VSDs on cargo proteins destined for the PSV. The Golgi-independent pathway utilized by LV resident proteins involves formation of ER bodies that apparently transport proteins directly to the LV, as no transport intermediates between ER bodies and the LV have yet been identified (Xiang et al., 2013). Research concerning Golgi-independent transport to the vacuole is discussed further in the following section.

Figure 1.4 Intracellular Targeting
Mitochondrial and chloroplastic proteins are translated in the cytosol, where they remain in an unfolded conformation supported by chaperones. This allows post-translational transport across the organellar membrane. These proteins have N-terminal or internal presequences (red line), known as transit sequences, that direct them to specific locations within the organelle. Mitchondria and chloroplasts both have outer and inner membranes, requiring two translocases for protein import to the inner matrix or stroma, respectively. Five pathways have been described for mitochondrial protein import **(A)**: the presequence pathway **(1)**, the carrier pathway **(2)**, the β-barrel (SAM) pathway **(3)**, the mitochondrial intermembrane space assembly (MIA) pathway **(4)**, and the α-helical insertion (Mim1) pathway **(5)**. The details of each pathway are described in the text. In chloroplasts **(B)** there are several chaperones that bind and direct proteins to the TOC complex in the outer membrane for import. Each chaperone set **(1, 2,** and **3)** targets precursor proteins to a different subunit or receptor of the TOC complex, as described in the text. Once in the IMS, proteins destined for the stroma bind Tic22 and are directed into the TIC channel. In the stroma, the N-terminal transit peptides are cleaved by SPP. In plants, proteins undergo both Golgi-dependent and Golgi-independent transport into the PSV and the LV **(C)**. DVs and PACs are derived from the TGN and fuse with the PSV, although DVs do first transition through the MVB. Proteins with VSSs are recognized by VSRs and are packaged into vesicles, whose formation is facilitated by either AP1 or AP3 (not shown). CCVs are formed from AP1 mediated formation and fuse with the LV. In the Golgi-independent pathways, PACs and ER bodies form directly from the ER and fuse with the PSV and LV, respectively.

AKR2, Ankyrin repeat-containing protein 2; AP1, adaptor protein 1; CCV, clathrin coated vesicle; ER, endoplasmic reticulum; DV, dense vesicles; Hsp, heat shock protein; IM, inner membrane; IMP, inner membrane peptidase; IMS, inner membrane space; LV, lytic vacuole; MIA, mitochondrial intermembrane space assembly pathway; MPP, mitochondrial processing peptidase; MVB, multivesicular body; OM, outer membrane; PAC; PM, plasma membrane; PSV, protein storage vacuole; SAM, sorting and assembly machinery; SPP, stromal processing peptidase; TGN, *trans*-Golgi network; TIC, translocon of the inner chloroplast membrane; TIM, translocon of the inner mitochondrial membrane; TOC, translocon of the outer chloroplast membrane; TOM, translocon of the outer mitochondrial membrane; VSR, vacuolar sorting receptor; VSS, vacuolar sorting signal

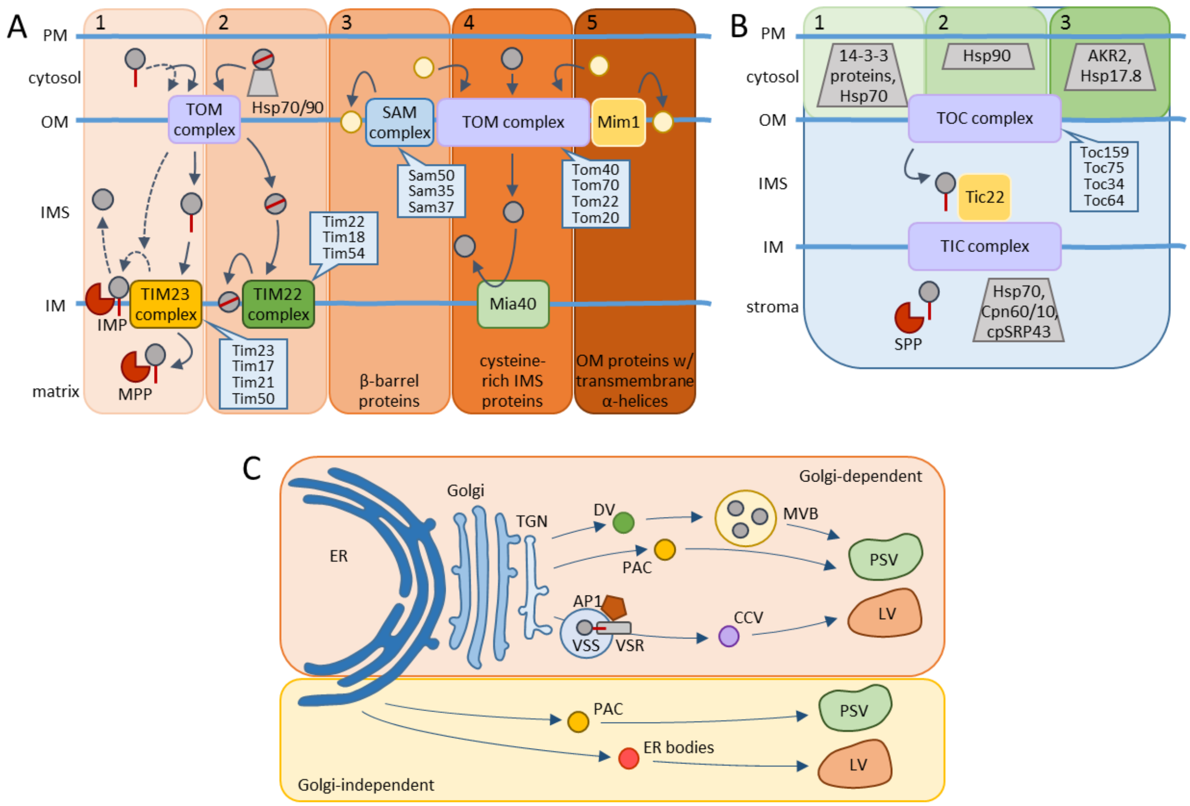
A
PM
cytosol
OM
IMS
IM
matrix
1
2
3
4
5
TOM complex
Hsp70/90
SAM complex
Sam50
Sam35
Sam37
TOM complex
Mim1
Tom40
Tom70
Tom22
Tom20
Tim22
Tim18
Tim54
IMP
TIM23 complex
TIM22 complex
Mia40
MPP
Tim23
Tim17
Tim21
Tim50
β-barrel proteins
cysteine-rich IMS proteins
OM proteins w/ transmembrane α-helices
B
PM
cytosol
OM
IMS
IM
stroma
14-3-3 proteins, Hsp70
Hsp90
AKR2, Hsp17.8
TOC complex
Toc159
Toc75
Toc34
Toc64
Tic22
TIC complex
SPP
Hsp70, Cpn60/10, cpSRP43
C
Golgi-dependent
ER
Golgi
TGN
DV
MVB
PAC
PSV
AP1
VSS
VSR
CCV
LV
PAC
PSV
ER bodies
LV
Golgi-independent

1.4 Unconventional, Golgi-Independent Secretion

1.4.1 Leaderless Secretion in Mammalian, Yeast, and Parasitic Cells

For decades the sole pathway for regulated protein secretion was believed to be via the ER/Golgi. However, in the mid-1980s, when Auron et al. (1984) sequenced the human interleukin 1 (IL-1) cDNA they found that, although it is secreted from human monocytes in response to an *Escherichia coli* endotoxin, it does not have a recognized signal sequence. Several years later, IL-1β was found to be actively secreted from human monocytes in the presence of brefeldin A (BFA), a known inhibitor of COPII vesicle formation, which prevents ER to Golgi transport (Rubartelli et al., 1990). Secretion of IL-1β was also observed in the presence of monensin (Rubartelli et al., 1990), an ionophore that inhibits conventional protein secretion by neutralizing and thereby disrupting the function of normally acidic compartments such as the Golgi (Mollenhauer et al., 1990). Since these initial reports, a large number of eukaryotic proteins have been found to be secreted via unconventional or Golgi-independent pathways. Although not an endogenous protein in most organisms, when exogenously expressed in animal and plant cells, the jellyfish green fluorescent protein (GFP), although a normally cytosolic protein, was found to be secreted. As with proteins like IL-1β, GFP lacks a known signal sequence, and secretion can occur in the presence of BFA when expressed in CHO (Chinese hamster ovary) cells as well as in NIH 3T3 (a standard fibroblast cell line), HEK293 (a human embryonic kidney cell line), and some cancer cell lines (Tanudji et al., 2002).

Although the emerging diversity of mechanisms makes classification problematic, unconventional protein secretion in animal and yeast systems is currently divided into four general types, described by Rabouille et al. (2012) **(Figure 1.5)**. First, mechanisms are classified as non-vesicular or vesicular secretion, and then further divided depending whether proteins utilizing these pathways are cytosolic or integral membrane proteins. Type I and Type II secretion mechanisms are both non-vesicular pathways for cytoplasmic proteins, involving translocation of proteins either directly across the PM or via ABC transporters, respectively. Secretion of proteins via what is termed the autophagy pathway (i.e. secretory autophagy [Jiang et al., 2013]) is classified as Type III, while proteins secreted by Golgi bypass mechanisms are termed Type IV secretion; both Type III and Type IV are vesicular pathways, although Type III is used in secretion of cytoplasmic proteins, while Type IV involves integral membrane proteins.

1.4.1.1 Type I – Direct Translocation Across the PM

The numerous studies on the secretion of fibroblast growth factor 2 (FGF2) have made it one of the best characterized examples of Type I unconventional secretion in the literature. An *in vitro* system of PM-derived, inside-out vesicles was used to assess FGF2 secretion. In this system, transport of the protein into the lumen of the vesicle is equivalent to export to the extracellular space (Schäfer et al., 2004). In these experiments, FGF2 was found to traverse the lipid bilayer unidirectionally, requiring both integral and peripheral membrane proteins (Schäfer et al., 2004). Galectin-1 (Gal-1) and FGF2 were also both observed to translocate directly across the membrane in this manner in mammalian cells in vivo (Schäfer et al., 2004). Using flow cytometry to detect protein-lipid interactions, FGF2 was determined to bind with high specificity to PtdIns(4,5)P2 (phosphatidylinositol 4,5-bisphosphate) on the inner/cytoplasmic leaflet of the PM lipid bilayer (Temmerman and Nickel, 2009; Nickel, 2011). It is hypothesized that PtdIns(4,5)P2 recruitment triggers oligomerization of FGF2 prior to membrane insertion (Nickel, 2010). Regardless of specific details, FGF2 then translocates across the PM in a folded conformation, ruling out the involvement of ABC transporters or protein channels (Backhaus et al., 2004; Torrado et al., 2009; Nickel, 2011). Once on the extracellular leaflet of the PM, heparin sulfate proteoglycans (HSPGs) are required for the release of FGF2 into the extracellular space (Zehe et al., 2006; Nickel, 2011). Zehe et al. (2006) suggests that HSPGs form a molecular trap to aid in the translation of FGF2 across the membrane. HSPGs bind to the C-terminal domain of FGF2, which has two lysine-rich loops on the surface that are responsible for the binding specificity

(Faham et al., 1996; Faham et al., 1998; Raman et al., 2003; Nickel, 2007). Two lines of evidence indicate that HSPG binding is necessary for FGF2 secretion. First, mutant FGF2 proteins with truncated C-terminal ends that were unable to bind HSPG could not be exported, while wild-type FGF2 could not be secreted from cells that lacked HSPG (Zehe et al., 2006). Extracellular FGF2 binds to HSPGs after which it interacts with high-affinity FGF receptors on the surface of target cells (Pellegrini et al., 2000; Schlessinger et al., 2000; Nickel, 2007). Finally, Tec kinase catalyzed phosphorylation of tyrosine 82 is also required for FGF2 secretion (Ebert et al., 2010), although the exact function of this phosphorylation is unknown (Nickel, 2011). Other proteins secreted by type I mechanisms include FGF1, HIV Tat, and annexins (Nickel, 2011). Membrane lipids, such as phosphoinositides or acidic phospholipids (e.g. phosphatidylserine), recruit these proteins to the cytoplasmic leaflet in preparation for translocation (Nickel, 2011). HIV Tat, FGF1, and annexin A2 have been shown to bind PtdIns(4,5)P2, while FGF1 and annexin A2 (Anxa2) bind phosphatidylserine to form the hetero-oligomeric complexes required for export (Rescher et al., 2004; Hayes et al., 2004; Hayes et al., 2009; Nickel, 2011).

1.4.1.2 Type II – ABC Transporter-Based

ABC (ATP-binding cassette) transporters are integral membrane proteins that use ATP (adenosine triphosphate) to move substrates across membranes (Hollenstein et al., 2007). ABC transporters are classified into two types: importers, found only in prokaryotes, and exporters (Hollenstein et al., 2007). Typically, they have two transmembrane domains (TMDs) and two cytoplasmic nucleotide-binding domains (NBDs). The NBDs, which have several conserved sequence motifs, bind and hydrolyze ATP at two ATP-binding sites formed by shared interface between the NBDs. The TMDs, however, are not conserved and vary in sequence, architecture, and length. Exporters have a core of twelve transmembrane helices, while in importers the number of helices can range from ten to twelve. ATP binding causes conformational changes in the NBDs that are then perceived by the TMDs, resulting in an outward-facing conformation. This allows for ATP hydrolysis, substrate dissociation on the extracellular side of the membrane, and the subsequent return of the transporter to its former inward-facing conformation. ABC transporters have been implicated in mediating translocation of lipid-modified peptides and proteins across the PM during unconventional secretion (Rabouille et al., 2012).

ABC transporters are known to mediate unconventional secretion in several species. In *Saccharomyces cerevisiae*, Ste6p (sterile), is an ABC transporter that is normally responsible for export of the mating pheromone a-factor (McGrath and Varshavsky, 1989; Kuchler et al., 1989; Michaelis, 1993). Mature a-factor is a peptide pheromone that contains 12 amino acid residues with a farnesylated and methylated C-terminal cysteine (Anderegg et al., 1988; Schafer et al., 1989). In Ste6p mutant lines, a-factor is not secreted and the mutant is sterile. In *Schizosaccharomyces pombe*, another peptide pheromone, M-factor, with the same C-terminal modifications as a-factor, is secreted by the ABC transporter Mam1 (mating type auxiliary gene, M cell specific) (Christensen and Nielsen, 1997). In *Drosophila melanogaster*, Mdr49 (multidrug resistance) mediates export of a geranylated germ cell attractant (Ricardo and Lehmann, 2009). The Mdr (multidrug resistance) class of transporters mediates export of a broad range of molecules, such as antibiotics and cancer chemotherapeutics (Higgins, 2007). The ABC transporters, Ste6, Mam1, and Mdr proteins, all contain 12 potential transmembrane domains and two ATP-binding sites (Christensen and Nielsen, 1997). When conservative amino acid substitutions are permitted, Ste6 and Mdr proteins have >60% sequence homology (Kuchler et al., 1989) and Mam1 has approximately 50% sequence homology when compared to Ste6 (a functional homolog of human Mdr3 [Ricardo and Lehmann, 2009]) and human Mdr1 (Christensen and Nielsen, 1997). Proteins exported by ABC transporters apparently require some sort of acylation for targeting and secretion. For example, HASPB (hydrophilic acylated surface protein B) (Denny et al., 2000; Stegmayer et al., 2005) and PfCDPK1 (*Plasmodium falciparum* Ca^{+2}-dependent protein kinase 1) (Möskes et al., 2004), both require dual acylation. In *Leishmania*, a protozoan parasite, N-myristoylation and palmitoylation of the HASPB N-terminal domain is required for localization to the extracellular leaflet of the PM (Denny et al., 2000). PfCDPK1, exported to the parasitophorous vacuole, needs addition of three acyl groups at its N-terminus for maximum membrane anchoring capability: N-myristoylation, palmitoylation, and a basic motif (Möskes et al., 2004). This dual acylation is reminiscent of Src (sarcoma)-family protein kinases anchoring to the membrane and associating with lipid rafts via myristoylation and palmitoylation; this is known as the two-signal model (Resh, 1999). It is possible that other lipid modifications are involved in export using ABC transporters, but only these few have been described to date.

1.4.1.3 Type III – Autophagy-Based

IL-1β (interleukin 1β), a cytoplasmic protein, was one of the first examples of unconventional secretion described (Rubartelli et al., 1990). IL-1β, IL-18, and IL-33 precursors are all cleaved by the protease caspase-1 prior to secretion (Nickel and Rabouille, 2009). Caspase-1 is known to be a key regulator of the inflammatory response and is activated by the inflammasome (Nickel and Rabouille, 2009), a multi-protein complex in the cell that becomes activated during infection or stress (Schroder and Tschopp, 2010). There are different types of inflammasomes, classified based on their protein composition (Petrilli et al., 2005). The mature form of IL-1β, however, might not be required for secretion as the IL-1β precursor has also been identified in supernatants from cells with inactive inflammasomes (Keller et al., 2008; Rabouille et al., 2012). Although the mechanism of IL-1β secretion has been under investigation for more than 25 years, many questions remain, including the type of vesicle transporting IL-1β, although secretory lysosomes, MVBs, and microvesicles have all been suggested in this role (Andrei et al., 1999; MacKenzie et al., 2001; Andrei et al., 2004; Qu et al., 2007; Rabouille et al., 2012).

Other examples of this class of secreted protein include the leaderless Acyl-CoA-binding protein (AcbA) from *Dictyostelium discoideum* and its yeast ortholog Acb1 that are secreted during cell starvation (Anjard and Loomis, 2005; Rabouille et al., 2012). Secretion of Acb1 involves interacting proteins associated with both the autophagy and MVB pathways, suggesting that an autophagosome-like vesicle could be involved in Acb1 secretion (Duran et al., 2010; Manjithaya et al., 2010;

Rabouille et al., 2012). Grh1 and GrpA, orthologues of mammalian GRASP65 (Golgi reassembly stacking protein) and GRASP55, proteins involved in Golgi cisternae stacking (Barr et al., 1997), are also required for secretion of Acb1 and AcbA, respectively (Kinseth et al., 2007; Bruns et al., 2011). During nutrient starvation, Grh1 localizes near ERES and promotes formation of CUPS (compartments for unconventional protein secretion), enriched in PtdIns3P (phosphatidylinsotol 3 phosphate) (Bruns et al., 2011). Both PtdIns3P and an N-terminal acetylation is required for membrane association of Grh1, which in turn recruits Vps23 (ESCRT-I), Atg8, and Atg9 (Axe et al., 2008; Bruns et al., 2011). Snf7 (ESCRT-III), however, is not found within CUPS, indicating that not all proteins required for the MVB or autophagy pathway are required for CUPS formation (Bruns et al., 2011). Other examples include Grh1, Bug1, Vps25/36 (ESCRT-II), and Vps20/2 (ESCRT-III), proteins required for formation of CUPS, but not required for autophagy (Bruns et al., 2011). Ssol, a PM t-SNARE, is also required for Acb1 secretion (Duran et al., 2010). In mammalian cells, starvation also triggers formation of compartments similar to CUPS, termed omegasomes (Axe et al., 2008; Matsunaga et al., 2010). CUPS and omegasomes both form near or associated with the ER and have membranes enriched in PtdIns3P (Bruns et al., 2011).

1.4.1.4 Type IV – Golgi Bypass

Proteins that use the Golgi bypass mechanism are defined as those that undergo anterograde transport to the PM that is resistant to BFA inhibition. Several proteins (Nickel and Rabouille, 2009; Rabouille et al., 2012), such as Hsp150 (heat shock protein) (Fatal et al., 2004), Ist2 (increased sodium tolerance) in yeast (Jüschke et al., 2005), CD45 (cluster of differentiation, a protein tyrosine phosphatase) (Baldwin and Ostergaard, 2002), and integrin αPS1 in *Drosophila melanogaster* (Schotman et al., 2008), with signal sequences/peptides use this pathway to reach the PM, with CFTR (cystic fibrosis transmembrane conductance regulator) (Yoo et al., 2002) being the best characterized. Direct transport of CFTR to the PM from the ER in COPII-coated vesicles (Wang et al., 2004) occurs without

Sar1 and Rab1 (Gee et al., 2011), which as previously described, are involved in vesicular trafficking, specifically tethering and coat formation. Syntaxin 5 (t-SNARE) is not required for transport of CFTR to the PM, but is required for transport of newly synthesized proteins from the ER to and through the Golgi stacks (Pelham, 2001), providing further evidence that CFTR does not go through the Golgi. Syntaxin 13 (t-SNARE), specific to the late endosome, however, is necessary for CFTR to reach the PM, indicating that CFTR-containing vesicles could be fusing to the late endosomal/lysosomal compartment prior to fusing with the PM (Yoo et al., 2002). This is further supported by studies that show CFTR first passing through ERGIC, or intermediate compartment (IC) (Marie et al., 2009), and then fusing to recycling endosomes to reach the PM (Prydz et al., 2013). Specific mechanisms and machinery that are involved in the Golgi bypass pathway are currently unknown.

Figure 1.5 Unconventional Secretory Pathways in Animal Cells
Four unconventional secretory pathways have been described in animal cells: Type I (direct translocation across the PM), Type II (ABC transported-based, Type III (autophagy-based), and Type IV (Golgi bypass mechanism). Proteins known to utilize each type of secretion (in colored boxes) and their corresponding transport components (in blue boxes) are listed; more details of each can be found in the text. FGF2, the best characterized protein to use Type I secretion (purple), requires integral and peripheral membrane proteins. FGF2 binds to PtdIns(4,5)P2 on the cytoplasmic leaflet of the PM and, using currently unknown mechanisms, translocates across the PM in a folded conformation. In Type II secretion (brown) the cargo protein binds the cytoplasmic face of the ABC transporters (Ste6p, Mam1, Mrd49). Energy provided by an ATPase subunit drives a conformational change to translocate and release the cargo into the extracellular space. Acb1 and AcbA are othologs that undergo Type III secretion (red) during cell starvation. Proteins involved in Golgi cisternae stacking (Grh1/GrpA) and the ESCRT pathway (Vps25/36 and Vps20/2) are required for formation of CUPS, enriched in PtdIns3P. Sso1, a PM t-SNARE, is also required for Acb1 secretion. Proteins that use Type IV secretion (green) undergo anterograde transport to the PM and are resistant to BFA inhibition. CFTR, for instance, is transported from the ER to the PM in COPII vesicles, first passing through ERGIC and fusing with recycling endosomes.

ABC, ATP-binding cassette; Acb, Acyl-CoA-binding protein; ADP, adenosine diphosphate; Anxa2, annexin A2; Atg, autophagy; ATP, adenosine triphosphate; BFA, brefeldin A; CD, cluster of differentiation; CFTR, cystic fibrosis transmembrane conductance regulator; COPII, coat protein II; CUPS, compartments for unconventional protein secretion; ER, endoplasmic reticulum; ERGIC, ER-Golgi intermediate compartment; ESCRT, endosomal sorting complexes required for transport; FGF2, fibroblast growth factor 2; HASPB, hydrophilic acylated surface protein B; Hsp, heat shock protein; IL-1β, interleukin 1-β; Ist, increased sodium tolerance; Mam1, mating type auxiliary gene, M cell specific; Mrd49, multidrug resistance 49; PfCDPK1, Plasmodium falciparum Ca+2-dependent protein kinase 1; PM, plasma membrane; PtdIns3P, phosphatidylinsotol 3 phosphate; PtdIns(4,5)P2, phosphatidylinositol 4,5-bisphosphate; Ste6p, sterile 6; TGN, *trans*-Golgi network; t-SNARE, soluble NSF (N-ethylmaleimide-sensitive factor) attachment protein receptor; Vps, vacuolar protein sorting

Adapted from Rabouille et al., 2012

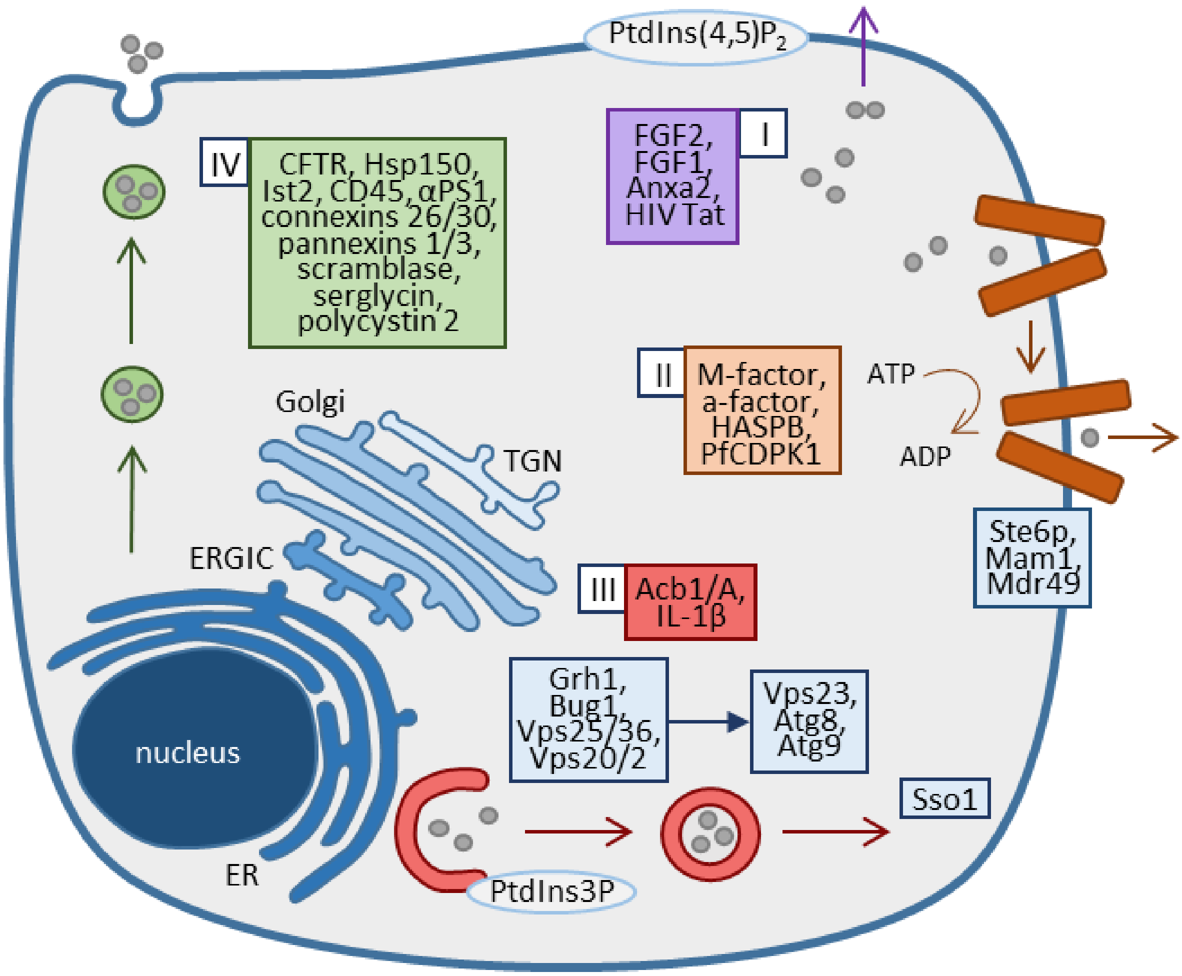
PtdIns(4,5)P2
I
FGF2,
FGF1,
Anxa2,
HIV Tat
IV
CFTR, Hsp150,
Ist2, CD45, αPS1,
connexins 26/30,
pannexins 1/3,
scramblase,
serglycin,
polycystin 2
II
M-factor,
a-factor,
HASPB,
PfCDPK1
ATP
ADP
Ste6p,
Mam1,
Mdr49
Golgi
TGN
ERGIC
III
Acb1/A,
IL-1β
nucleus
ER
Grh1,
Bug1,
Vps25/36,
Vps20/2
Vps23,
Atg8,
Atg9
Sso1
PtdIns3P

1.4.2 Unconventional Protein Secretion in Plants

Although extracellular localization of a number of plant proteins that lack recognized signal sequences has been observed numerous times over the last 20 years, the idea that at least some of these proteins might be secreted or localized by a defined non-Golgi pathway has been proposed only in the past few years. Research on seed storage proteins, lectins, and superoxide dismutases (SODs) provided some of the first hints that leaderless protein secretion existed in plants. Initial studies beginning in the late 1980s/early 1990s, and briefly outlined below, led to the discovery of unconventional protein transport and secretion in plants and provided much of the impetus for continued research that is leading to the description of the mechanisms involved. Specific proteins, such has mannitol dehydrogenase (MTD) and hygromycin phosphotransferase (HYG^R), have also been studied.

1.4.2.1 Storage Proteins

Seeds store energy and carbon in a number of compounds, including carbohydrates, lipids and proteins. Prolamins are the main endosperm storage proteins in a number of cereal grains including wheat (glutenins and gliadins), maize (zeins), and barley (hordeins) (Shewry and Halford, 2002). Early experiments in which these storage protein genes were overexpressed in dicots to study protein storage body formation found that the 19 kDa zein protein, when expressed by itself in Petunia, did not accumulate significantly even though RNA levels were substantial (Williamson et al., 1988). Because the exogenously expressed zein migrated as a 19 kDa protein, it was assumed that zein signal peptides were cleaved as the protein was made (Williamson et al., 1988). In localization studies, zeins were seen to accumulate in the seed of transformed plants and both dispersed and in aggregates at the cell surface (Williamson et al., 1988), suggesting that export of non-complexed zein might occur via some unconventional mechanism. Much later, work showed that, in maize and rice, protein bodies containing zeins form and are retained in the lumen of the rough ER, even though these zeins lacked traditional ER retention signals (Coleman et al., 1996). Using immunoblotting and immunogold labeling, studies on maize α-zein and γ-zeins expressed in tobacco indicate that γ-zeins may assist in localizing and stabilizing the accumulation of α-zeins in protein bodies, which form initially as aggregates of β- and γ-zeins before interior α-zein accumulation (Coleman et al., 1996). Protein bodies were seen in both the cytoplasm and in protein storage vacuoles, suggesting transport via an autophagy pathway (Coleman et al., 1996). Further research using the yeast two-hybrid system uncovered specific interactions between the various zein types. These include interactions between the γ-zeins (50, 27, and 16 kDa) and the 15 kDa β-zein, between the α-zeins (19 and 22 kDa) and the 10 kDa δ-zein, and interaction of α-/δ-zeins with 16 kDa γ-zein and 15 kDa β-zein (Kim et al., 2002). Not long thereafter, work on the transport of wheat storage proteins to vacuoles also implicated non-Golgi pathways (Levanony et al., 1992). Protein bodies (PBs) (defined as the result of storage vacuole fragmentation [Galili et al., 1993]), containing wheat storage proteins were examined using immunoelectron microscopy (immunoEM) (Levanony et al., 1992). PBs were observed to form in the rough ER and colocalize with BiP, a known ER-localized protein, but not with the Golgi (Levanony et al., 1992).

1.4.2.2 Lectins

Lectins, carbohydrate-binding proteins, have been observed to accumulate in vacuoles, and are secreted in response to pathogen attack (Chrispeels and Raikhel, 1991). How lectins, reached the extracellular space, since they lack the signal sequence previously thought to be necessary for secretion, was a persistent puzzle. More recent studies on the *Helianthus annuus* jacalin-related lectin strongly suggest that secretion occurs via unconventional pathways (Regente et al., 2012; Pinedo et al., 2012) and as described below is triggered by salicylic acid (SA) (Cheng et al., 2009a), an endogenous inducer of defense responses in plants (Malamy et al., 1990).

1.4.2.3 Superoxide Dismutases (SODs)

Superoxide dismutatses (SODs), metalloenzymes that catalyze the disproportionation reaction of the superoxide radical to hydrogen peroxide or molecular oxygen, remove reactive oxygen species (ROS) generated both within the cell and in the extracellular space. Unlike animal ecSODs (extracelluar SODs), plant SODs all lack a leader sequence, so it was assumed that they could not be extracellular/apoplastic. This led to the biochemically and physiologically awkward peroxidase hypothesis that suggested that the appearance of hydrogen peroxide in the apoplast during infection was the result of a reverse reaction catalyzed by peroxidases secreted in response to pathogen attack (Corpas et al., 2001; Bolwell et al., 2002; Bolwell, 1999; Neill et al., 2002). Unfortunately this hypothesis persisted in spite of extensive data pointing to the existence of ecSODs in plants. For instance, SOD isoforms of were found in extracellular spaces and washing fluid from *Pinus sylvestris* L. (Scots pine) needles (Streller and Wingsle, 1994; Karpinska et al., 2001), in the apoplast of *Hordeum vulgare* L. leaves after inoculation with *B. graminis f. sp. hordei* (Vanaker et al., 1998), and in the apoplast of *Pisum sativum* cultivars under salt stress (Hernández et al., 2001). Finally, using LC/MS^E Cheng et al. (2009b), showed that the *Arabidopsis* Cu/Zn SOD is secreted in the absence of cell lysis during treatment with SA. This, together with previous studies, suggests that SOD isozyme is being secreted via unconventional mechanisms.

1.4.2.4 Mannitol Dehydrogenase (MTD)

Mannitol, a six-carbon sugar alcohol, functions as a metabolite and osmoprotectant in a number of plant species (Stoop et al., 1996; Cheng et al., 2009b). The catabolic enzyme mannitol dehydrogenase (MTD), an NAD-dependent 1-oxidoreductase that oxidizes mannitol to mannose for use as a carbon and energy source, was first characterized in celery, a plant that translocates a large portion of its fixed carbon as mannitol (Stoop et al., 1996). While MTD, which lacks a signal sequence for conventional secretion, is normally found to be cytosolic and nuclear

(Zamski et al., 1996; Yamamoto et al., 1997), it is specifically translocated to the apoplast after treatment with salicylic acid (SA), making MTD a member of the SA-regulated class of pathogenesis-related (PR) proteins (Zamski et al., 2001; Cheng et al., 2009b). Interestingly, MTD homologs are found in non-mannitol producing plants such as *Arabidopsis*, ELI3 mRNA and tobacco where their accumulation and secretion is induced in response to infection (Patel and Williamson, 2016; Kiedrowski et al., 1992; Williamson et al., 1995; Jennings et al., 1998). Using *Nicotiana tabacum* cells transformed with celery MTD, Cheng et al. (2009b) demonstrated that SA-triggered MTD secretion into the apoplast is not affected by BFA, suggesting that MTD secretion is by unconventional means. The extracellular media from the SA-induced cells contained MTD that still had activity but no hexokinase (HK), a cytoplasmic protein marker, indicating that extracellular localization was not the result of cell lysis (Cheng et al., 2009b). Although the secretion of MTD has been assessed and verified using a variety of approaches, potential mechanisms of secretion are only now being explored.

1.4.2.5 Hygromycin Phosphotransferase (HYG^R)

Streptomyces hygroscopicus produces hygromycin B, an aminoglycoside antibiotic that inhibits protein synthesis in prokaryotic and eukaryotic cells (Pittenger et al., 1953; McGaha and Champney, 2007; Zhang et al., 2011). Hygromycin phosphotransferase (HYG^R) inactivates hygromycin B via phosphorylation, and is often used as a selectable marker in transgenic cells (Miki and McHugh, 2004). It was reported that not only does HYG^R lack a signal sequence (Miki and McHugh, 2004; Zhang et al., 2011), but its secretion by *A. thaliana*, is insensitive to BFA. Interestingly, although the transport and secretion of HYG^R from the cytosol to the extracellular matrix is BFA resistant, it requires synaptotagmin (SYT2). SYT2, a Golgi-localized protein, is required for truncation of the HYG^R C-terminus. Cells deficient in SYT2 could not process HYG^R, resulting in accumulation of HYG^R in prevacuolar compartments (PVCs) and vacuoles (Zhang et al., 2011).

1.4.3 Mechanisms of Unconventional Secretion and Trafficking in Plants

Although much less is known about unconventional secretion/transport in plants than in animals, particularly for cytosolic proteins secreted in the presence of BFA, several general pathways are beginning to emerge **(Figure 1.6)**. Potential pathways or mechanisms summarized by Drakakaki and Dandekar (2013) include transport by MVBs, or EXPOs (exocyst positive organelles, described later), or the fusion of vacuoles with the PM. Although protein transport to the vacuole is not necessarily via non-Golgi mechanisms, secretion of vacuolar proteins by PM fusion is considered unconventional.

1.4.3.1 Golgi-Independent Transport from ER to Vacuoles

As mentioned previously, proteins can be delivered to the vacuole by either Golgi-dependent or Golgi-independent methods. Tonoplast intrinsic proteins (TIPs) for instance can bypass the Golgi and be delivered directly from the ER to the PVC/vacuole (De Marchis et al., 2013). Studies on phytohemagglutinin (PHA) (a soluble vacuolar protein) and α-TIP in transformed tobacco plants show that BFA and monensin inhibit PHA transport to the vacuole, but have no effect on α-TIP transport (Gomez and Chrispeels, 1993). Rivera-Serrano et al. (2012) used inhibitory chemicals, particularly C834 (9-(5-bromo-2-propoxyphenyl)-10-ethyl-3,4,6,7,8,10-hexahydro-1,8(2H,5H)-acridinedione) (Rojas-Pierce, 2013), which is proposed to be an inhibitor of BFA-insensitive pathways, to further distinguish and verify Golgi-dependent vs. -independent pathways for TIPs in *Arabidopsis*. Upon treatment with C834, TIP3;1 (α-TIP) and TIP2;1 (δ-TIP) transport to the PVC and thus the vacuole were inhibited, but TIP1;1 (γ-TIP) transport remains unaffected. In the presence of BFA, however, the opposite is true – TIP3;1 and TIP2;1 transport is unaffected, while TIP1;1 transport from the ER to Golgi is inhibited; these results parallel with those obtained previously by Gomez and Chrispeels (1993). In another study, rice two-pore K^+ channel (TPK) isoforms normally located in the lytic vacuole (LV) (TpKa) and on the surface of the protein storage vacuole (PSV)-like compartments (TpKb) are shown to use the Golgi-dependent and Golgi-independent pathways, respectively (Isayenkov et al., 2011).

Many studies have provided evidence of this direct route from the ER to the vacuole, the Ervt (ER-vacuole trafficking) pathway, which is only selective to storage protein transport (Michaeli et al., 2014a). ER bodies, mentioned earlier in the discussion of intracellular protein targeting/transport, are able to mediate unconventional protein transport to the vacuole (De Marchis et al., 2013). Originally used by Hayashi et al. (2001), the term ER bodies, also known as protein bodies (Levanony et al., 1992) or PVCs (Reyes et al., 2011b), refers to ER-derived compartments that are usually larger than secretory vesicles (e.g. DVs) or CCVs (De Marchis et al., 2013). This mechanism has been shown to mainly transport storage proteins and enzymes (De Marchis et al., 2013), and there are several studies that support this statement. Zeins, as previously discussed, form aggregates in the ER and are transported in protein bodies until they are later delivered to storage vacuoles (Levanony et al., 1992) along with α-globulin and legumin-1 in *Zea mays* (maize) aleurone cells, a main cell type in cereal endosperm (Reyes et al., 2011b). The prevacuolar compartments containing zeins do not have Atg8 (autophagy-related protein 8), a known autophagosomal marker, or a double membrane, which suggests they are not autophagosomes (Reyes et al., 2011b). Michaeli et al. (2014a), however, argue the possibility of a transient interaction that would be hard to detect via microscopy between Atg8 and cargo receptor proteins. During selective autophagy, Atg8 binds AIM (Atg8-family interacting) or LIR (LC3 [light chain 3]-interaction region) motifs (Noda et al., 2010; Birgisdottir et al., 2013). Michaeli et al. (2014b) show that ATI1, containing AIM motifs and a transmembrane domain (Honig et al., 2012), interact with plastid proteins and ATG8f in the plastid bodies for delivery to the vacuole. Using electron microscopy, glycinin (11S), one of the major storage proteins in *Glycine max* L. (soybean), is seen to be transported to the PSV from the ER in protein bodies in soybean cotyledons (Mori et al., 2004). In rice endosperm, glutenins and α-globulins accumulate in PAC-like vesicles and colocalize with BiP, implying that these vesicles originate directly from the ER (Takahashi et al., 2005).

1.4.3.2 Fusion of Vacuole and PM

In *A. thaliana*, vacuoles fuse with the PM to release antibacterial proteins, such as lectins and vacuolar proteolytic enzymes (Hara-Nishimura and Hatsugai, 2011), into the extracellular space in response to *Pseudomonas syringae* infection (Hatsugai et al., 2009). This fusion is proteasome-dependent, and not only results in secretion of proteases, but also promotes cell death of nearby cells to inhibit bacterial growth (Hatsugai and Hara-Nishimura, 2010). All three catalytic subunits of the *A. thaliana* proteasome, which has caspase-3-like activity (Hatsugai and Hara-Nishimura, 2010), (PBA1, PBB, and PBE) are required for this process, indicating that the proteasome somehow regulates fusion of the vacuole to the PM (Hatsugai et al., 2009).

1.4.3.3 Vesicles/MVBs (Multivesicular Bodies)

Although the specifics of this type of unconventional secretion in plants have not been fully clarified, there is growing evidence that vesicles/MVBs are involved in unconventional secretion of a number of proteins. The examples briefly outlined below have been hypothesized to use an exosome-mediated pathway, reminiscent of the well-defined autophagy-based mechanisms (Type III secretion) in animal cells. Secretion via vesicles/MVBs would likely give rise, at least transiently, to extracellular exosome-like vesicles and is hypothesized to be triggered both by stimuli or occur as a part of normal cellular activity (Ding et al., 2014a). Regente et al. (2008) found phospholipids, particularly phosphatidic acid (PA) and phosphatidylinositol (PI), in the extracellular fluid of *Helianthus annuus* sunflower seedlings. Further investigation using ultracentrifugation to fractionate extracellular fluids combined with transmission electron microscopy found the appearance of these phospholipids correlated with the appearance of vesicle-like particles with phospholipid membranes in the apoplast (Regente et al., 2009). MALDI-TOF/MS (Matrix-Assisted Laser Desorption/Ionization – Time of Flight/Mass Spectrometry) analysis of the same extracellular fluids identified a putative Rab GTPase, Rab 11A, which is commonly involved in vesicular trafficking (Regente et al., 2009). Again, using *H. annuus* seedlings, a leaderless *Helianthus annuus* jacalin-related lectin (Helja) whose secretion is resistant to BFA, was found in the secretome (Regente et al., 2012; Pinedo et al., 2012). Immunofluorescent labeling and fractionation detected Helja in the apoplast (Pinedo et al., 2012) and in the isolated vesicular exosome-like fraction (Regente et al., 2012), respectively. Interestingly, several different jacalin-related lectins, which all lack signal peptides, are also secreted in response to SA in *Arabidopsis* cell suspension cultures (Cheng et al., 2009a).

Using confocal laser scanning microscopy (CLSM) and transmission electron microscopy (TEM), Prado et al. (2014) have also observed the release of nanovesicles, which they termed pollensomes, from pollen grains during pollen germination and pollen tube growth in olive (*Olea europaea*). This nanovesicular proteome was analyzed using mass spectrometry and the resulting proteins categorized by function, such as metabolism/signaling and protein synthesis/processing (Prado et al., 2014). The functional diversity of these proteins suggests that release of pollensomes assists in regulating various aspects of pollen tube growth and development (Prado et al., 2014).

As indicated earlier, protein secretion by the vesicular/MVP pathway can be a part of normal cell activity – *A. thaliana* and *A. lyrata*, for example, both release vesicles at the stigmatic papillae, while *Brassica napus* seems to release MVBs in response to compatible pollen (Safavian and Goring, 2013). Although the proteins contained in these vesicles and MVBs have not yet been identified, it seems likely, based on previous results that at least some will lack signal peptides. Finally, analysis by immunofluorescent and immunoEM show that VSRs (vacuolar sorting receptors), previously described as part of Golgi-dependent vacuolar sorting mechanisms, are localized in PVCs/MVBs, the TGN, and the PM, suggesting that MVBs could also have a role in secretion of VSRs at the membrane (Wang et al., 2011).

1.4.3.4 EXPO (Exocyst Positive Organelle)

AtExo70E2, one of 23 paralogues of mammalian Exo70 found in *A. thaliana*, is required for recruiting subunits for formation of EXPO, a spherical double-membrane cytoplasmic compartment resembling autophagomes (Wang et al., 2010; Ding et al., 2014b). Formation of EXPOs, however, is not triggered the same way as autophagosome formation, nor does AtExo70E2, an EXPO marker protein, colocalize with the autophagosome membrane marker, Atg8e (Yoshimoto et al., 2004; Contento et al., 2005; Wang et al., 2010) suggesting that EXPOs do not fuse with endosomes or lytic vacuoles. Further, Wang et al. (2010) used immunoEM to visualize AtExo70E2 localization to the PM as well as its presence in EXPOs, which are unaffected by inhibitors of conventional secretion (e.g. BFA) and endocytosis (e.g. wortmannin). EXPOs were observed both as distinct cytoplasmic structures as well as bodies in the process of fusing with the PM, which results in a single-membrane extracellular vesicle containing secreted proteins (Wang et al., 2010). SAMS2 (S-adenosyl-methionine synthetase 2), a cytosolic protein lacking a signal peptide, was seen to colocalize with AtExo70E2 in EXPO, but was not detected extracellularly (Wang et al., 2010).

Figure 1.6 Proposed Unconventional Secretory Pathways in Plant Cells
Several unconventional secretory pathways have been proposed in plant cells: fusion of the vacuole with the PM **(1)**, secretion via MVBs **(2)**, and secretion via EXPOs **(3)**. The secretory mechanisms of cytosolic proteins **(4)**, such as MTD and HYG^R, have not yet been deciphered. Proteins can also be directly transported from the ER to the vacuole **(5)**, and although part of the pathway does not include secretion, they arrive at the vacuole via unconventional means and can be secreted by vacuolar fusion with the PM. The ER-vacuole trafficking pathway uses ER bodies (also called protein bodies or PVCs) which are ER-derived compartments mainly involved in transporting storage proteins and enzymes. Release of antibacterial proteins into the extracellular space can occur through fusion of the vacuole with the PM. This fusion is proteasome-dependent and promotes cell death to prevent bacterial growth. Protein secretion via MVBs in plants is reminiscent of the autophagy-based unconventional secretion (Type III) in animals. Helja, a jacalin-related lectin lacking a signal peptide and whose secretion is BFA resistant, has been detected in both the vesicular exosome-like fraction as well as in the apoplast. In general, lectins are found in the vacuole and undergo unconventional secretion, however, the exact pathway they use has not yet been determined. Formation of EXPOs, double membrane compartments resembling autophagosomes, requires AtExo70E2, also found localized at the PM. EXPOs have been observed as distinct cytoplasmic structures as well as bodies in the process of PM fusion. It is unknown where EXPOs originate (indicated by dashed lines), however, they share similarities with CUPS in animal cells.

BFA, brefeldin A; CUPS, compartments for unconventional protein secretion; ER, endoplasmic reticulum; ERGIC, ER-Golgi intermediate compartment; EXPO, exocyst positive organelle; HYG^R, hygromycin phosphotransferase; MTD, mannitol dehydrogenase; MVB, multivesicular body; PVC, prevacuolar compartments; TGN, *trans*-Golgi network

Adapted from Drakakaki and Dandekar, 2013 and Ding et al., 2014

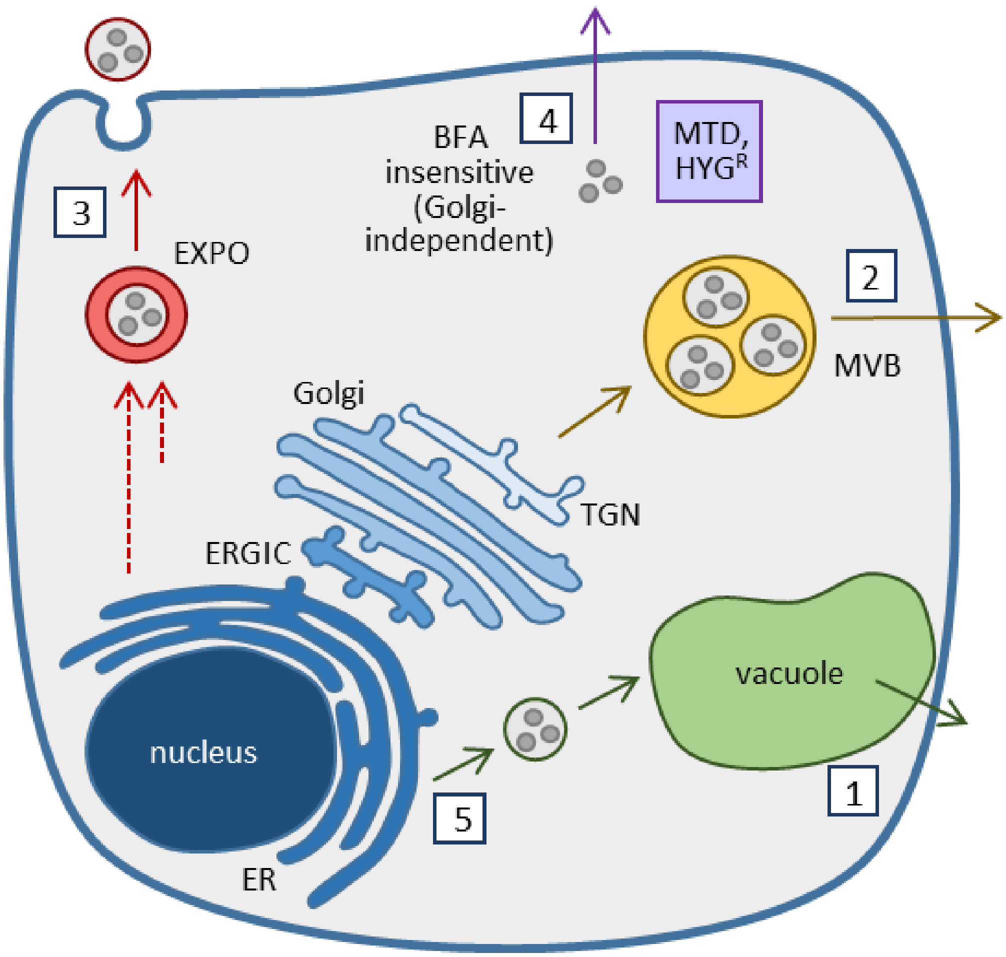
4
BFA
insensitive
(Golgi-
independent)
MTD,
HYG^R
3
EXPO
2
MVB
Golgi
TGN
ERGIC
vacuole
nucleus
5
1
ER

1.5 Methods of Protein-Protein Interaction Analysis

Protein trafficking is involved in most cellular pathways, therefore, understanding the mechanisms involved can provide an insight into multiple aspects of cell function. A particularly crucial aspect of understanding trafficking is the mechanisms and regulation of these processes through protein-protein interactions (PPIs). Rao et al. (2014) summarize methods of protein-protein interaction analysis, categorizing these methods into three main classes: *in vitro*, *in vivo*, or *in silico*. In vitro techniques are performed in a controlled environment, outside the normal context of a cell or an organism; examples of this are affinity chromatography, co-immunoprecipitations, X-ray crystallography, and NMR (nuclear magnetic resonance) spectroscopy. Yeast two-hybrid assays are an example of an *in vivo* approach, where the procedure is performed in whole, living organisms. *In silico* techniques involve computer simulation(s) and include sequence/structure-based predictive approaches. Here, the focus will be on *in vitro* and *in vivo* methods commonly used to assess protein-protein interactions during trafficking.

It is unlikely that any single approach described below has the ability to fully assess even one of these facets. For instance, cell fractionation can be used to detect protein presence in a given cellular component, but cannot be used to unambiguously validate compartmentation. Electron microscopy, however, can be used to unambiguously validate compartmentation of a particular antibody-crossreacting protein, but it cannot be used to unambiguously verify protein identity or activity. Only by combining a variety of approaches can any one aspect of trafficking be thoroughly evaluated.

1.5.1 Cell Fractionation and Immunoblot Analysis

Cell fractionation, separating cellular components using centrifugation or filtration, combined with various protein analytical methods such as immunoblotting, ELISA and enzyme activity assays, has been widely used to assess protein localization and trafficking. After collection of the extracellular fluids either by infiltration-centrifugation of leaf tissue (e.g. O'Leary et al., 2014) or centrifugation/filtration of cells from cell cultures, cell contents are fractionated using various methods. In the most common approaches, cells or tissues are ground or sonicated to disrupt the cell wall and/or plasma membrane, while leaving organelles and vesicles intact. These cellular components are of different densities and so can be separated by differential centrifugation. Different particles will pellet or sediment at different rates under different g-forces; for instance, at low speeds (1000xg) whole cells, nuclei, and large cytoskeletal fragments will form a pellet. At medium (20,000xg) and high speeds (80,000xg), mitochondria, lysosomes, and perixosomes or microsomes and small vesicles, respectively, will be separated from the cell homogenate, or extract. At very high speeds (150,000xg), ribosomes, viruses, and large macromolecules will sediment. In addition, various membranes can be separated into microsomal and plasma membrane fractions by 2-phase partitioning (Mitra et al., 2015). Used in conjunction with immunoblotting and or enzyme assays, cell fractionation provides an unambiguous and relatively easy way to quickly assess cellular location of a protein. Visualization is generally done after gel separation to maximize signal intensity. A primary antibody is first used that binds specifically to the protein of interest, followed by a secondary antibody that binds to the primary antibody. There are a variety of ways to visualize the protein, depending on the moiety bound to the secondary antibody (e.g. alkaline phosphatase, fluorescent tags, etc.). Although these are straightforward methods, cross-contamination between cell fractions and variation in sample preparation can be problematic. Also, there is no way to guarantee complete recovery of each cell fraction, which can result in misleading information concerning protein quantitation. Immunoblotting itself can also be problematic due to binding of an antibody to proteins other than the original antigen.

1.5.2 Electron Microscopy

Electron microscopy has been a traditional workhorse in the study of protein localization. Although antibodies can be labeled with different electron-opaque metals for visualization, many of the studies above utilized immunogold labeling and electron microscopy (EM) to assess localization of specific proteins. Traditionally, samples are fixed before sectioning (cutting the sample into slices approximately 60-80 nm) and staining (Winey et al., 2013). Target proteins can be identified using gold labeling of the relevant antibody, which can be used pre- (before fixing) or post-embedding (Winey et al., 2013). Colloidal gold particles, first proposed for use by Faulk and Taylor (1971), are conjugated to secondary antibodies that recognize and bind a primary antibody, which in turn binds the target protein or molecule. This labeling technique can be used in conjunction with both transmission EM (TEM) and scanning EM (SEM). In EM, an electron beam is passed through the prepared sample, where the electrons are absorbed and scattered (Winey et al., 2013). The high electron density of gold causes an increase in electron scatter, producing a high contrast “spot” on the image that highlights or “labels” the protein or molecule of interest. The advantages and disadvantages of each type of EM analyses are summarized by Wilson and Bacic (2012). Both TEM and SEM can provide more specific information regarding protein localization than cell fractionation, but only produce static images. TEM can distinguish intracellular details up to a resolution of 0.2 nm, but relatively lengthy traditional fixation and sample preparation methods can introduce artifacts. Likewise for SEM, dehydration can distort cellular features and produce artifacts. In addition, coating with conductive materials can thicken the sample, obscuring structural details. Sample preparation using cryo-TEM, which involves cryofixation and freeze substitution overcomes many of the problems associated with traditional fixation techniques, and results in superior preservation of cellular membranes and structures. During freeze substitution, tissues are rapidly frozen followed by replacement of ice with a fixative such as glutaraldehyde and uranyl acetate in acetone (Feder and Sidman, 1958; Giddings, 2003). Unfortunately, it requires relatively costly equipment and resulting images are low-contrast.

1.5.3 Confocal Microscopy

Confocal microscopy is a technique for imaging thin slices or planes of tissue that are then combined to reconstruct 3-dimensional images of the tissue structure (Nwaneshiudu et al., 2012). For confocal imaging, incoming light, the excitation beam, passes through an aperture to focus it on a spot inside the tissue. An image or this spot is then detected on the other side of the sample. More point images are obtained as the focal point changes in the X-Y plane and the image of a particular slice is created. In fluorescence confocal microscopy, fluorophores added to the specimen (or structure of interest) fluoresce upon stimulation by specific wavelengths of light, providing sharper imaging. Many assays, such as immunofluorescence, fluorescent stains, and BiFC (bimolecular fluorescence complementation) have been developed using this general principle. BiFC is particularly relavent for these analyses as it can be used to assess protein-protein interactions or complexes using two nonfluoresecent fragments of a normally fluorescent protein (Kerppola, 2013). Two proteins, presumed interactors, are each fused with a part of the fluorescent protein. If the proteins are true interactors, they bring the fluorescent protein fragments in vicinity of each other, causing them to associate and fluoresce.

Confocal microscopy has obvious advantages over conventional microscopy with its ability to reconstruct 3-dimensional images while providing high-resolution, high-contrast images. Since confocal microscopy uses fresh tissues, there are fewer artifacts induced by sample/slide preparation. Confocal microscopy, however, is relatively slow and expensive compared to other imaging methods. In addition, photobleaching, the irreversible fading of fluorophores over time when exposed to excitation light, limits the application of fluorescence confocal microscopy. Finally, BiFC, although a powerful technique for assessing colocalization of proteins, is too cumbersome to assess real-time formation of complexes or detect complex dissociation.

1.5.4 Mass Spectrometry in Proteomics

While other approaches still have significant advantages, mass spectrometry, particularly with the advent of more sensitive techniques and more robust analytical techniques, is becoming, if not the sole method of choice, a desirable companion approach to the methods described above. Mass spectrometry, for instance, is often coupled with various *in vitro* and *in vivo* techniques to unambiguously determine protein identity and PTMs.

Mass spectrometry allows precise measurement of the mass-to-charge ratio (*m/z*) and relative abundance of ionized analytes in the gas phase. This has many applications in proteomics, including protein identification and quantitation, peptide sequencing, PTM analysis, and identification of protein-protein interactions. Mass spectrometers consist of an ion source (ionization of proteins or peptides for analysis), a mass analyzer (measurement of *m/z*), and a detector (measurement of the number of ions or ion current at each *m/z*), which are each described in greater detail below and in several notable reviews (Aebersold and Mann, 2003; Walther and Mann, 2010).

1.5.4.1 Proteomic Approaches

Discovery-based proteomics is divided into two categories: the “bottom-up” approach and the “top-down” approach (Chait, 2006). For protein identification and sequence, as well as determination of post translational modifications (PTMs), the “bottom-up” approach is used (Aebersold and Mann, 2003). Generally, proteins are digested with an enzyme (i.e. trypsin) producing peptides that are then analyzed via mass spectrometry. The initial MS scan (MS1) produces *m/z* values and relative intensity of precursor ions of the peptides resulting from enzymatic digestion. For peptide sequencing and PTM identification, tandem mass spectrometry (MS/MS or MS^2) is required (Biemann, 1992; Papayannopoulos, 1995). This involves fragmentation (explained below) of the precursor ions to produce a set of smaller fragments called product ions, that can be used to determine the amino acid residue sequence of the peptide. Depending on the protein sequence and the enzyme(s) used to produce the original precursor ions, this approach, however, can result in the detection of an incomplete set of digested peptides. In the “top-down” approach, intact protein ions are analyzed and fragmented in the mass spectrometer, providing better protein primary structure descriptions and identification of modifications (Chait, 2006). This approach is better suited for PTM and alternative splice variant identification (Chait, 2006), but requires a mass spectrometer with high resolving power.

1.5.4.2 Data Acquisition Methods

Data-dependent acquisition (DDA) is a commonly utilized method of data selection/acquisition used in discovery-based analyses (Ducret et al., 1998). Data obtained from the MS1 scan is used to determine which peptides will be fragmented for sequence identification (Stahl et al., 1996; Egertson et al., 2013). Although DDA is a widely used acquisition strategy, it has several limitations. Since fragmentation and the resulting peptides sampled are based on relative abundance, there is a bias toward high abundance peptides. If a peptide is above the detection limit, but masked by background interference it might not be selected (Michalski et al., 2011). In addition, when the instrument is acquiring MS/MS data, precursor ion detection does not occur. This can result in further loss of peptide and protein identifications (Egertson et al., 2013). An alternative to DDA is DIA (data-independent acquisition), where peptides selected for MS/MS scans occur independently of precursor ion information (Egertson et al., 2013). There are many variations of DIA, such as ion mobility-MS (Myung 2003) as well as using wider (Venable et al., 2004) or narrower (Panchaud et al., 2009) isolation windows. Because MS/MS spectra are more complex for DIA than DDA, peptide identification can be less effective when using traditional database search strategies (Egertson et al., 2013).

1.5.4.3 Separation, Ionization, and Mass Analyzers

ESI (electrospray ionization) and MALDI (matrix-assisted laser desorption/ionization) are two common ionization techniques used in MS analyses (Aebersold and Mann, 2003). For ESI a high voltage is applied to a solution to ionize analytes (Fenn et al., 1989), whereas for MALDI, a laser is used to sublimate and ionize analytes from a dry, crystalline matrix (Karas and Hillenkamp, 1988). Liquid-chromatography (LC), and other liquid-based separation methods, are frequently coupled to a mass spectrometer (LC-MS) via ESI to provide additional separation of components and thus simplify analysis of complex samples (Aebersold and Mann, 2003). There are four main types of mass analyzers: ion trap, time-of-flight (TOF), quadrapole, and Fourier transform ion cyclotron (FT-MS) (Aebersold and Mann, 2003). Like choosing an ion source, the type of mass analyzer used depends on the analysis, with all options having advantages and disadvantages. TOF analyzers are often coupled to a MALDI ion source (MALDI-TOF) for analysis of intact peptides, whereas ESI is more frequently used in combination with ion traps and triple quadrapole instruments for peptide fragmentation analysis, known as tandem mass spectrometry (MS/MS or MS^2) (Aebersold and Goodlett, 2001; Aebersold and Mann, 2003).

The current hybrid mass analyzers, combining the capabilities of individual mass analyzers, include the linear ion trap-Orbitrap, the quadrapole-Orbitrap, and the quadrupole-ion trap-Orbitrap (Perry et al., 2008; Zubarev and Makarov, 2013; Senko et al., 2013).

1.5.4.4 Fragmentation Methods

There are a number of methods available for peptide fragmentation; commonly used modes being CID (collision-induced dissociation), ETD (electron-transfer dissociation), and HCD (high-energy collisional dissociation) (Guthals and Bandeira, 2012). CID/HCD and ETD are considered complementary techniques for several reasons.

In CID, the collision of gas molecules with peptides results in a vibrational excitement that dissociates amide bonds between the carbonyl and amine groups (Molina et al., 2008). Fragments that include the N-terminus and C-terminus of the peptide are termed b-ions and y-ions, respectively (Roepstorff and Fohlman, 1984). During HCD, which can be performed on orbitrap instruments, precursor ions are transferred into what is termed the C-trap, where ions are normally stored from an ion trap, which traps ions in an electrostatic field, on the way to the orbitrap, an orbital ion trap (Makarov, 2000; Olsen et al., 2007). In the C-trap, peptides undergo higher energy collisional dissociation events with nitrogen, or another neutral gas using radiofrequency voltages for peptide fragmentation (Olsen et al., 2007). HCD fragmentation results in b-ions and y-ions, as well as immonium ions (Olsen et al., 2007) that have the general structure $RCH=NH_2^+$ (Hohmann et al., 2008). In ETD, radical anions are generated by ion/ion reactions that results in an electron transfer reaction that converts positively charged peptides into peptide cation radicals. This peptide fragmentation requires more reaction time relative to CID and HCD (Syka et al., 2004). The instability of these radicals results in fragmentation of the peptides, with dissociation occurring between amide nitrogen and α-carbons in the peptide backbone (Syka et al., 2004; Molina et al., 2008), creating product ions containing either the N-terminus or the C-terminus of the peptide, or c-ions or z-ions, respectively (Roepstorff and Fohlman, 1984). CID and HCD are more commonly used in peptide sequencing, while the use of ETD is more advantageous for PTM identifications (Kim and Pandey, 2012). ETD, unlike CID and HCD, does not cleave the most labile bond first and is considered a “soft” fragmentation method, making it superior for PTM analyses (Syka et al., 2004). On the other hand, HCD produces higher quality spectra than CID and so is more often used in proteomics studies (Jedrychowski et al., 2011).

1.5.5 Summary

As discussed above, each approach described in Sections 1.5.1 to 1.5.4 is capable of producing useful analyses of a specific aspect of protein localization and trafficking. A combination of methods is, however, necessary to construct a complete picture of trafficking at any particular stage of protein secretion. In Cheng et al. (2009b), MTD secretion in response to SA was evaluated using immunoEM, immunoblotting, immunotitration, and enzyme activity assays. EM imaging showed MTD relocalization in response to treatment. Immunoblotting confirmed that MTD was being secreted into the media from the cytosol and immunotitration and enzyme activity assays showed that MTD was still a functional protein. These three techniques together were required to produce the data necessary to rigorously validate both the secretion of cytosolic MTD in response to SA and the functionality of the secreted MTD. In the work presented in this thesis, a combination of analytical methods, particularly crosslinking and MS analysis, is likewise necessary to construct and assess a hypothesis describing a mechanism for the unconventional secretion of MTD.

1.6 References

Aebersold R, Goodlett DR (2001) Mass spectrometry in proteomics. Chem Rev **101**:269-296

Aebersold R, Mann M (2003) Mass spectrometry-based proteomics. Nature **422**:198–207

Anderegg RJ, Betz R, Carr SA, Crabb JW, Duntze W (1988) Structure of *Saccharomyces cerevisiae* mating hormone a-factor. J Biol Chem **263**:18236-18240

Andrei C, Dazzi C, Lotti L, Torrisi MR, Chimini G, Rubartelli A (1999) The secretory route of the leaderless protein interleukin 1β Involves exocytosis of endolysosome-related vesicles. Mol Biol Cell **10**:1463-1475

Andrei C, Margiocco P, Poggi A, Lotti LV, Torrisi MR, Rubartelli A (2004) Phospholipases C and A2 control lysosome-mediated IL-1β secretion: implications for inflammatory processes. Proc Natl Acad Sci USA **101**:9745-9750

Anjard C, Loomis WF (2005) Peptide Signaling during terminal differentiation of *Dictyostelium*. Proc Natl Acad Sci USA **102**:7607-7611

Auron PE, Webb AC, Rosenwasser LJ, Mucci SF, Rich A, Wolff SM, Dinarello CA (1984) Nucleotide sequence of human monocyte interleukin 1 precursor cDNA. Proc Natl Acad Sci USA **81**:7907-7911

Axe EL, Walker SA, Manifava M, Chandra P, Roderick HL, Habermann A, Griffiths G, Ktistakis N (2008) Autophagosome formation from membrane compartments enriched in phosphatidylinositol 3-phosphate and dynamically connected to the endoplasmic reticulum. J Cell Biol **182**:685-701

Backhaus R, Zehe C, Wegehingel S, Kehlenbach A, Schwappach B, Nickel W (2004) Unconventional protein secretion: membrane translocation of FGF-2 does not require protein unfolding. J Cell Sci **117**:1727-1736

Baldwin TA, Ostergaard HL (2002) The protein-tyrosine phosphatase CD45 reaches the cell surface via golgi-dependent and -independent pathways. J Biol Chem **277**:50333-50340

Barr FA, Puype M, Vandekerckhove J, Warren G (1997) GRASP65, a protein involved in the stacking of golgi cisternae. Cell **91**:253-262

Becker T, Böttinger L, Pfanner N (2012) Mitochondrial protein import: from transport pathways to an integrated network. Trends Biochem Sci **37**:85-91

Biemann K (1992) Mass spectrometry of peptides and proteins. Annu Rev Biochem **61**:977-1010

Birgisdottir ÅB, Lamark T, Johansen T (2013) The LIR motif - crucial for selective autophagy. J Cell Sci **126**:3237-3247

Bjørkøy G, Lamark T, Brech A, Outzen H, Perander M, Øvervatn A, Stenmark H, Johansen T (2005) p62/SQSTM1 forms protein aggregates degraded by autophagy and has a protective effect on huntingtin-induced cell death. J Cell Biol **171**:603-614

Bolwell PG (1999) Role of active oxygen species and NO in plant defence responses. Curr Opin Plant Biol **2**:287-294

Bolwell PG, Bindschedler LV, Blee KA, Butt VS, Davies DR, Gardner SL, Gerrish C, Minibayeva F (2002) The apoplastic oxidative burst in response to biotic stress in plants: a three-component system. J Exp Bot **53**:1367-1376

Braakman I, Bulleid NJ (2011) Protein folding and modification in the mammalian endoplasmic reticulum. Annu Rev Biochem **80**:71-99

Braakman I, Hebert DN (2013) Protein folding in the endoplasmic reticulum. Cold Spring Harb Perspect Biol **5**:a013201/1-17

Brandizzi F, Barlowe C (2013) Organization of the ER-golgi interface for membrane traffic control. Nat Rev Mol Cell Biol **14**:382-392

Bruns C, McCaffery JM, Curwin AJ, Duran JM, Malhotra V (2011) Biogenesis of a novel compartment for autophagosome-mediated unconventional protein secretion. J Cell Biol **195**:979-992

Campelo F, Malhotra V (2012) Membrane fission: the biogenesis of transport carriers. Annu Rev Biochem **81**:407-427

Cancino J, Jung JE, Luini A (2013) Regulation of golgi signaling and trafficking by the KDEL receptor. Histochem Cell Biol **140**:395-405

Capitani M, Sallese M (2009) The KDEL receptor: new functions for an old protein. FEBS Lett **583**:3863-3871

Chait BT (2006) Mass spectrometry: bottom-up or top-down. Science **214**:65-66

Chen YA, Scheller RH (2001) Snare-mediated membrane fusion. Nat Rev Mol Cell Biol **2**:98-106

Cheng FY, Blackburn K, Lin YM, Goshe MB, Williamson JD (2009a) Absolute protein quantification by LC/MS^E for global analysis of salicylic acid-induced plant protein secretion responses. J Proteome Res **8**:82-93

Cheng FY, Zamski E, Guo WW, Pharr DM, Williamson JD (2009b) Salicylic acid stimulates secretion of the normally symplastic enzyme mannitol dehydrogenase: a possible defense against mannitol-secreting fungal pathogens. Planta **230**:1093-1103

Chrispeels MJ, Raikhel NV (1991) Lectins, lectin genes, and their role in plant defense. Plant Cell **3**:1-9

Christensen PU, Davey J, Nielsen O (1997) The *Schizosaccharomyces pombe* mam1 gene encodes an ABC transporter mediating secretion of M-factor. MGG **255**:226-236

Coleman C, Herman EM, Takasaki K, Larkins BA (1996) The maize γ-zein sequesters α-zein and stabilizes its accumulation in protein bodies of transgenic tobacco endosperm. Plant Cell **8**:2335-2345

Conner SD, Schmid SL (2003) Regulated portals of entry into the cell. Nature **422**:37-44

Contento AL, Xiong Y, Bassham DC (2005) Visualization of autophagy in *Arabidopsis* using the fluorescent dye monodansylcadaverine and a GFP-AtATG8e fusion protein. Plant J **42**:598-608

Corpas FJ, Barroso JB, del Río LA (2001) Peroxisomes as a source of reactive oxygen species and nitric oxide signal molecules in plant cells. Trends Plant Sci **6**:145-150

Cross BCS, Sinning I, Luirink J, High S (2009) Delivering proteins for export from the cytosol. Nat Rev Mol Cell Biol **10**:225-264

De Marchis F, Bellucci M, Pompa A (2013) Unconventional pathways of secretory plant proteins from the endoplasmic reticulum to the vacuole bypassing the golgi complex. Plant Signal Behav **8**:25129/1-5

De Matteis MA, Luini A (2008) Exiting the golgi complex. Nat Rev Mol Cell Biol **9**:273-284

Denny PW, Gokool S, Russell DG, Field MC, Smith DF (2000) Acylation-dependent protein export in *Leishmania*. J Biol Chem **275**:11017-11025

Ding Y, Robinson DG, Jiang L (2014a) Unconventional protein secretion (UPS) pathways in plants. Curr Opin Cell Biol **29**:107-115

Ding Y, Wang J, Lai JHC, Chan VHL, Wang X, Cai Y, Tan X, Bao Y, Xia J, Robinson DG, Jiang L (2014b) Exo70E2 is essential for exocyst subunit recruitment and EXPO formation in both plants and animals. Mol Biol Cell **25**:412-426

Doherty GJ, McMahon HT (2009) Mechanisms of endocytosis. Annu Rev Biochem **78**:857-902

Drakakaki G, Dandekar A (2013) Protein secretion: How many secretory routes does a plant cell have? Plant Sci **203-204**:74-78

Ducret A, van Oostveen I, Eng JK, Yates JR III (1998) High throughput protein characterization by automated reverse-phase chromatography/electrospray tandem mass spectrometry. Protein Sci **7**:706-719

Duden R (2003) ER-to-golgi transport: COP I and COP II function (Review). Mol Membr Biol **20**:197-207

Duran JM, Anjard C, Stefan C, Loomis WF, Malhotra V (2010) Unconventional secretion of Acb 1 is mediated by autophagosomes. J Cell Biol **188**:527-536

Ebert AD, Laußmann M, Wegehingel S, Kaderali L, Erfle H, Reichert J, Lechner J, Beer JD, Pepperkok R, Nickel W (2010) Tec-kinase-mediated phosphorylation of fibroblast growth factor 2 is essential for unconventional secretion. Traffic **11**:813-826

Egertson JD, Kuehn A, Merrihew GE, Bateman NW, MacLean BX, Ting YS, Canterbury JD, Marsh DM, Kellmann M, Zabrouskov V, Wu CC, MacCoss MJ (2013) Multiplexed MS/MS for improved data-independent acquisition. Nat Methods **10**:744-748

Fabrikant G, Lata S, Riches JD, Briggs JAG, Weissenhorn W, Kozlov MM (2009) Computational model of membrane fission catalyzed by ESCRT-III. PLoS Comput Biol **5**:1000575/1-11

Faham S, Hileman RE, Fromm JR, Linhardt RT, Rees DC (1996) Heparin structure and interactions with basic fibroblast growth factor. Science **271**:1116-1120

Faham S, Linhardt RJ, Rees DC (1998) Diversity does make a difference: fibroblast growth factor-heparin interactions. Curr Opin Struct Biol **8**:578-586

Fatal N, Karhinen L, Jokitalo E, Makarow M (2004) Active and specific recruitment of a soluble cargo protein for endoplasmic reticulum exit in the absence of functional COPII component Sec24p. J Cell Sci **117**:1665-1673

Faulk PW, Taylor MG (1971) Communication to the editors an immunocolloid method for the electron microscope. Immunochemistry **8**:1081-1083

Feder N, Sidman RL (1958) Methods and principles of fixation by freeze-substitution. J Biophysic and Biochem Cytol **4**:593-602

Fenn JB, Mann M, Meng CK, Wong SF, Whitehouse CM (1989) Electrospray Ionization for mass spectrometry of large biomolecules. Science **246**:64-71

Flores-Pérez Ú, Jarvis P (2013) Molecular chaperone involvement in chloroplast protein import. Biochim Biophys Acta **1833**:332-340

Galili G, Altschuler Y, Levanony H (1993) Assembly and transport of seed storage proteins. Trends Cell Biol **3**:437-442

Gao C, Cai Y, Wang Y, Kang BH, Aniento F, Robinson DG, Jiang L (2014) Retention mechanisms for ER and golgi membrane proteins. Trends Plant Sci **19**:508-515

Gee HY, Noh SH, Tang BL, Kim KH, Lee MG (2011) Rescue of ΔF508-CFTR trafficking via a GRASP-dependent unconventional secretion pathway. Cell **146**:746-760

Giddings TH (2003) Freeze-substitution protocols for improved visualization of membranes in high-pressure frozen samples. J Microsc **212**:53-61

Gierasch LM (1989) Signal sequences. Biochemistry **28**:923-930

Gillon AD, Latham CF, Miller EA (2012) Vesicle-mediated ER export of proteins and lipids. Biochim Biophys Acta **1821**:1040-1049

Gomez L, Chrispeels MJ (1993) Tonoplast and soluble vacuolar proteins are targeted by different mechanisms. Plant Cell **5**:1113-1124

Grant BD, Donaldson JG (2009) Pathways and mechanisms of endocytic recycling. Nat Rev Mol Cell Biol **10**:597-608

Guo W, Grant A, Novick P (1999) Exo84p is an exocyst protein essential for secretion. J Biol Chem **274**:23558-23564

Guthals A, Bandeira N (2012) Peptide identification by tandem mass spectrometry with alternate fragmentation modes. MCP **11**:550-557

Halic M, Beckmann R (2005) The signal recognition particle and its interactions during protein targeting. Curr Opin Struct Biol **15**:116-125

Hara-Nishimura I, Hatsugai N (2011) The role of vacuole in plant cell death. Cell Death Differ **18**:1298-1304

Hara T, Takamura A, Kishi C, Iemura SI, Natsume T, Guan JL, Mizushima N (2008) FIP200, a ULK-interacting protein, is required for autophagosome formation in mammalian cells. J Cell Biol **181**:497-510

Hatsugai N, Hara-Nishimura I (2010) Two vacuole-mediated defense strategies in plants. Plant Signal Behav **5**:1568-1570

Hatsugai N, Iwasaki S, Tamura K, Kondo M, Fuji K, Ogasawara K, Nishimura M, Hara-Nishimura I (2009) A novel membrane fusion-mediated plant immunity against bacterial pathogens. Genes Dev **23**:2496-2506

Hayashi Y, Yamada K, Shimada T, Matsushima R, Nishizawa N, Mikio N, Hara-Nishimura I (2001) A proteinase-storing body that prepares for cell death or stresses in the epidermal cells of *Arabidopsis*. Plant Cell Physiol **42**:894-899

Hayes MJ, Merrifield CJ, Shao D, Ayala-Sanmartin J, D'Souza Schorey C, Levine TP, Proust J, Curran J, Bailly M, Moss SE (2004) Annexin 2 binding to phosphatidylinositol 4,5-bisphosphate on endocytic vesicles is regulated by the stress response pathway. J Biol Chem **279**:14157-14164

Hayes MJ, Shao DM, Grieve A, Levine T, Bailly M, Moss SE (2009) Annexin A2 at the interface between F-actin and membranes enriched in phosphatidylinositol 4,5,-bisphosphate. Biochim Biophys Acta **1793**:1086-1095

He C, Klionsky DJ (2009) Regulation mechanisms and signaling pathways of autophagy. Annu Rev Genet **43**:67-93

Hegde R, Bernsteir H (2006) The surprising complexity of signal sequences. Trends Biochem Sci **31**:563-571

Heider MR, Munson M (2012) Exorcising the exocyst complex. Traffic **13**:898-907

Henne WM, Buchkovich NJ, Emr SD (2011) The ESCRT pathway. Dev Cell **21**:77-91

Hernández JA, Ferrer MA, Jiménez A, Barceló AR, Sevilla F (2001) Antioxidant systems and O2.-/H2O2 production in the apoplast of pea leaves. It's relation with salt-induced necrotic lesions in minor veins. Plant Physiol **127**:817-831

Higgins CF (2007) Multiple molecular mechanisms for multidrug resistance transporters. Nature **446**:749-757

Hohmann LJ, Eng JK, Gemill A, Klimek J, Vitek O, Reid GE, Martin DB (2008) Quantification of the compositional information provided by immonium ions on a quadrupole-time-of-flight mass spectrometer. Anal Chem **80**:5596-5606

Hollenstein K, Dawson RJP, Locher KP (2007) Structure and mechanism of ABC transporter proteins. Curr Opin Struct Biol **17**:412-418

Honig A, Avin-Wittenberg T, Ufaz S, Galili G (2012) A new type of compartment, defined by plant-specific Atg8-interacting proteins, is induced upon exposure of *Arabidopsis* plants to carbon starvation. Plant Cell **24**:288-303

Hsu SC, Ting AE, Hazuka CD, Davanger S, Kenny JW, Kee Y, Scheller RH (1996) The mammalian brain rsec6/8 complex. Neuron **17**:1209-1219

Huotari J, Helenius A (2011) Endosome maturation. EMBO J **30**:3481-3500

Hwang I, Robinson DG (2009) Transport vesicle formation in plant cells. Curr Opin Plant Biol **12**:660-669

Hyman SE (2005) Neurotransmitters. Curr Biol **15**:R154-R158

Isayenkov S, Isner JC, Maathuis FJM (2011) Rice two-pore K^+ channels are expressed in different types of vacuoles. Plant Cell **23**:756-768

Itakura E, Kishi C, Inoue K, Mizushima N (2008) Beclin 1 forms two distinct phosphatidylinositol 3-kinase complexes with mammalian Atg14 and UVRAG. Mol Biol Cell **19**:5360-5372

Jäger S, Bucci C, Tanida I, Ueno T, Kominami E, Saftig P, Eskelinen EL (2004) Role for Rab7 in maturation of late autophagic vacuoles. J Cell Sci **117**:4837-4848

Jedrychowski MP, Huttlin EL, Haas W, Sowa ME, Rad R, Gygi SP (2011) Evaluation of HCD- and CID-type fragmentation within their respective detection platforms for murine phosphoproteomics. MCP **10**:M111.009910/1-9

Jennings DB, Ehrenshaft M, Pharr MD, Williamson JD (1998) Roles for mannitol and mannitol dehydrogenase in active oxygen-mediated plant defense. Proc Natl Acad Sci USA **95**:15129-15133

Jiang S, Dupont N, Castillo EF, Deretic V (2013) Secretory versus degradative autophagy: unconventional secretion of inflammatory mediators. J Innate Immun **5**:471-479

Jung CH, Jun CB, Ro SH, Kim YM, Otto MN, Cao J, Kundu M, Kim DH (2009) ULK-Atg13-FIP200 complexes mediate mTOR signaling to the autophagy machinery. Mol Biol Cell **20**:1992-2003

Jüschke C, Wächter A, Schwappach B, Seedorf M (2005) SEC18 /NSF-independent, protein-sorting pathway from the yeast cortical ER to the plasma membrane. J Cell Biol **169**:613-622

Kang R, Zeh HJ, Lotze MT, Tang D (2011) The Beclin 1 network regulates autophagy and apoptosis. Cell Death Differ **18**:571-580

Karas M, Hillenkamp F (1988) Laser desorption ionization of proteins with molecular masses exceeding 10,000 daltons. Anal Chem **60**:2299-2301

Karpinska B, Karlsson M, Schinkel H, Streller S, Süss KH, Melzer M, Wingsle G (2001) A novel superoxide dismutase with a high isoelectric point in higher plants. expression, regulation, and protein localization. Plant Physiol **126**:1668-1677

Keller M, Rüegg A, Werner S, Beer HD (2008) Active caspase-1 is a regulator of unconventional protein secretion. Cell **132**:818-831

Kerppola TK (2013) Design of fusion proteins for bimolecular fluorescence complementation (BiFC). CSH Protoc **2013**:714-719

Kiedrowski S, Kawalleck P, Hahlbrock K, Somssich IE, Dangl JL (1992) Rapid activation of a novel plant defense gene is strictly dependent on the *Arabidopsis* RPM1 disease resistance locus. EMBO J **11**:4677-4684

Kienzle C, von Blume J (2014) Secretory cargo sorting at the *trans*-golgi network. Trends Cell Biol **24**:584-593

Kihara A, Noda T, Ishihara N, Ohsumi Y (2001) Two distinct Vps34 phosphatidylinositol 3-kinase complexes function in autophagy and carboxypeptidase Y sorting in *Saccharomyces cerevisiae*. J Cell Biol **152**:519-530

Kim CS, Woo YM, Clore AM, Burnett RJ, Carneiro NP, Larkins BA (2002) Zein protein interactions, rather than the asymmetric distribution of Zein mRNAs on endoplasmic reticulum membranes, influence protein body formation in maize endosperm. Plant Cell **14**:655-672

Kim MS, Pandey A (2012) Electron transfer dissociation mass spectrometry in proteomics. Proteomics **12**:530-542

Kim PK, Hailey DW, Mullen RT, Lippincott-Schwartz J (2008) Ubiquitin signals autophagic degradation of cytosolic proteins and peroxisomes. Proc Natl Acad Sci USA **105**:20567-20574

Kinseth MA, Anjard C, Fuller D, Guizzunti G, Loomis WF, Malhotra V (2007) The golgi-associated protein GRASP is required for unconventional protein secretion during development. Cell **130**:524-534

Kirisako T, Ichimura Y, Okada H, Kabeya Y, Mizushima N, Yoshimori T, Ohsumi M, Takao T, Noda T, Ohsumi Y (2000) The reversible modification regulates the membrane-binding state of Apg8/Aut7 essential for autophagy and the cytoplasm to vacuole targeting pathway. J Cell Biol **151**:263-275

Klionsky DJ (2005) The molecular machinery of autophagy: unanswered questions. J Cell Sci **118**:7-18

Kuchler K, Sterne RE, Thorner J (1989) *Saccharomyces cerevisiae* STE6 gene product: a novel pathway for protein export in eukaryotic cells. EMBO J **8**:3973-3984

Lee DW, Jung C, Hwang I (2013) Cytosolic events involved in chloroplast protein targeting. Biochim Biophys Acta **1833**:245-252

Lee MCS, Miller EA, Goldberg J, Orci L, Schekman R (2004) Bi-directional protein transport between the ER and golgi. Annu Rev Cell Dev Biol **20**:87-123

Lemus L, Goder V (2014) Regulation of endoplasmic reticulum-associated protein degradation (ERAD) by ubiquitin. Cell **3**:824-847

Lenz M, Crow DJG, Joanny JF (2009) Membrane buckling induced by curved filaments. Phys Rev Lett **103**:38101/1-4

Levanony H, Rubin R, Altschuler Y, Galili G (1992) Evidence for a novel route of wheat storage proteins to vacuoles. J Cell Biol **119**:1117-1128

Levine B, Klionsky DJ (2004) Development by self-digestion: molecular mechanisms and biological functions of autophagy. Dev Cell **6**:463-477

Liang XH, Jackson S, Seaman M, Brown K, Kempkes B, Hibshoosh H, Levine B (1999) Induction of autophagy and inhibition of tumorigenesis by beclin 1. Nature **402**:672-676

Liu Y, Bassham DC (2012) Autophagy: pathways for self-eating in plant cells. Annu Rev Plant Biol **63**:215-237

Luirink J, Sinning I (2004) SRP-mediated protein targeting: structure and function revisited. Biochim Biophys Acta **1694**:17-35

Mackenzie A, Wilson HL, Kiss-Toth E, Dower SK, North RA, Surprenant A (2001) Rapid secretion of interleukin-1β by microvesicle shedding. Immunity **15**:825-835

Makarov A (2000) Electrostatic axially harmonic orbital trapping: a high-performance technique of mass analysis. Anal Chem **72**:1156-1162

Malamy J, Carr JP, Klessig DF, Raskin I (1990) Salicylic acid: a likely endogenous signal in the resistance response of tobacco to viral infection. Science **250**:1002-1004

Manjithaya R, Anjard C, Loomis WF, Subramani S (2010) Unconventional secretion of *Pichia pastoris* Acb 1 is dependent on GRASP protein, peroxisomal functions, and autophagosome formation. J Cell Biol **188**:537-546

Marie M, Dale HA, Sannerud R, Saraste J (2009) The function of the intermediate compartment in pre-golgi trafficking involves its stable connection with the centrosome. Mol Biol Cell **20**:4458-4470

Matsunaga K, Morita E, Saitoh T, Akira S, Ktistakis NT, Lzumi T, Noda T, Yoshimori T (2010) Autophagy requires endoplasmic reticulum targeting of the PI3-kinase complex via Atg14L. J Cell Biol **190**:511-521

McGaha SM, Champney SW (2007) Hygromycin B inhibition of protein synthesis and ribosome biogenesis in *Escherichia Coli*. Antimicrob Agents Chemother **51**:591-596

McGarth JP, Varshavsky A (1989) The yeast STE6 gene encodes a homologue of the mammalian multidrug resistance P-glycoprotein. Nature **340**:400-404

Michaeli S, Avin-Wittenberg T, Galili G (2014a) Involvement of autophagy in the direct ER to vacuole protein trafficking route in plants. Front Plant Sci **5**:134/1-5

Michaeli S, Simon; Honig A, Levanony H, Peled-Zehavi H, Galili G (2014b) *Arabidopsis* ATG8-interacting protein1 is Involved in autophagy-dependent vesicular trafficking of plastid proteins to the vacuole. Plant Cell **26**:4084-4101

Michaelis S (1993) STE-6, the yeast a-factor transporter. Semin Cell Biol **4**:17-27

Michalski A, Cox J, Mann M (2011) More than 100,000 detectable peptide species elute in single shotgun proteomics runs but the majority if inaccessible to data-dependent LC/MS/MS. J Proteome Res **10**:1785-1793

Miki B, McHugh S (2004) Selectable marker genes in transgenic plants: applications, alternatives and biosafety. J Biotechnol **107**:193-232

Molina H, Matthiesen R, Kandasamy K, Pandey A (2008) Comprehensive comparison of collision induced dissociation and electron transfer dissociation. Anal Chem **80**:4825-4835

Mollenhauer HH, Morré JD, Rowe LD (1990) Alteration of intracellular traffic by monensin; mechanism, specificity and relationship to toxicity. Biochim Biophys Acta **1031**:225-246

Moremen KW, Tiemeyer M, Nairn AV (2012) Vertebrate protein glycosylation: diversity, synthesis and function. Nat Rev Mol Cell Biol **13**:448-462

Mori T, Maruyama N, Nishizawa K, Higasa T, Yagasaki K, Ishimoto M, Utsumi S (2004) The composition of newly synthesized proteins in the endoplasmic reticulum determines the transport pathways of soybean seed storage proteins. Plant J **40**:238-249

Mosavi LK, Cammett TJ, Desrosiers DC, Peng ZY (2004) The ankyrin repeat as molecular architecture for protein recognition. Protein Sci **13**:1435-1448

Möskes C, Burghaus PA, Wernli B, Sauder U, Dürrenberger M, Kappes B (2004) Export of *Plasmodium falciparum* calcium-dependent protein kinase 1 to the parasitophorous vacuole is dependent on three N-terminal membrane anchor motifs. Mol Microbiol **54**:676-691

Myung S, Lee YJ, Moon MH, Taraszka J, Sowell R, Koeniger S, Hilderbrand AE, Valentine SJ, Cherbas L, Kaufmann TC, Miller DF, Mechref Y, Novotny MV, Ewing MA, Sporleder RC, Clemmer DE (2003) Development of high-sensitivity ion trap ion mobility spectrometry time-of-flight techniques: a high-throughput Nano-LC-IMS-TOF separation of peptides arising from a *drosophila* protein extract. Anal Chem **75**:5137-5145

Nakano A, Luini A (2010) Passage through the golgi. Curr Opin Cell Biol **22**:471-478

Neill S, Desikan R, Hancock J (2002) Hydrogen peroxide signaling. Curr Opin Plant Biol **5**:388-395

Neupert W, Herrmann JM (2007) Translocation of proteins into mitochondria. Annu Rev Biochem **76**:723-749

Nezis IP, Simonsen A, Sagona AP, Finley K, Gaumer S, Contamine D, Rusten TE, Stenmark H, Brech A (2008) Ref(2)P, the *Drosophila melanogaster* homologue of mammalian p62, is required for the formation of protein aggregates in adult brain. J Cell Biol **180**:1065-1071

Nice DC, Sato TK, Stromhaug PE, Emr SD, Klionsky DJ (2002) Cooperative binding of the cytoplasm to vacuole targeting pathway proteins, Cvt13 and Cvt20, to phosphatidylinositol 3-phosphate at the pre-autophagosomal structure is required for selective autophagy. J Biol Chem **277**:30198-30207

Nickel W (2010) Pathways of unconventional protein secretion. Curr Opin Biotechnol **21**:621-626

Nickel W (2007) Unconventional secretion: an extracellular trap for export of fibroblast growth factor 2.J Cell Sci **120**:295-2299

Nickel W (2011) The unconventional secretory machinery of fibroblast growth factor 2. Traffic **12**:799-805

Nickel W, Rabouille C (2009) Mechanisms of regulated unconventional protein secretion. Nat Rev Mol Cell Biol **10**:148-155

Noda NN, Yoshinori O, Inagaki F (2010) Atg8-family interacting motif crucial for selective autophagy. FEBS Lett **584**:1379-1385

Nwaneshiudu A, Kuschal C, Sakamoto FH, Anderson RR (2012) Introduction to confocal microscopy. J Invest Dermatol **132**:1-5

Obara K, Sekito T, Niimi K, Ohsumi Y (2008) The Atg18-Atg2 complex is recruited to autophagic membranes via phosphatidylinositol 3-phosphate and exerts an essential function. J Biol Chem **283**:23972-23980

O'Leary BM, Rico A, McCraw S, Fones HN, Preston GM (2014) The infiltration-centrifugation technique for extraction of apoplastic fluid from plant leaves using *Phaseolus vulgaris* as an example. J Vis Exp **19**:94

Olsen JV, Nacek B, Lange O, Makarov A, Horning S, Mann M (2007) Higher-energy C-trap dissociation for peptide modification analysis. Nat Methods **4**:709-712

Panchaud A, Scherl A, Shaffer SA, Haller PD, Kulasekara HD, Miller SI, Goodlett DR (2009) Precursor acquisition independent from ion count: how to dive deeper into the proteomics ocean. Anal Chem **81**:6481-6488

Pankiv S, Clausen TH, Lamark T, Brech A, Bruun JA, Outzen H, Øvervatn A, Bjørkøy G, Johansen T (2007) p62/SQSTM1 binds directly to Atg8/LC3 to facilitate degradation of ubiquitinated protein aggregates by autophagy. J Biol Chem **282**:24131-24145

Papayannopoulos IA (1995) The interpretation of collision-induced dissociation tandem mass spectra of peptides. Mass Spectrom Rev **14**:49-73

Pardo N, de Dios Alche J, Casado-Vela J, Mas S, Villalba M, Rodriguez R, Batanero E (2014) Nanovesicles are secreted during pollen germination and pollen tube growth: a possible role in fertilization. Mol Plant **7**:573-577

Paris N, Stanley MC, Jones RL (1996) Plant cells contain two functionally distinct vacuolar compartments. Cell **85**:563-572

Patel T, Williamson JD (2016) Mannitol in Plants, Fungi, and Plant-Fungal Interactions. Trends Plant Sci http://dx.doi.org/10.1016/j.tplants.2016.01.006

Patterson GH, Hirschberg K, Polishchuk RS, Gerlich D, Phair RD, Lippincott-Schwartz J (2008) Transport through the golgi apparatus by rapid partitioning within a two-phase membrane system. Cell **133**:1055-1067

Pelham HRB (2001) SNAREs and the specificity of membrane fusion. Trends Cell Biol **11**:99-101

Pellegrini L, Burke DF, von Delft F, Mulloy B, Blundell TL (2000) Crystal structure of fibroblast growth factor receptor ectodomain bound to ligand and heparin. Nature **407**:1029-1034

Perry RH, Cooks GR, Noll RJ (2008) Orbitrap mass spectrometry: instrumentation, ion motion and applications. Mass Spectrom Rev **27**:661-669

Petrilli V, Papin S, Tschopp J (2005) The inflammasome. Curr Biol **15**:R581

Pinedo M, Regente M, Elizalde M, Quiroga IY, Pagnussat LA, Jorrín-Novo J, Maldonado A, de la Canal L (2012) Extracellular sunflower proteins: evidence on non-classical secretion of a jacalin-related lectin. Protein Pept Lett **19**:270-276

Pittenger RC, Wolfe RN, Hoehn MM, Marks PN, Daily WA, McGuire JM (1953) Hygromycin. I. Preliminary studies on the production and biologic activity of a new antibiotic. Antibiot Chemother **3**:1268-1278

Pohl C, Jentsch S (2009) Midbody ring disposal by autophagy is a post-abscission event of cytokinesis. Nat Cell Biol **11**:65-70

Prydz K, Tveit H, VedelerA, Saraste J (2013) Arrivals and departures at the plasma membrane: direct and indirect transport routes. Cell Tissue Res **352**:5-20

Qu Y, Franchi L, Nunez G, Dubyak GR (2007) Nonclassical IL-1β secretion stimulated by P2X7 receptors is dependent on inflammasome activation and correlated with exosome release in murine macrophages. J Immunol **179**:1913-1925

Rabouille C, Malhotra V, Nickel W (2012) Diversity in unconventional protein secretion. J Cell Sci **125**:5251-5255

Raman R, Venkataraman G, Ernst S, Sasisekharan V, Sasisekharan R (2003) Structural specificity of heparin binding in the fibroblast growth factor family of proteins. Proc Natl Acad Sci USA **100**:2357-2362

Rao SV, Srinivas K, Sujini GN, Kumar SGN (2014) Protein-protein interaction detection: methods and analysis. Int J Proteomics **2014**:1-12

Regente M, Monzón GC, de la Canal L (2008) Phospholipids are present in extracellular fluids of imbibing sunflower seeds and are modulated by hormonal treatments. J Exp Bot **59**:553-562

Regente M, Monzón GC, Maldonado AM, Pinedo M, Jorrín J, de la Canal L (2009) Vesicular fractions of sunflower apoplastic fluids are associated with potential exosome marker proteins. FEBS Lett **583**:3363-3366

Regente M, Pinedo M, Elizalde M, de la Canal L (2012) Apoplastic exosome-like vesicles: a new way of protein secretion in plants? Plant Signal Behav **7**:544-546

Rescher U, Ruhe D, Ludwig C, Zobiack N, Gerke V (2004) Annexin 2 is a phosphatidylinositol (4,5)-bisphosphate binding protein recruited to actin assembly sites at cellular membranes. J Cell Sci **117**:3473-3480

Resh MD (1999) Fatty acylation of proteins: new insights into membrane targeting of myristoylated and palmitoylated proteins. Biochim Biophys Acta **1451**:1-16

Reyes FC, Buono R, Otegui M (2011a) Plant endosomal trafficking pathways. Curr Opin Plant Biol **14**:666-673

Reyes FC, Chung T, Holding D, Jung R, Vierstra R, Otegui MS (2011b) Delivery of prolamins to the protein storage vacuole in maize aleurone cells. Plant Cell **23**:769-784

Ricardo S, Lehmann R (2009) An ABC transporter controls export of a *Drosophila* germ cell attractant. Science **323**:943-946

Richter S, Voß U, Jürgens G (2009) Post-golgi traffic in plants. Traffic **10**:849-828

Rivera-Serrano E, Rodriguez-Welsh MF, Hicks GR, Rojas-Pierce M (2012) A small molecule inhibitor partitions two distinct pathways for trafficking of tonoplast intrinsic proteins in *Arabidopsis*. PloS One **7**:44735/1-11

Robinson DG, Pimpl P (2014) Clathrin and post-golgi trafficking: a very complicated issue. Trends Plant Sci **19**:134-139

Roepstorff P, Fohlman J (1984) Proposal for a common nomenclature for sequence ions in mass spectra of peptides. Biomed Mass Spectrom **11**:601

Rojas-Pierce M (2013) Targeting of tonoplast proteins to the vacuole. Plant Sci **211**:132-136

Rubartelli A, Cozzolino F, Talio M, Sitia R (1990) A novel secretory pathway for interleukin - 1β, a protein lacking a signal sequence. EMBO J **9**:1503-1510

Safavian D, Goring DR (2013) Secretory activity is rapidly induced in stigmatic papillae by compatible pollen, but inhibited for self-incompatible pollen in the *Brassicaceae*. PloS One **8**:84286/1-13

Schäfer T, Zentgraf H, Zehe C, Brügger B, Bernhagen J, Nickel W (2004) Unconventional secretion of fibroblast growth factor 2 is mediated by direct translocation across the plasma membrane of mammalian cells. J Biol Chem **279**:6244-6251

Schafer WR, Kim R, Sterne R, Thorner J, Kim SH, Rine J (1989) Genetic and pharmacological suppression of oncogenic mutations in RAS genes of yeast and humans. Science **245**:379-385

Schlessinger J, Plotnikov AN, Ibrahimi OA, Eliseenkova AV, Yeh BK, Yayon A, Linhardt RJ, Mohammadi M (2000) Crystal structure of a ternary FGF-FGFR-Heparin complex reveals a dual role for heparin in FGFR binding and dimerization. Mol Cell **6**:743-750

Schmidt O, Teis D (2012) The ESCRT machinery. Curr Biol **22**:116-120

Schotman H, Karhinen L, Rabouille C (2008) dGRASP-mediated noncanonical integrin secretion is required for *Drosophila* epithelial remodeling. Dev Cell **14**:171-182

Schroder K, Tschopp J (2010) The inflammasomes. Cell **140**:821-832

Schünemann D (2007) Mechanisms of protein import into thylakoids of chloroplasts. Biol Chem **388**:907-915

Scott SV, Guan J, Mutchins MU, Kim J, Klionsky DJ (2001) Cvt19 is a receptor for the cytoplasm-to-vacuole targeting pathway. Mol Cell **7**:1131-1141

Senko MW, Remes PM, Canterbury JD, Mathur R, Song Q, Eliuk SM, Mullen C, Earley L, Hardman M, Blethrow JD, Bui H, Specht A, Lane O, Denisov E, Makarov A, Horning S, Zabrouskov V (2013) Novel parallelized quadrupole/linear ion trap/orbitrap tribrid mass spectrometer improving proteome coverage and peptide identification rate. Anal Chem **85**:11710-11714

Shewry PR, Halford NG (2002) Cereal seed storage proteins: structures, properties and role in grain utilization. J Exp Bot **53**:947-958

Shintani T, Huang WP, Stromhaug PE, Klionsky DJ (2002) Mechanism of cargo selection in the cytoplasm to vacuole targeting pathway. Dev Cell **3**:825-837

Soll J, Schleiff E (2004) Protein import into chloroplasts. Nat Rev Mol Cell Biol **5**:198-208

Stahl DC, Swiderek KM, Davis MT, Lee TD (1996) Data-controlled automation of liquid chromatography/tandem mass spectrometry analysis of peptide mixtures. J Am Soc Mass Spectrom **7**:532-540

Stanley P (2011) Golgi glycosylation. Cold Spring Harb Perspect Biol **3**:a005199/1-13

Stegmayer C, Kehlenbach A, Tournaviti S, Wegehingel S, Zehe C, Denny P, Smith DF, Schwappach B, Nickel W (2005) Direct transport across the plasma membrane of mammalian cells of *Leishmania* HASPB as revealed by a CHO export mutant. J Cell Sci **118**:517-527

Stoop JMH, Williamson JD, Pharr MD (1996) Mannitol metabolism in plants: a method for coping with stress. Trends Plant Sci **1**:139-144

Streller S, Wingsle G (1994) *Pinus sylvestris* L. needles contain extracellular CuZn Superoxide dismutase. Planta **192**:195-201

Strømhaug PE, Reggiori F, Guan J, Wang CW, Klionsky DJ (2004) Atg21 is a phosphoinositide binding protein required for efficient lipidation and localization of Atg8 during uptake of aminopeptidase I by selective autophagy. Mol Biol Cell **15**:3553-3566

Stroud RM, Walter P (1999) Signal sequence recognition and protein targeting. Annu Rev Cell Dev Biol **10**:87-119

Sun Q, Fan W, Chen K, Ding X, Chen S, Zhong Q (2008) Identification of barkor as a mammalian autophagy-specific factor for beclin 1 and class III phosphatidylinositol 3-kinase. Proc Natl Acad Sci USA **105**:19211-19216

Suzuki K, Kirisako T, Kamada Y, Mizushima N, Noda T, Ohsumi Y (2001) The pre-autophagosomal structure organized by concerted functions of APG genes is essential for autophagosome formation. EMBO J **20**:5971-5981

Suzuki K, Kubota Y, Sekito T, Ohsumi Y (2007) Hierarchy of Atg proteins in pre-autophagosomal structure organization. Genes Cells **12**:209-218

Syka JEP, Coon JJ, Schroeder MJ, Shabanowitz J, Hunt DF (2004) Peptide and protein sequence analysis by electron transfer dissociation mass spectrometry. Proc Natl Acad Sci USA **101**:9528-9533

Szul T, Sztul E (2011) COPII and COPI traffic at the ER-golgi Interface. Am J Physiol **26**:348-364

Takahashi H, Saito Y, Kitagawa T, Morita S, Masumura T, Tanaka K (2005) A novel vesicle derived directly from endoplasmic reticulum is involved in the transport of vacuolar storage proteins in rice endosperm. Plant Cell Physiol **46**:245-249

Tanaka Y, Guhde G, Suter A, Eskelinen EL, Hartmann D, Lüllmann-Rauch R, Janssen PML, Blanz J, von Figura K, Saftig P (2000) Accumulation of autophagic vacuoles and cardiomyopathy in LAMP-2-deficient mice. Nature **406**:902-906

Tanida I (2011) Autophagy basics. Microbiol Immunol **55**:1-11

Tanudji M, Hevi S, Chuck SL (2002) Improperly folded green fluorescent protein is secreted via a non-classical pathway. J Cell Sci **115**:3849-3857

Temmerman K, Nickel W (2009) A novel flow cytometric assay to quantify interactions between proteins and membrane lipids. J Lipid Res **50**:1245-1254

TerBush DR, Maurice T, Roth D, Novick P (1996) The exocyst is a multiprotein complex required for exocytosis in *Saccharomyces cerevisiae*. EMBO J **15**:6483-6494

Torrado LC, Temmerman K, Müller HM, Mayer MP, Seelenmeyer C, Backhaus R, Nickel W (2009) An intrinsic quality-control mechanism ensures unconventional secretion of fibroblast growth factor 2 in a folded conformation. J Cell Sci **122**:3322-3329

Vanacker H, Carver TLW, Foyer CH (1998) Pathogen-induced changes in the antioxidant status of the apoplast in barley leaves. Plant Physiol **117**:1103-1114

Venable JD, Dong MQ, Wohlschlegel J, Dillin A, Yates JR III (2004) Automated approach for quantitative analysis of complex peptide mixtures from tandem mass spectra. Nat Methods **1**:39-45

von Heijne G (1990) The signal peptide. J Membr Biol **115**:195-201

Walther TC, Mann M (2010) Mass spectrometry-based proteomics in cell biology. J Cell Biol **190**:491-500

Wang H, Zhuang XH, Hillmer S, Robinson DG, Jiang LW (2011) Vacuolar sorting receptor (VSR) proteins reach the plasma membrane in germinating pollen tubes. Mol Plant **4**:845-853

Wang J, Ding Y, Wang J, Hillmer S, Miao Y, Lo SW, Wang X, Robinson DG, Jiang L (2010) EXPO, an exocyst-positive organelle distinct from multivesicular endosomes and autophagosomes, mediates cytosol to cell wall exocytosis in *Arabidopsis* and tobacco cells. Plant Cell **22**:4009-4030

Wang X, Matteson J, An Y, Moyer B, Yoo JS, Bannykh S, Wilson IA, Riordan JR, Balch WE (2004) COPII-dependent export of cystic fibrosis transmembrane conductance regulator from the ER uses a di-acidic exit code. J Cell Biol **167**:65-74

Watson P, Stephens DJ (2005) ER-to-golgi transport: form and formation of vesicular and tubular carriers. Biochim Biophys Acta **174**4:304-315

Williamson JD, Galili G, Larkins BA, Gelvin SB (1988) The synthesis of a 19 kilodalton zein protein in transgenic petunia plants. Plant Physiol **88**:1002-1007

Williamson JD, Stoop JMH, Massel MO, Conkling MA, Pharr DM (1995) Sequence analysis of a mannitol dehydrogenase cDNA from plants reveals a function for the pathogenesis-related protein ELI3. Proc Natl Acad Sci US **92**:7148-7152

Wilson SM, Bacic A (2012) Preparation of plant cells for transmission electron microscopy to optimize immunogold labeling of carbohydrate and protein epitopes. Nat Protoc **7**:1716-1727

Winey M, Meehl JB, O'Toole ET, Giddings TH (2013) Conventional transmission electron microscopy. Mol Biol Cell **25**:319-323

Xiang L, Etxeberria E, Van den Ende W (2013) Vacuolar protein sorting mechanisms in plants. FEBS J **280**:979-993

Yamamoto K, Fujii R, Toyofuku Y, Saito T, Koseki H, Hsu VW, Aoe T (2001) The KDEL receptor mediates a retrieval mechanism that contributes to quality control at the endoplasmic reticulum. EMBO J **20**:3082-3091

Yamamoto YT, Zamski E, Williamson JD, Conkling MA, Pharr MD (1997) Subcellular localization of celery mannitol dehydrogenase: a cytosolic metabolic enzyme in nuclei. Plant Physiol **115**:1397-1403

Yoo JS, Moyer BD, Bannykh S, Yoo HM, Riordan JR, Balch WE (2002) Non-conventional trafficking of the cystic fibrosis transmembrane conductance requlator through the early secretory pathway. J Biol Chem **277**:11401-11409

Yoshimoto K, Hanaoka H, Sato S, Kato T, Tabata S, Noda T, Ohsumi Y (2004) Processing of ATG8s, ubiquitin-like proteins, and their deconjugation by ATG4s are essential for plant autophagy plant. Cell **16**:2967-2983

Zamski E, Yamamoto YT, Williamson JD, Conkling MA, Pharr MD (1996) Immunolocalization of mannitol dehydrogenase in celery plants and cells. Plant Physiol **112**:931-938

Zehe C, Engling A, Wegehingel S, Schäfer T, Nickel W (2006) Cell-surface heparan sulfate proteoglycans are essential components of the unconventional export machinery of FGF-2. Proc Natl Acad Sci USA **103**:15479-15484

Zhang C, Hicks GR, Raikhel NV (2014) Plant vacuole morphology and vacuolar trafficking. Front Plant Sci **5**:476/1-9

Zhang H, Zhang L, Gao B, Fan H, Jin J, Botella MA, Jiang L, Lin J (2011) Golgi apparatus-localized synaptotagmin 2 is required for unconventional secretion in *Arabidopsis*. PloS One **6**:26477/1-14

Zubarev RA, Makarov A (2013) Orbitrap mass spectrometry. Anal Chem **85**:5288-5296

CHAPTER 2

Elucidating the Mannitol Deyhdrogenase (MTD) Interactome Associated with Unconventional Secretion

2.1 Abstract

Golgi-dependent secretion was long believed to be the sole protein secretory pathway in cells, however, more recent evidence has supported that unconventional, non-Golgi secretion occurs in both animal and plants. Specific mechanisms involved in this process have not been completely elucidated. We used a transformed *Arabidopsis thaliana* cell line to express celery mannitol dehydrogenase (MTD), a protein known to be secreted by unconventional/leaderless means, to identify components of its secretory interactome/complex. *In vivo* formaldehyde crosslinking was used to preserve protein interactions triggered by the endogenous pathogen response signal salicylic acid (SA). The MTD-interacting complex was "captured" using co-immunopurification and interacting protein components were determined using quantitative liquid chromatography-tandem mass spectrometry (LC/MS/MS). After analyzing biological replicates and utilizing statistical analysis, 30 candidate proteins emerged that were not only crosslinked to MTD, but also displayed significant increases/decreases in response to SA. Many of these proteins (e.g. kinases, chaperones, and AAA-ATPases) have been implicated in various trafficking pathways, including exocytosis and autophagy.

2.2 Introduction

Protein trafficking is required at some point in most cellular processes, making it a crucial part of cell function and survival. Until relatively recently, protein trafficking was thought to occur by two major mechanisms: Golgi-dependent (classical) trafficking, where the nascent protein is recognized by the presence of an N-terminal signal sequence and cotranslationally inserted into the lumen of the endoplasmic reticulum (ER) for subsequent routing via the Golgi to the vacuole or the extracellular space. Other proteins, such as nuclear-encoded mitochondrial and chloroplast proteins, are initially translated in the cytosol prior to being directed into their respective organelles via “transit” peptide-mediated insertion that is independent of the ER/Golgi apparatus. Classical, Golgi-mediated secretion largely restricts control of secretion to regulation by activation of gene expression. This is, or can be, relatively slow, because it not only requires gene activation and production of a new protein, but also requires trafficking through the entire ER/Golgi pathway for secretion.

More recently, many proteins have been found to traffic independent of the Golgi, contradicting long established dogma concerning protein trafficking. Proteins that undergo Golgi-independent or unconventional secretion, either constitutively or in response to stress/stimulus-regulated signals, can be further categorized by whether or not they enter the ER. Those that are Golgi-independent, but are first inserted into the ER from whence they are transported directly to their final destination, are said to be transported by a “Golgi bypass” mechanism (Michaeli et al., 2014). Other secreted proteins circumvent both the ER and the Golgi since they lack a signal peptide for ER insertion; their secretion is often termed “leaderless.” Secretion by both of these mechanisms is insensitive to brefeldin A (BFA), an inhibitor of COPII vesicle formation, which prevents ER to Golgi transport (Rubartelli et al., 1990).

Proteins secreted by unconventional, Golgi-independent mechanisms follow a much shorter pathway than those secreted by classical means, and so their secretion is typically much more rapid. In animal cells, although research is ongoing, four types unconventional secretion are recognized, as reviewed by Rabouille et al. (2012). Proteins that undergo direct translocation across the plasma membrane (Type I), often requiring the assistance of both integral and peripheral membrane proteins. ABC transporters, and other integral membrane proteins, also assist in Type II secretion, using ATP to move substrates across membranes. Type III secretion is based on autophagy, recycling proteins and damaged organelles via sequestration and formation of subcellular membranes. Lastly, proteins categorized under Type IV or Golgi-bypass secretion are transported directly from the ER to the PM. Although a number of these mechanisms, along with associated protein interactors, have been validated in animal cells, many components of the secretion machinery are still to be identified and aspects of these mechanisms are not fully understood. Even less known about unconventional secretion in plant cells, where its existence was only reported recently and where pathways are only beginning to be defined (Drakakaki and Dandekar, 2013).

In plants, some of the initial clues that there was more to protein trafficking than the classically recognized pathways came as early as the late 1980s. Some of the earliest involved the apparent mislocalization of the maize storage proteins (zeins) when expressed in petunia and tobacco (Williamson et al., 1988; Coleman et al., 1996). Because they did not package into the expected protein storage bodies, it was assumed that their signal peptides were somehow cleaved during protein synthesis (Williamson et al., 1988). Subsequent studies showed that although zeins lack ER retention signals, in an appropriate system they are normally retained in the lumen of the rough ER and ultimately localized in protein bodies in the cytoplasm and protein storage vacuoles, suggesting utilization of the autophagy pathway (Coleman and Herman, 1996). Additionally, plant lectins, carbohydrate-binding proteins such as the jacalin-related lectins, were known to accumulate in vacuoles and, although the mechanism was unknown, these vacuolar proteins were then secreted in response to pathogen attack (Chrispeels and Raikhel, 1991). Jacalin-related lectins bind mannose or maltose and when secreted during infection have a defensive function against bacteria and fungi by binding to these moieties in the pathogen cell wall. (Van Damme et al., 1998). More recently, a number of biochemical, cytological and physical analyses suggested that the normally cytosolic plant Cu/Zn SODs, which all lack signal sequences, relocalize to the apoplast in response to infection (Streller and Wingsle, 1994; Karpinska et al., 2001; Cheng et al., 2009a). The initial reports of secretion of proteins lacking a classical signal peptide such as these provided much of the impetus for current research on unconventional secretion in plants. In both animal and plant cells, however, many of the mechanisms and proteins involved have remained a mystery for over two decades since these findings pointed toward the existence of unconventional secretion.

One of the first plant proteins whose leaderless, pathogen induced secretion was rigorously confirmed by multiple approaches was mannitol dehydrogenase (MTD), an NAD-dependent 1-oxidoreductase first characterized for its role in mannitol metabolism in celery, *Apium graveolens* L. MTD oxidizes mannitol to mannose (Stoop et al., 1996) in the cytosol and given its normally symplastic (cytosolic and nuclear) localization in uninfected plants (Zamski et al., 1996; Yamamoto et al., 1997), not surprisingly lacks a recognized signal sequence (Williamson et al., 1995). In *Nicotiana tabacum* expressing celery MTD under regulation of a CaMV 35S promoter, translocation of MTD to the apoplast after treatment with salicylic acid (SA), an inducer of pathogenesis-related (PR) responses, was first observed by Cheng et al. (2009b). This SA-triggered secretion was not inhibited by BFA, and immunoelectron microscopy failed to detect MTD in Golgi during the secretory timeframe, suggesting that secretion occurred by an unconventional pathway (Cheng et al., 2009b). Since using a heterologous system to analyze a global mechanism can result in artifacts, the specific secretion of MTD (i.e. not a result of cell lysis) was also confirmed using liquid chromatography-tandem mass spectrometry (LC/MS/MS) analysis of the secretome of SA-treated celery cells (Blackburn et al., 2010).

As with leaderless secretion mechanisms characterized to date in animals, we hypothesize that secretion of the normally symplastic, leaderless MTD involves the SA-triggered association of MTD with the various components of its secretory machinery. Although immunoelectron and confocal microscopy are powerful tools for assessing protein localization, transport, and secretion, these methods have limitations that make them less than ideal for identifying assessing multiple protein interactors simultaneously. Concurrent isolation and identification of multiple protein interactors, however, has proven feasible using a combination of protein crosslinking, imunnopurification, and mass spectrometric protein identification. Using these procedures we identified putative components of the MTD secretory complex in the cytoplasm of transformed *A. thaliana* cells expressing a FLAG-tagged celery MTD immediately following treatment with SA. Herein we describe the resulting identification of multiple interactors participating, at least transiently, in the SA-triggered, of MTD secretory interactome.

2.3 Experimental

2.3.1 Materials

All chemicals and reagents were from Thermo Fisher Scientific or Sigma-Aldrich unless otherwise stated. Sequencing grade modified trypsin was from Promega.

2.3.2 Construction and Transformation of 35S-MTD-FLAG

An in-frame FLAG peptide (D-Y-K-D-D-D-D-K) was inserted at the C-terminus of the celery mannitol dehydrogenase (*AgMtd*) cDNA (GenBank accession U24561) using recombinant PCR. Forward (F31) 5’-TGCCCAAGTCTGGTACACAA-3’ and reverse primers (R51) 5’-AGCTGGATCCTATTTGTCATCGTCATCCTTGTAATCC TCCATTGCGGTGTTCACAT-3’ containing a FLAG encoding sequence were used. The PCR product was digested with BamH1, inserted into the BamH1 site of the *AgMtd*-containing clone p9-41 (Jennings et al., 2002), screened for orientation, and sequenced. The construct contains the first 359 of 365 amino acids from MTD plus the FLAG epitope (37.6 kDa), under the control of a CaMV 35S promoter.

The resulting plasmid (p9-41-FLAG) was transformed into *Agrobacterium tumefaciens* strain EHA105 (Hood et al., 1993) for transformation into *Arabidopsis thaliana* cells (Clough and Bent, 1998). Seed was collected and germinated on kanamycin for selection. Cell suspension cultures were established from kanamycin resistant (50 mg/ml) shoots as described by Mathur and Koncz (1998). Resulting MTD-FLAG expressing cultures were screened using immunoblot analysis as described below and a robust MTD expressing line, 2W1, was selected for these analyses.

2.3.3 Cell Maintenance and Treatment

Wild-type (wt) *Arabidopsis thaliana* (Columbia, Col) and 2W1 (transformed *A. thaliana* cells expressing celery MTD, as described by Zamski et al. [2001]) cell suspension cultures were maintained on 7-8 day transfer cycles in 50 ml MS media (Murashige and Skoog, 1962) on a rotator (150 rpms) at room temperature (approximately 25°C). On the 7^{th} day post-transfer, cells (approximately 5-6 ml packed cell volume per 50 ml MS media) were treated with 0.5 ml of 100 mM salicylic acid (SA) (a working concentration of 1 mM SA) for 10 or 20 min. After treatment, cells were rinsed with deionized water, crosslinked for 20 min using 1% formaldehyde (25ml or enough to submerge cells), and then quenched using 300 mM glycine as described by Vasilescu et al. (2004). Crosslinked cells were flash frozen using liquid nitrogen and stored at -80°C until further use.

2.3.4 Protein Extraction

Frozen cells were powdered in liquid N_2 using mortar and pestle, proteins were extracted in extraction buffer (20 mM Tris, 150 mM NaCl, 1 mM EDTA, 20% glycerol, 20 mM NaF, 1 mM PMSF, 50 nM Microcystin, protease inhibitor cocktail [1 tablet/50 ml], pH 8.8) at a 2:1 ratio (e.g. 1 ml extraction buffer/2 g cells) and centrifuged at 10,000xg for 20 min. The supernatant was decanted and stored at -20°C.

2.3.5 Co-Immunopurification (Co-IP) of MTD-Complex

Anti-FLAG magnetic beads (Sigma, M8823) were used to immunopurify the formaldehyde crosslinked MTD-interacting complexes; a packed bead volume of 200 μl were incubated with the extract above (containing 10 mg of total protein, determined by the method of Bradford (Bradford, 1976) adjusted to 3.5-8 ml with the extraction buffer depending on the concentration of the extract for 2 hours at room temperature (approximately 25°C). The flow-through was saved and the beads rinsed 3X with TBS (15 mM NaCl, 0.2 mM KCl, 2.5 mM Tris, pH 7.4) before eluting the bound proteins with 2X Laemmli buffer (65.8 mM Tris, 2.1% SDS, 26.3% (w/v) glycerol, 0.01% bromophenol blue, pH 6.8). Beads were incubated at a 1:1 buffer-to-bead volume ratio on a rocker for 10 min at room temperature after which the buffer containing the eluted proteins was collected. A sequential co-IP using the protocols above was performed using 75 μl of 5X Laemmli buffer and 125 μl the previous elution (now 1X Laemmli buffer) to produce 2X Laemmli buffer to elute the beads from the sequential co-IP. These elutions from both co-IPs were combined and stored at -20°C.

2.3.6 Immunoblotting

Proteins blotted onto nitrocellulose are incubated with a blocking agent (5% nonfat milk in TBST [TBS, 0.01% Tween]) for 30 min, then incubated with a ratio 1:2000 of 1° antibody (anti-MTD):TBST for 1 hour after discarding the blocking agent. The nitrocellulose is rinsed 3X with TBST and incubated with an alkaline phosphatase (AP)-labeled 2° antibody (anti-rabbit, Promega):TBST ratio of 1:2400 for 1 hour and then rinsed 3X again with TBST. Lastly, the nitrocellulose is incubated with NBT/BCIP (Promega, S3771)/Alkaline Phosphatase buffer (100 mM Tris, 150 mM NaCl, 1 mM $MgCl_2$, pH 9.0) at 66 μl:33 μl:5 ml ratio for at least 10 min or until there is enough color development. All incubations are done on a rocker at room temperature.

2.3.7 In-Gel Tryptic Digestion and LC/MS/MS

Proteins obtained from the co-IP were separated by gradient (4-15%) SDS-PAGE. Bands/fractions (F1-11, starting at the base of the well lane to produce fractions no thicker than 5 mm and no thinner than 1 mm) were excised using MW markers as a reference and subjected to overnight trypsin digestion. Resulting tryptic digests were dried down using a speed vacuum to appropriate volumes and filtered using a filter pipette tip into a microtiter plate for analysis via LC/MS/MS.

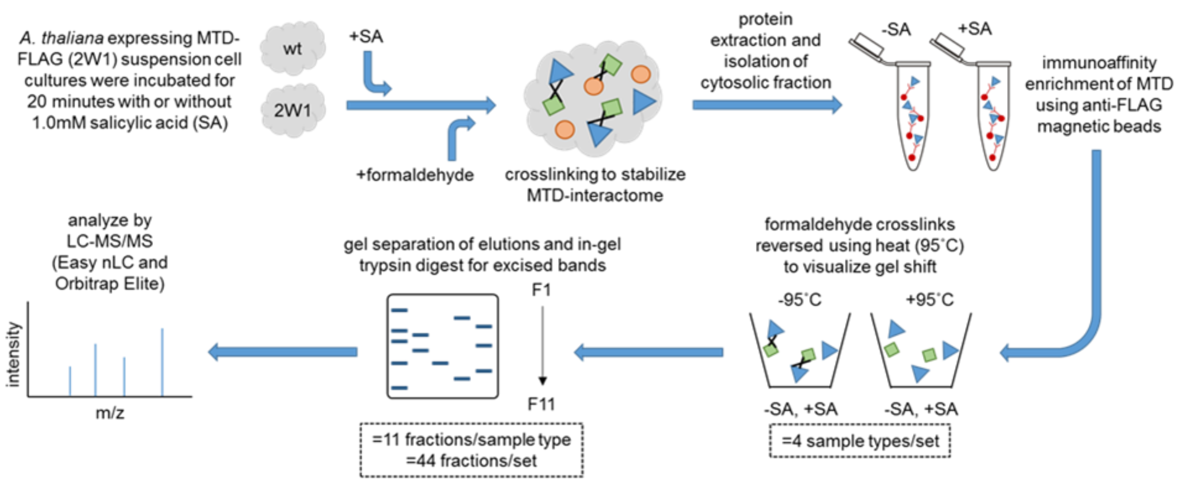

Figure 2.1 Sample Preparation Workflow

Wild-type (wt) and transformed cells (2W1) were both treated with SA and formaldehyde crosslinked. After protein extraction, the cytosolic fraction was isolated and incubated with anti-FLAG magnetic beads. Elutions resulting from co-immunopurification were treated with or without heat to reverse (data not shown) or preserve the crosslinks, respectively. Proteins were separated using SDS-PAGE and bands were excised. Samples were prepared for LC/MS/MS after overnight trypsin digestion.

2.3.8 LC/MS/MS Data Acquisition

LC/MS/MS analyses were performed on an Easy nLC 1000 liquid chromatograph coupled to an LTQ Orbitrap Elite mass spectrometer (Thermo Fisher). Samples were injected onto a PepMap 100 C18, 5 µm, trapping column (Thermo Fisher) and separated by in-line gradient elution onto a Self-Pack PicoFrit column, 75 µm id x 20 cm (New Objective), packed in-house with HALO, 2.7µm, C18 stationary phase (Advanced Materials Technology). A 90 minute linear gradient of 5%-40% of Mobile Phase B (Mobile Phase A: 0.1 formic acid/2% acetonitrile in water; Mobile Phase B: 0.1% formic acid in acetonitrile) at a 300nl/min flow rate was used for peptide separation. Data-dependent acquisition was used to select the top 5 most intense precursors for HCD fragmentation.

2.3.9 Data Normalization and Comparisons

Spectra from the LC/MS/MS (Easy nLC-Orbitrap Elite) was processed through Proteome Discoverer and protein identifications made by searching the TAIR 7.0 database using MASCOT. Although all eleven gel fractions, F1-F11, were analyzed via LC/MS/MS, only the 956 proteins identified in fractions F2-F8 **(Figure B.1)** were processed further. Fraction F1 was not assessed as it contained large crosslinked complexes and residual membrane fragments that were not resolved on the implemented gel system. MTD and any crosslinked complexes should be found above F7 (MW range of ca. 38-49 kDa), thus Fractions 9-11 were not used in the analysis; F8, however, was processed further to ensure that all MTD would be analyzed in case of “smearing” or aberrant migration. Protein intensities from these seven fractions were determined using Scaffold (Proteome Software) intensities without normalization, with minimum normalization, or with Scaffold normalization and were compared using Principal Component Analysis (PCA). Minimum normalization entailed calculating the median of all identified protein intensities, then dividing each protein median intensity by the lowest median protein intensity in the sample set to obtain a normalization factor. All intensities were individually multiplied by the normalization factor, producing normalized values for further analysis. Scaffold normalized intensity values were derived using Scaffold's "Quantitative Analysis" function.

Results of different normalization techniques of treated/untreated cells were compared using the entire/whole set of identified proteins, including sliding duplicates (e.g. F2+F3, F3+F4, etc.), as well as individual fractions/gel slices. Intensities were $\log_2(x)$ transformed using Perseus (http://www.perseus-framework.org) to create a more Gaussian distribution. Protein data was then filtered for reproducibility; requiring a protein to be present at least two out of three times per treatment group (e.g. if protein X is present in two replicates of the treated sample, but none in the untreated sample, it is kept; if protein X is present in one replicate in both the treated and untreated sample, it is eliminated). This left 610 proteins in the 20-minute SA treatment, out of an original 956 identified proteins in both the treated/untreated samples and approximately 200-440 proteins in each fraction in all three replicates combined. In the 10-minute SA treatment, 1 replicate was prepared which resulted in 437 protein identifications. Missing values were replaced using random, low abundance (level of detection +/-) values that reflect values seen in the data set from a normal distribution. Replacing missing data allowed median and statistically significant calculations of changes in relative protein abundance later on.

Optimal normalization and comparison methods were determined using principle component analysis (PCA) scatter plots **(Figure C.1)** after data processing. In whole sample sets and sliding duplicates, data points grouped by replicate, suggesting that replicates are more different than treatment groups. Data in individual band comparisons, however, largely grouped by treatment rather than replicate, indicating there is a significant treatment effect (i.e. a significant difference in proteins interacting with MTD in untreated vs. treated cells). It seems likely that in whole sample sets and sliding duplicates, the protein samples are simply too complex to distinguish differences between treatments. Individual band comparisons, however, contain fewer proteins due to electrophoretic separations of proteins by molecular weight, allowing treatment differences to be distinguished. Although gel slice/fraction F2, did not resolve by treatment regardless of the normalization method, Scaffold normalization produced the best data separation for all remaining gel bands, F3-F8 **(Figure C.1)**, and was thus used in all further analyses.

2.3.10 Data Filtration and Ratio Calculations

To eliminate from our data any proteins interacting nonspecifically with the bead-linked FLAG antibody, or with the beads themselves, crosslinked proteins were isolated from nontransformed, wild-type (wt) *Arabidopsis* cell cultures and subjected to FLAG-IP as performed with the MTD-FLAG transformed cells. A total of 695 proteins were identified in crosslinked, immunopurified extracts from both treated and untreated wt cells. These were removed from the list of proteins found in the XL2W1 samples (i.e. subtracted as being nonspecific interactors) to produce a list of proteins unique to XL2W1 (+/-SA). Changes in relative protein abundance were then calculated for the remaining 44 and 105 proteins in the 10 and 20-minute treatments, respectively, by first calculating the median intensity of each treatment group normalized in Scaffold. The treated median intensity of a given protein was then divided by its untreated median intensity to calculate the ratio of protein abundance.

Figure 2.2 Data Analysis Workflow
Samples were obtained from 3 replicate treatments at 20 minutes (SA20) and 1 replicate treatment at 10 minutes (SA10) of XL2W1 +/-SA. Protein identifications (+/-SA, fractions F2-F8) were made from raw data using MASCOT, which uses peptide mass lists acquired using Proteome Discoverer to search the TAIR database. Scaffold was used to visualize protein IDs, as well as quantitate, and normalize peptide intensities. These values were uploaded into Perseus, where they were filtered based on two valid values per treatment group (-SA or +SA) and log2(x) transformed. Missing data was replaced using random, low abundance values from a normal distribution. Proteins unique to XL2W1 treatments were identified by comparing them to XLwt proteins and subtracting nonspecific binding. Changes in relative protein abundance were calculated based on two separate medians from treated and untreated cells. Values in circles indicate proteins remaining after each data filtering step.

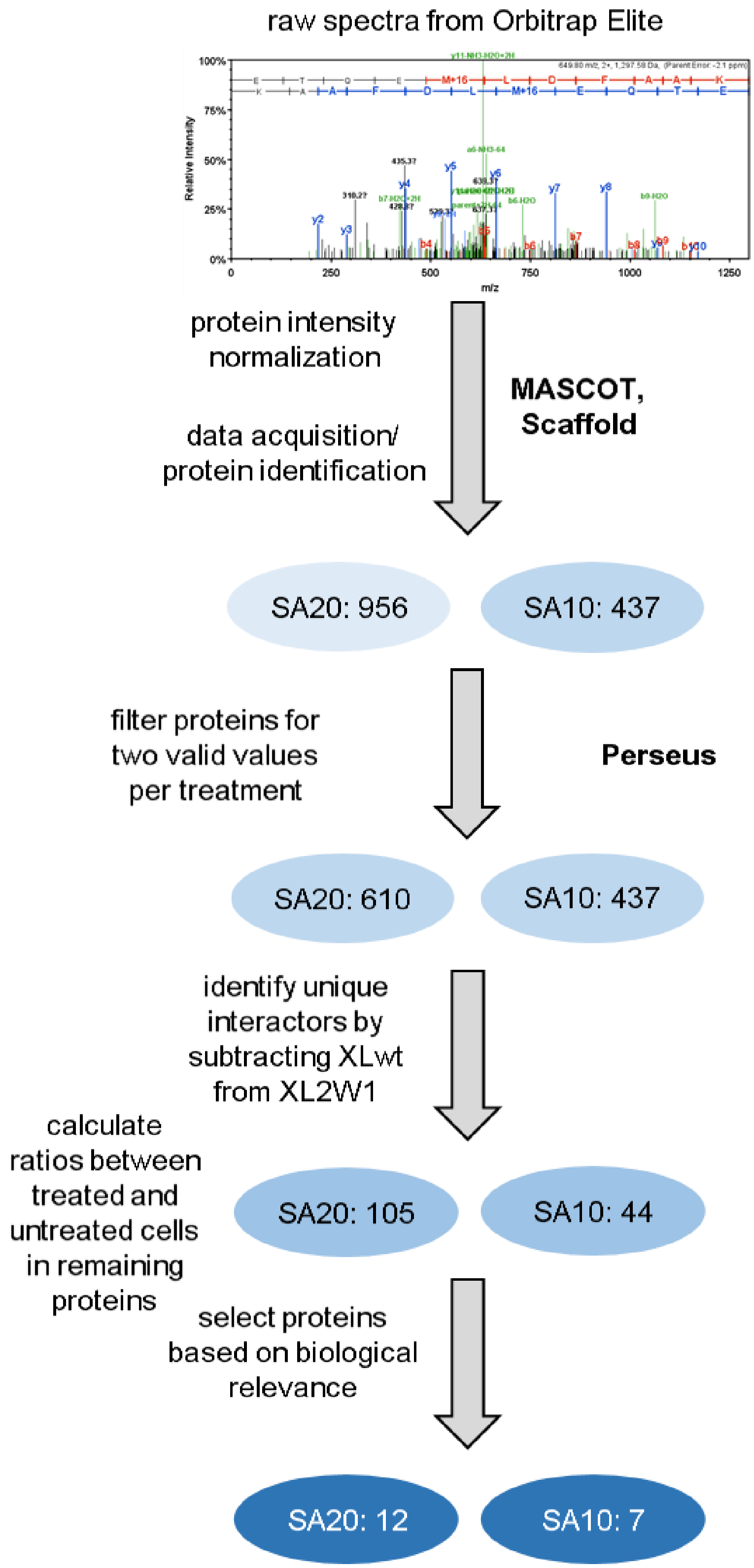
raw spectra from Orbitrap Elite
Relative Intensity
m/z
protein intensity normalization
data acquisition/ protein identification
MASCOT, Scaffold
SA20: 956
SA10: 437
filter proteins for two valid values per treatment
Perseus
SA20: 610
SA10: 437
identify unique interactors by subtracting XLwt from XL2W1
calculate ratios between treated and untreated cells in remaining proteins
SA20: 105
SA10: 44
select proteins based on biological relevance
SA20: 12
SA10: 7

2.4 Results and Discussion

2.4.1 SA Triggers Formation of an MTD-Interacting Complex; Crosslinking Preserves the MTD-Interactome

We have perviously shown that SA induces secretion of MTD in both native celery and in transgenic tobacco (Blackburn et al., 2010; Cheng et al., 2009b). Since this hypothetically involves the formation of an MTD-complex consisting of proteins required for its secretion, we used formaldehyde crosslinking to preserve these complexes during extraction. The resulting crosslinked interactome would be shifted to a higher molecular weight after SDS-PAGE. To assess the presence of MTD in these complexes, eluates obtained from co-immunopurification (co-IP) of formaldehyde crosslinked extracts from both SA treated and untreated *A. thaliana* cells expressing a FLAG-tagged celery MTD (cell line 2W1) were heated to reverse formaldehyde crosslinking, separated by SDS-PAGE gel electrophoresis and Coomassie stained **(Figure 2.3A, B)**. The gel region corresponding to the native 40 kDa molecular weight of MTD (37 kDa-50 kDa) was excised and analyzed via LC/MS/MS **(Figure 2.3C)** to verify the presence of MTD in the immunopurified complex. MTD was identified in both + and -SA treated 2W1 cells, but not in the wild-type, which expresses ELI3, not the FLAG-tagged celery MTD. At high stringency identification requirements, 95% protein and peptide identity threshold in Scaffold, one peptide and four peptides were identified in the treated sample and untreated sample, respectively **(Figure 2.3C)**. Both proteins share a common identified peptide (VGDNVGIGCLVGSCR), however, peak area intensities were 4.6×10^6 and 2.7×10^6 for untreated and treated 2W1 cells, respectively. This decrease is consistent with the previous observation that MTD is decreasing in the cytosol in response to SA (Cheng et al., 2009b). Eluates obtained from co-IP of MTD-FLAG in untreated, crosslinked (XL) 2W1 extracts were also separated by SDS-PAGE gel and assessed by immunoblotting **(Figure 2.3A, B)** to visualize the presence of MTD in the crosslinked complex. MTD crossreacting material was largely present in the higher MW region of the gel in the unheated (-95°C) sample. The light smearing in the unheated eluate could result from instability during separation, or intermediate complex formation, since permeation of cell calli by SA and formaldehyde could vary. In the heated (+95°C) sample, where crosslinking is reversed, MTD returns to its original 40 kDa MW, as seen in the flow though (FT). Immunoblots of treated XL2W1 samples also show MTD-complexes shifted to higher MWs.

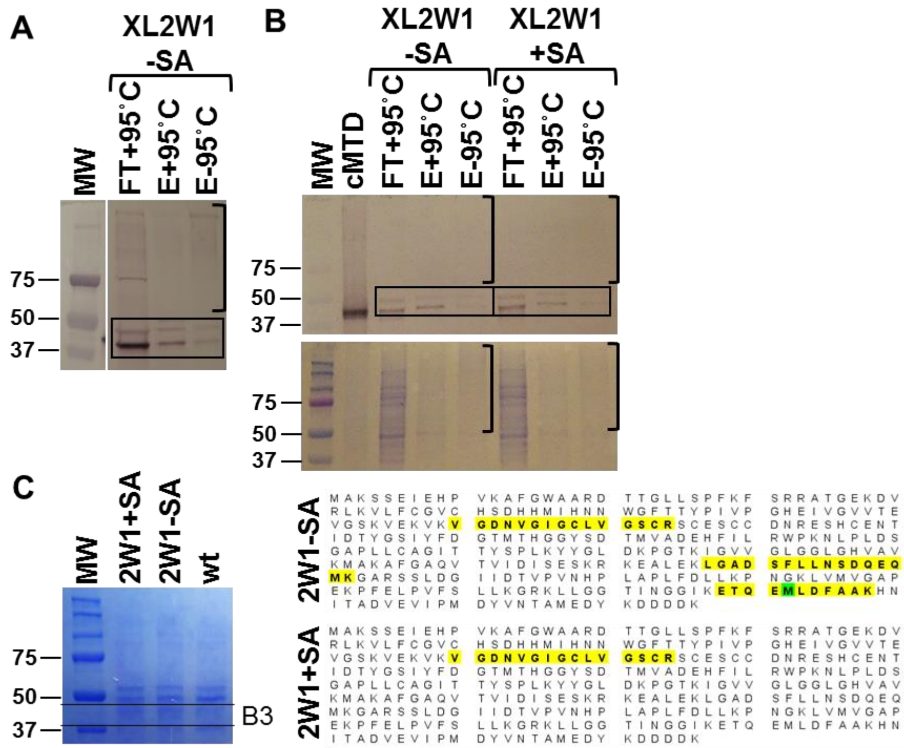

Figure 2.3 MTD is Present in Immunopurified, Crosslinked Complexes
(A, B) MTD is present in both heated and unheated elutions from crosslinked (XL) 2W1 crude extract. Heat reverses crosslinking, returning MTD to its original 40 kDa MW. Without heat, however, MTD-complexes are seen in higher MW regions of the immunoblot indicated by a bracket (]). These MTD-interacting complexes are visualized using an anti-MTD antibody. **(C)** Coomassie stained gel of elutions derived from 2W1 cells. The presence of MTD at 40 kDa was verified by excision of the indicated gel region, followed by in-gel tryptic digestion and LC/MS/MS analysis. Four high quality peptides were identified in the untreated sample and one in the treated, representing 12% and 4% protein coverage, respectively, at 95% protein and peptide identity thresholds.

2.4.2 Assessing the MTD Interactome following 10 minutes after SA Treatment

Having verified that we can recover MTD-interacting complexes using crosslinking and FLAG-immunopurification, we began assessing the components of these complexes. Intact, formaldehyde crosslinked, interacting complexes were recovered by separating unheated FLAG-IP samples using gel electrophoresis as described above, in this case for samples 10 minutes after SA treatment. Seven 2-5 mm gel slices/fractions, spanning approximately the range from 300 (F2) to 36 kDa (F8) were excised, subjected to in-gel tryptic digestion and assessed by LC/MS/MS analysis. After subtracting proteins present in untransformed, wild-type controls, presumably representing nonspecific protein interactions with the FLAG matrix, relative abundance in remaining proteins in untreated samples (XL2W1) were compared to unique proteins in samples from 10 minute SA-treated cells (XL2W1+SA). The resulting protein responses were categorized as follows: those with increased/decreased abundance that migrated at or near their unshifted, native molecular weights (i.e. appeared to be uncomplexed) and those with increased or decreased abundance at shifted molecular weights (i.e. appeared to be part of a complex) or were degraded, respectively.

Forty-four (44) protein interactors unique to the 10 minute, SA-treated XL2W1 cells were identified. A subset of these proteins (designated SA10) that has previously reported associations with cellular responses to SA and/or protein trafficking is listed in **Table 2.1**. Proteins identified from co-IPed eluates of the 10-minute SA treatment overlapped the set of proteins identified in the 20-minute treatment, shown later, indicating that, although we performed only one replicate of the 10-minute treatment, they are reproducible identifications. Among the identified proteins that show an increase in response to SA are, not unexpectedly, stress response/signaling proteins such as kinases. Additionally, a number of interactors were proteins involved in binding to the cellular scaffold (e.g. SNX1), suggesting the existence of a preexisting, scaffold-linked MTD complex. Finally, although several proteins previously identified as being involved in protein trafficking show a quantitative increase after the 10-minute SA treatment, none of these quantitative increases are associated with a shift in apparent MW/mobility.

Among these is MAP kinase 4 (AT4G01370), a stress response protein, that increases by a ratio of 2.2. Three vesicular trafficking proteins were also identified, two transducin/WD40 repeat family proteins (AT1G52730 and AT3G18860) and NSF AAA-ATPase (AT4G04910). Both WD40 repeat family proteins also showed an increase in relative abundance after SA treatment at their respective MW fractions, suggesting the formation of an initial complex involved in the MTD secretory pathway. The ATPase (NSF), however, shows a slight decrease. Two proteins, Hsp93-III (AT3G48870), a Clp protease associated ATPase, and VH1-interacting kinase (VIK, AT1G14000), previously reported to be involved in import into the chloroplast and the vacuole, respectively, were also identified. Hsp93-III in MW fractions F2 and F5 decreased to 0.5 and 0.6 relative to levels in untreated cells, respectively; VIK showed a ratio of 3.9, but no shift in apparent MW. Finally, RPT4A (AT5G43010), a regulatory protein associated with proteasomal complexes, was identified in fraction F7, consistent with its unshifted MW.

Table 2.1 The MTD Interactome 10 minutes after SA Treatment (SA10)
Unique MTD-interacting proteins that appear in response to the 10 minute SA treatment are listed by their ratios relative to levels in untreated cells.

Accession No.	**Protein/Function**	**MW** (kDa)	**F2** >250 kDa[a]	**F3** 151-250 kDa	**F4** 100-150 kDa	**F5** 51-99 kDa	**F6** 49-51 kDa	**F7** 38-49 kDa	**F8** 36-38 kDa
AT1G14000[b]	VIK | VH1-interacting kinase	49					*	**3.9***	
AT4G01370[b]	MPK4 | MAP kinase 4	43						*	**2.2**
AT1G52730	Transducin/WD40 repeat family protein	38						*	**2.2***
AT5G43010[b]	RPT4A | regulatory particle AAA-ATPase	45						**1.5***	
AT3G18860[b]	Transducin/WD40 repeat family protein	84				**1.4***			
AT3G48870[b]	HSP93-III | Clp ATPase	106	**0.5**		*	**0.6**			
AT4G04910[b]	NSF | AAA-type ATPase family protein	81				**0.5***			

(light green, ratio >2; light red, ratio <0.5). * native MW, [a] MW ranges are approximate and may vary slightly, [b] protein also present at 20 minutes in SA treated samples.

2.4.3 The MTD Interactome 20 Minutes after SA Treatment

Using the same methods described for assessing extracts from the 10 minute treatment, the MTD interactome was examined at 20 minutes. Three replicates were performed for both untreated and 20-minute SA treated cells, and proteins present in at least 2 out of 3 replicates (in either sample type) were retained for further analysis. This resulted in the identification of 105 unique proteins which included a subset of 12 proteins (SA20) **(Table 2.2)** with previously reported associations with SA response and/or protein trafficking.

Six proteins present in the 20 minutes post SA interactome were also present in the 10 minute SA interactome, but with different amounts relative to untreated cells as well as different mobility shifts **(Table 2.2)**. Two proteins, NSF (AT4G04910) and RPT4A (AT5G43010), although present in the 10 minute interactome, do not increase relative to samples from untreated cells until the 20 minute time point, at which time they have ratios of 10 and 18, in F5 and F7, respectively. Although isolated as part of the crosslinked IPed interactome, and not present in samples from wild-type cells, NSF and RPT4A do not display MW shifts, only increases.

Other unique interactors, Hsp93-III (AT3G48870) and MPK4 (AT4G01370) show smaller increases (ratios of 2.1 and 2.4, respectively). In contrast, VIK (AT1G14000) is the only protein showing a decrease in the 20-minute treatment samples, consistent with the idea that it is an earlier interactor during MTD secretion. Finally, one protein, the WD40 repeat family protein (AT3G18860), shows approximately the same relative levels in both SA10 and SA20; ca. a 1.4 ratio compared to untreated cells after 10 minutes and a 1.5 ratio after 20 minutes. Interestingly, although these proteins were all isolated as part of a crosslinked complex, a number appear on the gel at their native MW or smaller. The first six proteins listed show relative increases at their native MW fractions, while the last six show decreases in fractions above their MWs as well as increases at their respective MWs.

Table 2.2 MTD Interacting Proteins 20 minutes after SA Treatment (SA20)
MTD-interacting proteins unique to XL2W1 in response to SA after 20 minutes are listed by their ratios relative to untreated XL2W1.

Accession No.	**Protein/Function**	**MW** (kDa)	**F2** >250 kDa[a]	**F3** 151-250 kDa	**F4** 100-150 kDa	**F5** 51-99 kDa	**F6** 49-51 kDa	**F7** 38-49 kDa	**F8** 36-38 kDa
AT5G43010[b]	RPT4A | regulatory particle AAA-ATPase	45						**18.3***	
AT4G04910[b]	NSF | AAA-type ATPase family protein	81		**1.1**		**10.2***			
AT1G14000[b]	VIK | VH1-interacting kinase	49					*****	**2.4***	
AT3G48870[b]	HSP93-III | Clp ATPase	106	**1.0**	**0.2**	**2.1***	**1.3**			
AT4G01370[b]	MPK4 | MAP kinase 4	43						**2.0***	**0.8**
AT5G42970	CSN4 | PCI domain protein	45						**2.0***	
AT5G50920	HSP93-V | CLPC homolog	103	**0.2**	**0.1**	**1.5***	**1.1**			
AT3G18860[b]	Transducin/WD-40 repeat family protein	84				**1.5***			
AT5G22060	J2 | DNAJ homolog 2	46	**0.4**				**0.8**	*****	
AT5G06140	SNX1 | sorting nexin 1	47						**0.7***	
AT5G20720[c]	CPN20, CPN10, CPN21 | chaperonin 20	27			**0.7**				
AT5G56000	Hsp90.4 | Heat Shock Protein	80	**0.003**		**0.005**	*****			

(dark green, ratio >10; light green, ratio >2; dark red, ratio >0.1; light red, ratio <0.5). * fraction corresponding to native MW, [a] MW ranges are approximate and may vary slightly, [b] protein present in Table 2.1, [c] MW <36 kDa and below F8

Overall, larger changes are observed 20 minutes after SA treatment (SA20) compared to 10 minutes. Several additional proteins that are implicated in protein trafficking are also present in the SA20 interactome. Four proteins, J2 (DNAJ homolog 2, AT5G22060), CPN20 (chaperonin 20, AT5G20720), Hsp90.4 (AT5G56000), and SNX1 (sorting nexin 1, AT5G06140), decrease at 20 minutes in treated vs. untreated cells, either in fractions above or at their native MWs. Interestingly, the first three proteins have all been implicated in protein binding and regulation or stabilization of protein folding. The ClpC homolog Hsp93-V (AT5G50920) is distributed over fractions F2 through F5, with its decreasing presence in the larger fractions being mirrored by an increase in F4. This is perhaps because it is becoming uncomplexed from the MTD interactome over this period. This also parallels the behavior of the Clp ATPase (Hsp93-III) suggesting ClpC and Clp ATPase might form a complex. Finally, CSN4 (AT5G42970), a subunit of the COP9 signalosome (CSN), which regulates the ubiquitin proteasome, increases by a ratio of 2 by 20 minutes after treatment with SA. Again, this roughly parallels the 18.3 ratio of the proteasome-associated protein, RPT4A. The increased relative abundance of ClpC and proteasomal proteins support the functional significance of these two groups in the MTD interactome.

2.4.4 Changes in the SA-Specific MTD Interactome between 10 and 20 Minutes

Increases/decreases in proteins interacting with MTD between the 10 and 20-minute SA treatments might offer insights into potential mechanisms of the MTD secretory machinery by providing functional grouping of protein presence. Comparing protein intensities at both treatment time points, changes in the MTD interactome were identified, shown in **Table 2.3**.

Proteins in **Table 2.3** might not be present in both **Tables 2.1** and **2.2**; because during data filtration, 20 minute proteins were seen in at least 2 replicates of treated cells, but might not have been present in the single 10-minute treatment. Therefore, the 10-minute value used for these calculations was based on low abundance values, as described in Methods. Also, the values seen in **Table 2.3** may not complement the values in **Tables 2.1** and **2.2** because untreated comparisons used for the 10 and 20 minute treated samples were different; the reason behind this was for consistency in sample preparation and analysis, as described in Methods. For instance, RPT4A has a 1.5 ratio in F7 at 10 minutes, an 18.3 ratio at 20 minutes, but a ratio of 1.4 between 10-20 minutes. The slight apparent inconsistencies are a result of normalization against different untreated control values at 10 and 20 minutes.

Table 2.3 MTD Interactome is Composed of Transient Complexes
Proteins unique to the MTD-interactome in response to SA are listed by ratios. Values indicate the ratio between 10 and 20 minute SA treatments.

Accession No.	**Protein/Function**	**MW** (kDa)	**F2** >250 kDa[a]	**F3** 151-250 kDa	**F4** 100-150 kDa	**F5** 51-99 kDa	**F6** 49-51 kDa	**F7** 38-49 kDa	**F8** 36-38 kDa
AT4G04910[b]	NSF | AAA-type ATPase family protein	81		**0.1**		**14.8***			
AT5G22060[c]	J2 | DNAJ homolog 2	46					**5.2**	*	
AT3G48870[b]	HSP93-III | Clp ATPase	106	**5.1**	**0.4**	**2.7***	**2.9**			
AT4G01370[b]	MPK4 | MAP kinase 4	43						**3.3***	**0.4**
AT5G42970[c]	CSN4 | PCI domain protein	45						**2.4***	
AT5G50920[c]	HSP93-V | CLPC homologue 1	103			**1.8***				
AT5G43010[b]	RPT4A | regulatory particle AAA-ATPase	45						**1.4***	
AT1G14000[b]	VIK | VH1-interacting kinase	49					*	**0.8***	
AT3G18860[b]	Transducin/WD40 repeat family protein	84				**0.2***			

(dark green, ratio >10; light green, ratio >2; dark red, ratio >0.1; light red, ratio >0.5). * fraction representing native MW, [a] MW ranges are approximate and may vary slightly, [b] present in both Tables 2.1 and 2.2, [c] present in Table 2.2.

Many of the unique MTD-interacting proteins identified show little change by 10 minutes post-treatment. However, a notable increase is seen at 20 minutes, resulting in an overall increase in relative abundance between the two treatment times. NSF, for instance, has a relative change of 0.5 and 10.2 in its uncomplexed fraction (F5) compared to levels in untreated cells, at 10 and 20 minutes, respectively. In **Table 2.3**, NSF has a ratio of 14.8 between the two time points. Although this behavior is most obvious with NSF, many other proteins also display this pattern. Hsp93-III, for example, was not identified in its uncomplexed fraction (F4) in SA10, but showed a slight decrease in abundance (0.5 and 0.6) in fractions above and below F4; in SA20, however, Hsp93-III increased in abundance by a ratio of 2.1 (F4). Comparing the two treatment times, Hsp93-III increased by a ratio of 2.7 in its native MW fraction and by a ratio of 5.1 in F2 between 10 and 20 minutes. MPK4 shows similar increases of 2.2 and 2.0 when comparing 10 and 20-minute treatments, respectively, to untreated cells. As seen in **Table 2.3**, however, MPK4 has a 3.3 ratio between the two time points; this likely reflects intensity values after normalization, indicating that despite the ratios in **Tables 2.1** and **2.2**, MPK4 levels increase further after 10 minutes. Using normalized intensity values MPK4 increases from 10 to 20 minutes **(Table 2.3)**, even though it appears decreased if one just compares the values in **Tables 2.1** and **2.2**. DNAJ and CSN4, which are not found in the 10-minute treatment samples, increase by ratios of 5.2 (F6, a fraction above its uncomplexed MW fraction) and 2.4 (F7, its uncomplexed fraction), respectively at 20 minutes. For these proteins identified in interacting complexes from 20 minute SA treated cells, ratios listed in **Table 2.3** were calculated relative to the 10 minute intensity values using randomly selected, low abundance values as described in Methods.

The remaining four proteins show a less than a 0.5 ratio in abundance between the 10 and 20 minute time points. The Hsp93-V, not identified at the 10 minute time point, shows a 1.5 ratio in its native MW fraction (F4) and complementary decreases in MW fractions above its native MW (F2, F3) between untreated and 20-minute treated cells. Hsp93-V was also seen in F5 at 20 minutes, but with little change in abundance (suggesting it was part of a preexisting complex). In the fractions above F4, Hsp93-V was not identified in at least 2 out of 3 replicate analyses in the 20 minute treatment. In F5, Hsp93-V was identified in 2 replicate analyses, however, because of the method of normalization (Scaffold) used with the 10 minute SA-treated cells, it was only reported in 1 replicate analysis of the 20-minute samples. This results in a reported value only for the F4 fraction in **Table 2.3**. Here**,** Hsp93-V increased in abundance by a ratio of 1.8 between 10 and 20 minutes of treatment in its native MW fraction; no other values are generated in fractions above or below its MW. For the ratio calculation of Hsp93-V reported in **Table 2.3**, a value was selected using the same methods as described for DNAJ and CSN4. Using this method RPT4A shows ratios of 1.5 and 18.3 in its native MW fraction (F7) at 10 and 20 minutes after SA treatment, respectively. When comparing the two time points, however, RPT4A displays only a 1.4 ratio due to normalization as described above. Overall, RPT4A increases in abundance in F7 at 20 minutes, despite the varying values. The values for VIK are much more consistent, increase in abundance in its native MW fraction (F7) by ratios of 3.9 and 2.4 compared to untreated cells at 10 and 20 minutes, respectively. Between the 10 and 20 minute treatments in **Table 2.3**, VIK showed a slight decrease in abundance (0.8) in F7, mirroring the changes seen in both **Tables 2.1 and 2.2**. Finally, one of the WD40 proteins (AT3G18860) was identified in both 10 and 20 minutes treatments, showing ratios of 1.4 and 1.5, respectively, in its native MW fraction (F7). In **Table 2.3**, however, the WD40 protein decreases substantially in abundance (10/20 min = 0.2) between the two time points. This indicates that this WD40 protein is more abundant in treated cells, but decreases in abundance at longer treatment times, thus suggesting its early interaction in the MTD-complex decreases over time.

Table 2.4 Interactors in the Transient Complexes Classified by Previously Reported Function

Proteins identified in either SA10 or SA20 can be categorized by reported functions (as indicated by the "+" sign). Many of these proteins have overlapping functions consistent with a role in secretion.

Protein/ Function	Stress Response	Regu- lation[d]	Protein Import	Vesicular Trafficking	Protea- some	Protein Binding	Protein Folding	Refs
MPK4[a]	+	+						1, 2, 3, 4
VIK[a]	+	+						5
CPN20[b]		+				+	+	6, 7, 8, 9
DNAJ2[b]						+	+	10, 11, 12
HSP93-III[a]		+	+			+	+	13, 14, 15, 16, 17, 18
HSP93-V[b]		+	+			+	+	13, 14, 15, 16, 17, 18
HSP90.4[b]			+	+		+		19, 20, 21, 22, 23
WD40 protein[c]				+		+		24, 25, 26
WD40 protein[a]				+		+		24, 25, 26
SNX1[b]				+		+		27, 28, 29, 30, 31, 32
NSF[a]				+				33, 34, 35
CSN4[b]				+	+			36, 37, 38
RPT4A[a]		+			+			39

[a] present in Tables 2.1 and 2.2, [b] present in Table 2.2, [c] present in Table 2.1
[d] protein is involved signaling of or regulating the enzymatic activity of another protein

[1] Broderson et al., 2006; [2] Peterson et al., 2000; [3] Qiu et al., 2008; [4] Zhang et al., 2015; [5] Ceserani et al., 2009; [6] Bertsch et al., 1992; [7] Hirohashi et al., 1999; [8] Kuo et al., 2013; [9] Weiss et al., 2009; [10] Ahmad et al., 2011; [11] Bukau et al., 2006; [12] Cuéllar et al., 2013; [13] Akita et al., 1997; [14] Flores-Pérez and Jarvis, 2013; [15] Kovacheva et al., 2007; [16] Nielsen et al., 1997; [17] Rosano et al., 2012; [18] Sjögren et al., 2014; [19] Faou and Hoogenraad, 2012; [20] Krishna and Gloor, 2001; [21] Lotz et al., 2008; [22] Shigeta et al., 2014; [23] Young et al., 2003; [24] Eugster et al., 2004; [25] Kim et al., 2012; [26] McMahon and Mills, 2004; [27] Burda et al, 2002; [28] Gokool et al., 2007; [29] Horazdovsky et al. 1997; [30] Mari et al., 2008; [31] Seaman et al., 1998; [32] Utskarpen et al., 2007; [33]Littleton et al., 2001; [34] Wickner and Schekman, 2008; [35] Wilson et al., 1992; [36] Dohmann et al., 2008; [37] Su et al., 2011; [38] Wei et al., 2008; [39] Hatsugai et al., 2009

Although notable progress has been made describing and validating components of unconventional protein trafficking in plants using techniques such as electron microscopy and fluorescent labeling, this is one of the first reports to simultaneously identify multiple, early components of a complex forming in response to a secretory signal, in this case salicylic acid (SA).

Futher examination of these identified proteins reveal that changes in the relative abundance and apparent mobility of these MTD-interacting proteins fall into several classes **(Table 2.4)**. First, protein mobility in gel electrophoresis relative to mobility predicted by their native molecular weights fell into three classes: fractions running above the native MW (higher MW), fractions running below the MW (lower MW), or fractions running at the predicted native MW. In addition, relative changes in protein abundance compared to untreated samples were either >1 or <1. Relative changes in higher MW fractions that are >1 between treatments, often accompanied by a decrease (a relative ratio of <0) in the native MW fraction suggest that the protein was being incorporated into a larger complex, presumably the MTD interactome.

Identified interactors into three main groups: 1) SA-induced signaling proteins, related to pathogen response and downstream signaling in the cell, 2) primary/pre-existing MTD-interacting proteins, present in the interactome prior to or within the first 10 minutes of SA treatment, and 3) elicited MTD-interacting proteins, present in the interactome after 10 minutes of SA treatment. Assignment of proteins to each class was based strictly on the ratios calculated from relative protein abundance in treated and untreated cells **(Tables 2.1, 2.2,** and **2.3)** and the fraction where each protein was identified. The proteins listed in **Table 2.4** are presented roughly in the sequence that the hypothesized interactions are occurring with MTD.

Table 2.5 Possible Interpretation of Indicated Ratios in Specific Fractions
Values >1 (green) or <0 (red) at higher or native MW fractions indicate whether a protein is becoming complexed to or uncomplexed from the MTD interactome.

Interaction State	Higher MW Fraction	Native MW Fraction
complexed	>1	<0
complexed	>1	
complexed, gone, degraded		<0
uncomplexed	<0	>1
uncomplexed, gone, degraded	<0	
uncomplexed		>1

2.4.5 SA-Induced Signaling Proteins

After both 10 and 20 minute SA treatments, the kinases, MPK4 and VIK, increased in abundance in the interactome in comparison to untreated cells. MPK4, the terminal kinase in the MEKK1-MKK1/2-MPK4 ROS signaling cascade (Pitzschke et al., 2009), negatively regulates plant innate immune responses (Peterson et al., 2000; Zhang et al., 2015). In the absence of pathogen challenge, MPK4 interacts with the nuclear transcription factor WRKY33 to suppress SA-dependent defense responses (Brodersen et al., 2006; Qiu et al., 2008). VIK, a MAP kinase kinase kinase, interacts with VH1/BRL2, a receptor-like kinase of the BRI1 family (Ceserani et al., 2009). The structure of VIK suggests it is a modular protein that bridges VH1/BRL2 to other proteins and facilitates downstream kinase activity (Ceserani et al., 2009). VH1/BRL2 itself is associated with three main cellular processes: targeted protein degradation, vesicular trafficking, and signal transduction (Ceserani et al., 2009). Increased levels of these proteins in the interactome after SA treatment are consistent with their reported functions. Interestingly, the observed increase in both MPK4 and VIK was at their native, uncomplexed MWs fractions, suggesting that while they were crosslinked at the time of immunopurification, they might have been at the periphery of the complex and disassociated during sample elution or separation. This is perhaps consistent with a role in phosphorylation of one of the MTD-interactors rather than MTD itself.

2.4.6 Initial Secretory Complex

Several interactors identified (CPN20, Hsp90.4, DNAJ, and Hsp93) have previously been annotated as chaperones, proteins that help other proteins achieve or maintain their functionally active conformation via interactive stabilization, but that are not a part of a final structure (Hartl et al., 2011). Heat shock proteins (HSPs) are a family of chaperones, classified by molecular weight. Hsp90s, Hsp70s, and Hsp60s (chaperonins) are ATP- and cofactor-regulated and are generally involved in protein folding and re-folding. Interestingly, all chaperones identified here show similar changes in specific fractions in both 10 and 20 minute post-SA treatments. They also tend to decrease in abundance at high MW fractions with respect to their native MW fraction at both 10 and 20 minutes after SA treatment in comparison to levels in untreated cells. This might suggest that they are disassociating from the MTD-interactome, although it is unclear whether they are actively disassociating from the secretory machinery as part of the secretory process, or if they are detaching during column elution or gel sample preparation. Some of the identified chaperones increase in abundance at their native MWs between the 10- and 20-minute time points, in parallel with the observed decrease in the high MW fractions. These trends in protein levels and mobility shifts suggest that chaperones are possibly early interactors in the secretory machinery, initially in complex with, but disassociating from MTD following SA treatment. Such preformed complexes could stabilize MTD or be part of a preformed complex, providing increased efficiency of MTD secretion, a pathogenesis-related protein, with consequent benefits to cellular defense responses.

CPN20 and Hsp90.4 both decrease in abundance at higher MW fractions by 20 minutes after SA treatment, suggesting that they are disassociating from the MTD-interactome relative to untreated cells. Although this suggests the existence of a preformed MTD-“chaperone” complex, neither CPN20 nor Hsp90.4 were identified at the 10-minute treatment time point. Again, this might be simply because they were on the periphery of the MTD-interacting complex and are thus easier to destabilize, or they might represent transient complexes that interact between 10-20 minutes. Of course, there simply might not have been enough replicates to capture these low abundance proteins. CPN20 is thought to be a co-chaperonin that assists chaperonin CPN60 in protein folding (Bertsch 1992, Hirohashi 1999, Weiss 2009). More recently, it has been implicated in the activation of the iron superoxide dismutase (FeSOD) in chloroplasts by direct interaction (Kuo et al., 2013). In *A. thaliana*, there are 7 proteins in the Hsp90 family, 4 of which are cytosolic (Hsp90.1-Hsp90.4), one localized to the chloroplast (Hsp90.5), one localized to the mitochondria (Hsp90.6), and one localized to the ER (Hsp90.7) (Krishna and Gloor, 2001). Hsp90s are molecular chaperones involved in protein folding, stabilization, trafficking, and degradation (Shigeta et al., 2014). Vesicular stomatitis virus glycoprotein (VSVG) transport between Golgi cisternae requires Hsp90 ATPase activity and it forming a complex with a co-chaperone, tetratricopeptide repeat domain 1 (TPR1) (Lotz et al., 2008). A final interesting functional correlation is that mitochondrial protein import requires both Hsp90 and Hsp70 to transfer preproteins to the TOM (translocase of the outer mitochondria membrane) complex (Young et al., 2003; Faou and Hoogenraad, 2012).

DNAJ, like the other HSPs identified in the 20-minute treatment interactome, decreases in abundance relative to untreated samples in fractions above its native MW. DNAJ, a member of the Hsp40 family, is a chaperone that works in conjunction with Hsp70s to assure proper folding of proteins in both healthy and stressed cells (Bukau et al., 2006; Ahmad et al., 2011). Generally, Hsp40 chaperones regulate the ATPase activity of their associated Hsp70s, as well as assist in binding and transferring their substrate proteins (Cuéllar et al., 2013). DNAJ can also act as an independent chaperone, preventing unfolded polypeptides from aggregating (Cuéllar et al., 2013).

In addition to having the same accumulation profile as CPN20, Hsp90.4, and DNAJ at the 20-minute time point, Hsp93-III also decreases in abundance in MW fractions higher than their native MW at 10 minutes. Not only do both Hsp93-III and Hsp93-V decrease in abundance at higher MW fractions at both 10 and 20 minutes, but they increase in abundance in their uncomplexed MW fraction at 20 minutes and between 10 and 20 minutes after treatment. This is consistent with the hypothesis that these chaperonins are early members of the secretory interactome. In *A. thaliana*, Hsp93-III (ClpC2) and Hsp93-V (ClpC1), paralogs on different chromosomes that share 91% sequence identity (Kovacheva et al., 2007), are essential for chloroplast function. Hsp93-III and Hsp93-V are two of the four total Hsp100 proteins found in plant chloroplasts (Sjögren et al., 2014). Although ClpC function of Hsp93 in plants in uncertain, a ClpC ortholog in *Synechococcus elongatus* was shown to prevent protein aggregation and resolubilize/refold aggregated polypeptides (Andersson et al., 2009). Chloroplast ClpC is a chaperone associated with the Clp protease complex, which is localized both in the stroma and on envelope membranes (Sjögren et al., 2014). The stromal Clp protease maintains protein homeostasis via degradation of damaged proteins and protein complexes (Sjögren et al., 2014). Because it is found at the envelope membrane in close proximity to Tic110, a subunit of the TIC (translocon on inner chloroplast membrane) complex (Akita et al., 1997; Nielsen et al., 1997), and has been found to bind transit peptides (Rosano et al., 2011), ClpC is thought to be involved in chloroplastic import of cytosolic preproteins (Flores-Pérez and Jarvis, 2013). The specific function of the Clp protease at the envelope membrane and how it might be involved in preprotein import is, however, currently unknown. (Sjögren et al., 2014).

The 5 initial MTD-interacting proteins (those that interact with MTD at <10 minutes post-treatment) identified in these analyses were selected based on data from both the 10 and 20 minute treatments. This included abundance and relative increases or decreases of these interactors in comparison to untreated cells. Upon further analysis, the similarity and functional overlap of these five proteins became apparent. CPN20, DNAJ, Hsp93-III, and Hsp93-V have all been implicated in protein folding, and therefore, protein binding. CPN20 and the Hsp93s regulate co-chaperones and proteases, respectively; and all 3 HSPs (Hsp93-III, Hsp93-V, and Hsp90.4) are involved in protein import into either the chloroplast or the mitochondria by binding substrate proteins. Based on the known functional roles of these chaperones and HSPs, they seem likely to be involved in MTD stabilization or transfer to other protein/complexes upon SA treatment. They could be stabilizing cytoplasmic MTD or be part of a preformed secretory complex, increasing the rapidity of MTD secretion in response to infection. Since some of these proteins have regulatory functions, it further suggests that they form a primed, partially preformed complex, awaiting a signal, such as a post-translational modification or the binding of another protein, for activation.

2.4.7 MTD-Interacting Proteins with Maximum Presence after 10 Minutes

Although the abundance of the identified components of the MTD interactome in this section have varying trends, all appear to be present at 10 minutes after SA treatment. Some of these proteins appear to display increases in abundance in native MW fractions that mirror decreases in higher MW fractions as proteins proposed to be associated with what is being called the "primary complex." The proteins discussed below (with the exception of NSF), however, are not present in higher MW fractions, but are only identified in their native MW fractions. Based on their functions, these proteins would have an important role the the primary complex involved in MTD secretion.

One or more WD40 repeat proteins increase in abundance in their native MW fractions both 10 and 20 minutes after treatment in comparison to untreated cells, although only one of them (WD40 protein [8860]) is detected at 20 minutes. Comparing the two time points, however, WD40-8860 has decreasing levels in its native MW fractions from 10 to 20 minutes. Together, these two observations suggest that SA increases levels of WD40 proteins, but as treatment time progresses, these proteins are degraded or disassociate from MTD. COPI subunits (α- and β'-COP) have terminal WD40 repeats that are required for interaction with other coatomer subunits (Kim et al., 2012) as well as cargo selection (Eugster et al., 2004; McMahon and Mills, 2004). COPII subunits (Sec13/31p) and clathrin also have terminal WD40 domains that recruit additional proteins during vesicle formation (McMahon and Mills, 2004).

SNX1 (sorting nexin 1) was detected only in the 20-minute SA treatment, with lower levels in its native MW fraction compared to untreated cells. Because it was not observed at 10 minutes, SNX1 might interact with the secretome transiently between the 10- and 20-minute time points. In yeast, Vps5p (vacuolar protein sorting) (a SNX1 homolog) is involved in endosomal trafficking as part of a retromer complex, composed of five subunits, that functions as a vesicle coat (Seaman et al., 1998). An analogous mammalian retromer has the same function as the yeast retromer (Gokool et al., 2007). SNX1 can bind to PtdIns3P (phosphatidylinositol 3-phosphate) and highly curved membranes via a region of Phox (PX) homology and Bin/Amphiphysin/Rvs (BAR) domains, respectively (Horazdovsky et al., 1997; Burda et al., 2002; Gokool et al., 2007). PX domain proteins form a diverse family that is involved is a variety of cellular functions, including cell signaling, and membrane trafficking and remodeling (Teasdale and Collins, 2012). The PX domain, a globular fold composed of β-strands and α-helices, is an important protein-protein interaction domain involved in binding endocytic/exocytic machinery and transmembrane proteins. The BAR domain superfamily has membrane-shaping proteins with the ability to induce, stabilize, or detect membrane curvature (Frost et al., 2009). Curvature caused by BAR domain proteins often recruits and facilitates binding of other BAR domain proteins in a positive feedback cycle; the BAR domain dimerizes into modules via its coiled-coils. The presence of SNX1 is consistent with the observation that cargo proteins, such as sortillin and the mannose 6-phosphate receptors (MPRs), are sorted at endosomal membranes by retromer complexes (Mari et al., 2008). These complexes can also mediate formation of vesicles and tubules for transport from endosomes to the TGN (Gokool et al., 2007). SNX1 and SNX2 also mediate retrograde transport of the Shiga toxin protein into the Golgi (Utskarpen et al., 2007).

CSN4 (COP9 signalosome 4) increases in its native MW fraction at 20 minutes relative to levels in untreated cells as well as increases between the 10- and 20-minute time points. Because it was not detected at 10 minutes, a random, low abundance value was selected for the ratio calculation, suggesting that CSN4 does not become part of the interactome until after 10 minutes of treatment. The COP9 signalosome (CSN), a conserved complex in all eukaryotes, is part of the ubiquitin-proteasome pathway and is composed of eight subunits, CSN1-CSN8 (Wei et al., 2008). CSN4, identified in SA20, affects cell division and causes arrest at G2

(Dohmann et al., 2008). In mice, CSN8/CSN was shown to be required for autophagosome maturation in the lysosomal pathway, likely through Rab7 regulation (Su et al., 2011).

RPT4A (regulatory particle triple-ATPase 4A) was identified at both treatment time points, showing increases in the native MW fractions, implying that RPT4A interaction with the MTD-interactome is triggered by SA. Although the increases compared to the untreated proteins are different between the two time points, the comparison of relative abundance indicates there are similar amounts of RPT4A in the interactome throughout treatment. The presence of this proteasomal regulatory protein is an intriguing result because fusion of the vacuolar membrane to the PM as a method of unconventional secretion is reported to require a catalytically active proteasome in *A. thaliana* (Hatsugai et al., 2009).

NSF (N-ethylmaleimide-sensitive factor) was detected at both time points, but showing very different profiles. At 10 minutes, NSF shows a slight decrease, while at 20 minutes it increases in abundance approximately by a ratio of 10. The comparison of relative NSF abundance between the two time points confirms that NSF levels at 20 minutes are substantially higher. Vesicular fusion involves NSF (Wilson et al., 1992), although it is not needed for the actual fusion itself. NSF, an AAA-ATPase chaperone, is required, however, for disassembling SNARE complexes after membrane fusion. This requires α-SNAP, an adapter protein that allows NSF to bind to the SNAP-SNARE complexes (Littleton et al., 2001; Wickner and Schekman, 2008).

The 6 elicited or SA-associated MTD-interacting proteins also share functionality. The 2 WD40 repeat proteins, SNX1, NSF, and CSN4 have all been implicated in various forms and stages of vesicular trafficking. WD40 proteins and SNX1 are both involved with vesicular coat formation; additionally, WD40 proteins are required for certain forms of cargo selection. CSN4 is required for autophagosome maturation and is a part of the COP9 signalosome, involved in the ubiquitin-proteasome pathway. RPT4A, a proteasomal regulatory protein, was also identified. Lastly, NSF is required for disassembling complexes responsible for membrane (e.g. vesicular) fusion. Together, these proteins suggest that MTD secretion utilizes some form of vesicular or endosomal trafficking. As mentioned previously, unconventional secretion in animal cells can occur similar to autophagy and it is not unlikely that a similar mechanism occurs in plants.

2.5 Conclusions and Future Perspectives

With the exception of the two early appearing (10 minutes), stress-induced kinases (MPK4 and VIK), the 11 remaining identified proteins have all been previously implicated in various aspects of vesicular trafficking. The 5 proteins hypothesized to be part of the pre-existing complex or initial secretory interactome included 3 molecular chaperones (Hsp90.4, Hsp93-III, Hsp93-V) as well as 2 co-chaperones (CPN20 and DNAJ). Interestingly, although these proteins are grouped solely based on observed changes in abundance and mobility shifts (interaction with MTD); this coincidentally resulted in similar functional grouping. This is an intriguing result because these proteins are involved in some way, whether alone or in conjunction with another protein, with stabilization and folding. Thus, the idea of a pre-formed complex stabilizing MTD in the cytosol, awaiting a secretory trigger, is plausible. The remaining 6 identified proteins were also only grouped by changes in abundance and mobility shift between untreated and treated cells. This group of proteins was also similar functionally, and although more diverse than the first group, all are involved in some stage of vesicular trafficking. Three proteins involved in cargo sorting and vesicular formation were identified. Two proteins had WD40 repeats (also seen in COPII and clathrin), that are responsible for cargo and coatomer interaction. The third protein, SNX1, a subunit of a retromer complex that functions as a vesicle coat with the ability to sort cargo, was also identified in this group. CSN4, a subunit of the COP9 signalosome, required for autophagosome maturation, was also part of this second group. The proteasomal regulatory protein RPT4A (identified in both treated groups) is required for vacuolar fusion to the PM and protein secretion into the extracellular space. Lastly, NSF was identified, a protein involved in SNARE complex disassembly. This second group of proteins supports the hypothesis that MTD is secreted by a vesicular trafficking mechanism.

Although these proteins might have been initially reported in unassociated vesicular trafficking pathways (not necessarily secretory pathways), at least one of the proteins in the second group was previously reported to be associated with a functional step of endosomal or vesicular trafficking (e.g. cargo selection, vesicle formation, vesicle maturation). These two groups combined create a model consisting of a pre-formed MTD complex, primed for secretion that upon receiving a secretory trigger is secreted via some sort of vesicular pathway.

Although the cellular signal(s) for MTD secretion has (have) not been identified, there are many possibilities, such as post-translation modifications (PTMs) to MTD or one of its interacting proteins. A similar approach (MTD-complex enrichment coupled with LC/MS/MS) will be used to assess the possible role of PTMs in signaling MTD secretion. Thus, elucidating an unconventional secretory pathway in plants can accelerate the understanding and future application of this important cellular function in all cell types.

2.6 References

Ahmad A, Bhattacharya A, McDonald RA, Cordes M, Ellington B, Bertelsen EB, Zuiderweg ERP (2011) Heat shock protein 70 kDa chaperone/DnaJ cochaperone complex employs an unusual dynamic interface. Proc Natl Acad Sci USA **108**:18966-18971

Akita M, Nielsen E, Keegstra K (1997) Identification of protein transport complexes in the chloroplastic envelope membranes via chemical cross-linking. J Cell Biol **136**:983-994

Andersson FI, Tryggvesson A, Sharon M, Diemand AV, Classen M, Best C, Schmidt R, Schelin J, Stanne TM, Bukau B, Robinson CV, Witt S, Mogk A, Clarke AK (2009) Structure and function of a novel type of ATP-dependent Clp protease. J Biol Chem **284**:13519-13532

Bertsch U, Jürgen S, Seetharam R, Viitanen P (1992) Identification, characterization, and DNA sequence of a functional “double” groES-like chaperonin from chloroplasts of higher plants. Proc Natl Acad Sci USA **89**:8696-8700

Blackburn K, Cheng FY, Williamson JD, Goshe MB (2010) Data-independent liquid chromatography/mass spectrometry (LC/MSE) detection and quantification of the secreted Apium graveolens pathogen defense protein mannitol dehydrogenase. Rapid Commun Mass Spectrom **24**:1009-1016

Bradford, MM (1976) A rapid and sensitive method for the quantitation of microgram quantifies of protein utilizing the principle of protein-dye binding. Anal Biochem **72**:248-254

Brodersen P, Petersen M, Nielsen HB, Zhu S, Newman MA, Shokat KM, Rietz S, Parker J, Mundy J (2006) *Arabidopsis* MAP kinase 4 regulates salicylic acid- and jasmonic acid/ethylene-dependent responses via EDS1 and PAD4. Plant J **47**:532-546

Bukau B, Weissman J, Horwich A (2006) Molecular chaperones and protein quality control. Cell **125**:443-451

Burda P, Padilla SM, Srimonti S, Emr SD (2002) Retromer function in endosome-to-golgi retrograde transport is regulated by the yeast Vps34 PtdIns 3-kinase. J Cell Sci **115**:3889-3900

Ceserani T, Trofka A, Gandotra N, Nelson T (2009) VH1/BRL2 receptor-like kinase interacts with vascular-specific adaptor proteins VIT and VIK to influence leaf venation. Plant J **57**:1000-1014

Cheng FY, Blackburn K, Lin LM, Goshe MB, Williamson JD (2009a) Absolute protein quantification by LC/MS^E for global analysis of salicylic acid-induced plant protein secretion responses. J Proteome Res **8**:82-93

Cheng FY, Zamski E, Guo WW, Pharr DM, Williamson JD (2009b) Salicylic acid stimulates secretion of the normally symplastic enzyme mannitol dehydrogenase: a possible defense against mannitol-secreting fungal pathogens. Planta **230**:1039-1103

Chrispeels MJ, Raikhel NV (1991) Lectins, lectin genes, and their role in plant defense. Plant Cell **3**:1-9

Chu CC, Li HM (2012) The amino-terminal domain of chloroplast hsp93 is important for its membrane association and functions *in vivo*. Plant Physiol **158**:1656-1665.

Clough SJ, Bent AF (1998) Floral dip: a simplified method for *Agrobacterium*-mediated transformation of *Arabidopsis thaliana*. Plant J **16**:735-743

Coleman CE, Herman EM, Takasaki K, Larkins BA (1996) The maize γ-zein sequesters α-zein and stabilizes its accumulation in protein bodies of transgenic tobacco endosperm. Plant Cell **8**:2335-2345

Cuéllar J, Perales-Calvo J, A. Muga A, Valpuesta JM, Moro F (2013) Structural insights into the chaperone activity of the 40-kda heat shock protein DnaJ. J Biol Chem **288**:15065-15074

Dohmann EMN, Levesque MP, De Veylder L, Reichardt I, Jürgens G, Schmid M, Schwechheimer C (2008) The *Arabidopsis* COP9 signalosome is essential for G2 phase progression and genomic stability. Development **135**:2013-2022

Drakakaki G, Dandekar A (2013) Protein secretion: How many secretory routes does a plant cell have? Plant Sci **203-204**:74-78

Eugster A, Frigerio G, Dale M, Duden R (2004) The α- and β'-COP WD40 domains mediate cargo-selective interactions with distincy di-lysine motifs. Mol Biol Cell **15**:1011-1023

Faou P, Hoogenraad NJ (2012) Tom34: A cytosolic cochaperone of the Hsp90/Hsp70 protein complex involved in mitochondrial protein import. Biochim Biophys Acta **1823**:348-357

Flores-Péres Ú, Jarvis P (2013) Molecular chaperone involvement in chloroplast protein import. Biochim Biophys Acta **1833**:332-340

Frost A, Unger VM, De Camilli P (2009) The bar domain superfamily: membrane-molding macromolecules. Cell **137**:191-196

Gokool S, Tattersall D, Seaman MNJ (2007) EHD1 interacts with retromer to stabilize SNX1 tubules and facilitate endosome-to-golgi retrieval. Traffic **8**:1873-1886

Hartl UF, Bracher A, Hayer-Hartl M (2011) Molecular chaperones in protein folding and proteostasis. Nature **475**:324-332

Hatsugai N, Iwasaki S, Tamura K, Kondo M, Fuji K, Ogasawara K, Nishimura M, Hara-Nishimura I (2009) A novel membrane fusion-mediated plant immunity against bacterial pathogens. Genes Dev **23**:2496-2506

He C, Klionsky DJ (2009) Regulation mechanisms and signaling pathways of autophagy. Annu Rev Genet **43**:67-93

Hirohashi T, Nishio K, Nakai M (1999) cDNA sequence and overexpression of chloroplast chaperonin 21 from *Arabidopsis thaliana*. Biochim Biophys Acta **1429**:512-515

Hood EE, Gelvin SB, Melchers LS, Hoekema A (1993) New *Agrobacterium* helper plasmids for gene transfer to plants. Transgenic Res **2**:208-218

Horazdovsky BF, Davies BA, Seaman MNJ, McLaughlin SA, Yoon SH, Emr SD (1997) A sorting nexin-1 homologue, Vps5p, forms a complex with Vps17p and is required for recycling the vacuolar protein-sorting receptor. Mol Biol Cell **8**:1529-1541

Jennings DB, Ehrenshaft M, Pharr DM, Williamson JD (1998) Roles for mannitol and mannitol dehydrogenase in active oxygen-mediated plant defense. Proc Natl Acad Sci USA **95**:15129-15133

Kadota Y, Shirasu K (2012) The HSP90 complex of plants. Biochim Biophys Acta **1823**:689-697

Karpinska B, Karlsson M, Schinkel H, Streller S, Süss KH, Melzer M, Wingsle G (2001) A novel superoxide dismutase with a high isoelectric point in higher plants. Expression, regulation, and protein localization. Plant Physiol **126**:1668-1677

Kim KH, Kim EK, Jeong KY, Park YH, Park HM (2012) Effects of mutations in the WD40 domain of α-COP on its interaction with the COPI coatomer in *Saccharomyces cerevisiae*. J Microbiol **50**:256-262

Kovacheva S, Bédard J, Wardle A, Patel R, Jarvis P (2007) Further *in vivo* studies on the role of the molecular chaperone, Hsp93, in plastid protein import. Plant J **50**:364-379

Krishna P, Gloor G (2001) The Hsp90 family of proteins in *Arabidopsis thaliana*. Cell Stress Chaperones **6**:238-246.

Kuo WY, Huang CH, Liu AC, Cheng CP, Li SH, Chang WC, Weiss C, Azem A, Jinn TL (2013) CHAPERONIN 20 mediates iron superoxide dismutase (FeSOD) activity independent of its co-chaperonin role in *Arabidopsis* chloroplasts. New Phytol **197**:99-110

Levine B, Klionsky DJ (2004) Development by self-digestion: molecular mechanisms and biological functions of autophagy. Dev Cell **6**:463-477

Littleton TJ, Barnard RJO, Titus SA, Slind J, Chapman ER, Ganetzky B (2001) SNARE-complex disassembly by NSF follows synaptic-vesicle fusion. Proc Natl Acad Sci USA **98**:12233-12238

Lotz GP, Brychzy A, Heinz S, Obermann WMJ (2008) A novel HSP90 chaperone complex regulates intracellular vesicle transport. J Cell Sci **121**:717-723

Mari M, Bujny MV, Zeuschner D, Geerts WJC, Griffith J, Petersen CM, Cullen PJ, Klumperman J, Geuze HJ (2008) SNX1 defines and early endosomal recycling exit for sortilin and mannose 6-phosphate receptors. Traffic **9**:380-393

Mathur J, Koncz C (1998) Establishment and maintenance of cell suspension cultures. Methods Mol Biol **82**:27-30

Mayer MP, Bukau B (2005) Hsp70 chaperones: cellular functions and molecular mechanism. Cell Mol Life Sci **62**:670-684

McMahon HT, Mills IG (2004) COP and clathrin-coated vesicle budding: different pathways, common approaches. Curr Opin Cell Biol **16**:379-391

Michaeli S, Avin-Wittenberg T, Galili G (2014) Involvement of autophagy in the direct ER to vacuole protein trafficking route in plants. Front Plant Sci **5**:1-5

Murashige T, Skoog F (1962) A revised medium for rapid growth and bioassays with tobacco tissue cultures. Physiol Plant **15**:473-497

Nielsen E, Akita M, Davila-Aponte J, Keegstra K (1997) Stable association of chloroplastic precursors with protein translocation complexes that contain proteins from both envelope membranes and a stromal Hsp100 molecular chaperone. EMBO J **16**:935-946

Petersen M, Brodersen P, Naested H, Anreasson E, Lindhart U, Johansen B, Nielsen HB, Lacy M, Austin MJ, Parker JE, Sharma S (2000) *Arabidopsis* MAP kinase 4 negatively regulates systemic acquired resistance. Cell **103**:1111-1120

Pitzschke A, Djamei A, Bitton F, Hirt H (2009) A major role of the MEKK1–MKK1/2–MPK4 pathway in ROS signalling. Mol Plant **2**:120–137

Qiu JL, Fiil BK, Petersen K, Nielsen HB, Botanga CJ, Thorgrimsen S, Palma K, Suarez-Rodriguez MC, Sandbech-Clausen S, Lichota J, Brodersen P, Grasser KD, Mattsson O, Glazebrook J, Mundy J, Petersen M (2008) *Arabidopsis* MAP kinase 4 regulates gene expression through transcription factor release in the nucleus. EMBO J **27**:2214-2221

Rabouille C, Malhotra V, Nickel W (2012) Diversity in unconventional protein secretion. J Cell Sci **125**:5251-5255

Rosano GL, Bruch EM, Colombo CV, Ceccarelli EA (2012) Toward a unified model of the action of CLP/HSP100 chaperones in chloroplasts. Plant Signal Behav **7**:672-674

Rubartelli A, Cozzolino F, Talio M, Sitia R (1990) A novel secretory pathway for interleukin-1β, a protein lacking a signal sequence. EMBO J **9**:1503-1510

Seaman MNJ, McCaffery JM, Emr SD (1998) A membrane coat complex essential for endosome-to-golgi retrograde transport in yeast. J Cell Biol **142**:665-681

Shigeta T, Zaizen Y, Asami T, Yoshida S, Nakamura Y, Okamoto S, Matsuo T, Sugimoto Y (2014) Molecular evidence of the involvement of heat shock protein 90 in brassinosteroid signaling in *Arabidopsis* T87 cultured cells. Plant Cell Rep **33**:499-510

Sjögren LLE, Tanabe N, Lymperopoulos P, Khan NZ, Rodermel SR, Aronsson H, Clarke AK (2014) Quantitative analysis of the chloroplast molecular chaperone ClpC/Hsp93 in *Arabidopsis* reveals new insights into its localization, interaction with the Clp proteolytic core, and functional importance. J Biol Chem **289**:11318-11330

Stoop JMH, Williamson JD, Pharr DM (1996) Mannitol metabolism in plants: a method for coping with stress. Trends Plant Sci **1**:139-144

Streller S, Wingsle G (1994) *Pinus sylvestris* L. needles contain extracellular CuZn superoxide dismutase. Planta **192**:195-201

Su H, Li F, Ranek MJ, Wei N, Wang X (2011) COP9 signalosome regulates autophagosome maturation. Circulation **124**:2117-2128

Teasdale RD, Collins BM (2012) Insights into the PX (phox-homology) domain and SNX (sorting nextin) protein families: structures, functions and roles in disease. Biochem J **441**:39-59

Utskarpen A, Slagsvold HH, Dyve AB, Skånland SS, Sandvig K (2007) SNX1 and SNX2 mediate retrograde transport of *Shiga* toxin. Biochem Biophys Res Commun **358**:566-570

Van Damme EJM, Peumans WJ, Barre A, Rougé P (1998) Plant lectins: a composite of several distinct families of structurally and evolutionary related proteins with diverse biological roles. Crit Rev Plant Sci **17**:575-692

Vasilescu J, Guo X, Kast J (2004) Identification of protein-protein interactions using *in vivo* cross-linking and mass spectrometry. Proteomics **4**:3845-3854

Wei N, Serino G, Deng XW (2008) The COP9 signalosome: more than a protease. Trends Biochem Sci **33**:592-600

Weiss C, Bonshtien A, Farchi-Pisanty O, Vitlin A, Azem A (2009) Cpn20: Siamese twins of the chaperonin world. Plant Mol. Biol **69**:227-238

Wickner W, Schekman R (2008) Membrane fusion. Nat Struct Mol Biol **15**:658-664

Williamson JD, Galili D, Larkins BA, Gelvin SB (1988) The synthesis of a 19 kilodalton zein protein in transgenic petunia plants. Plant Physiol **88**:1002-1007

Williamson JD, Stoop JMH, Massel MO,Conkling MA, Pharr DM (1995) Sequence analysis of a mannitol dehydrogenase cDNA from plants reveals a function for the pathogenesis-related protein ELI3. Proc Natl Acad Sci USA **92**:7148-7152

Wilson DW, Whiteheart SW, Wiedmann M, Brunner M, Rothman JE (1992) A multisubunit particle implicated in membrane fusion. J Cell Biol **117**:531-538

Yamamoto YT, Zamski E, Williamson JD, Conkling MA, Pharr DM (1997) Subcellular localization of celery mannitol dehydrogenase: a cytosolic metabolic enzyme in nuclei. Plant Physiol **115**:1397-1403

Young JC, Hoogenraad NJ, Hartl FU (2003) Molecular chaperones Hsp90 and Hsp70 deliver preproteins to the mitchondrial import receptor Tom70. Cell **112**:41-50

Zamski E, Guo WW, Yamamoto YT, Pharr DM, Williamson JD (2001) Analysis of celery (*Apium graveolens*) mannitol dehydrogenase (Mtd) promoter regulation in *Arabidopsis* suggests roles for MTD in key environmental and metabolic responses. Plant Mol Biol **47**:621-631

Zamski E, Yamamoto YT, Williamson JD, Conkling MA, Pharr DM (1996) Immunolocalization of mannitol dehydrogenase in celery plants and cells. Plant Physiol **112**:931-938

Zhang T, Zhu M, Song WY, Harmon AC, Chen S (2015) Oxidation and phosphorylation of MAP kinase 4 cause protein aggregation. Biochim Biophys Acta **1854**:156-165

APPENDICES

APPENDIX A

Verification of MTD-Complex via Immunoblotting

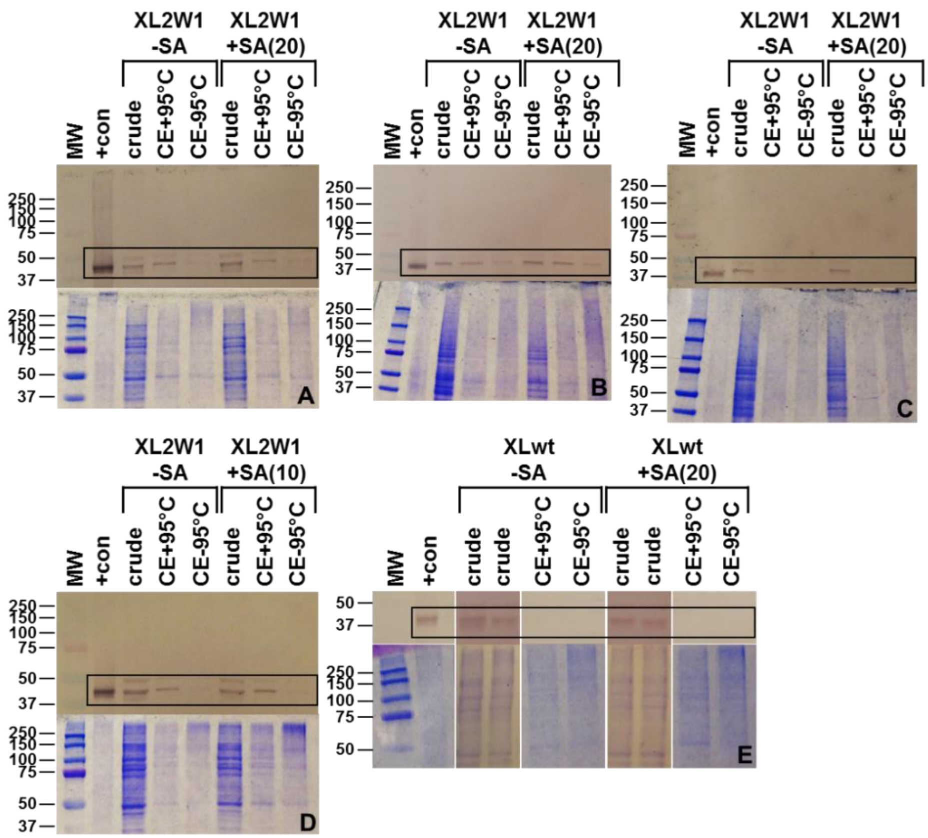

Figure A.1. MTD-Complex Co-Immunopurification
After blotting, gels stained with Coomassie Blue are shown below their corresponding immunoblots. Heavier banding at higher MWs and decreased MTD at its native MW at 40 kDa (indicated by a black box) in unheated samples, indicate the presence of anti-MTD reactive complexes preserved by crosslinking, and are visible on both the gel and immunoblot. MTD was detected and visualized using alkaline phosphatase (AP)-labeled 2° (anti-rabbit) antibody following 1° (anti-MTD) antibody. MTD and its location indicated by black rectangles. **A-C)** 20-minute SA treatment of XL2W1 cells. Gel shift visible in Rep1 (A) and Rep2 (B); there is less contrast in Rep3 (C), but still visible using Coomassie Blue. **D)** 10-minute SA treatment of XL2W1 cells with MTD present in the elutions. **E)** No MTD present in the combined elution from wt cells, but present in crude extract.

+con, celery MTD (positive control); 2W1, transformed cells; XL, crosslinked; SA, salicylic acid; CE, combined elution; FT, flow through; E, elution; MW, molecular weights; WT, wild-type

APPENDIX B

In-Gel Tryptic Digestion Excisions

Figure B.1. In-Gel Digestion Fractions
A total of 11 fractions (F1-F11) were excised from each lane using MW for reference. Sample replicates from each individual gel were combined (i.e. lanes 2-4 and 6-8). Protein contained in the gel pieces were digested using trypsin and resulting peptides were analyzed via LC/MS/MS. Each set of untreated cells has corresponding SA-treated cells. Three replicates, Rep1 **(A, B)**, Rep2 **(C, D)**, and Rep3 **(E, F)**, of untreated XL2W1 **(A, C, E)** with corresponding SA-treated (20min) **(B, D, F)** cells. Untreated XL2W1 with corresponding SA-treated (10min) cells **(G, H)**. Untreated wt with corresponding SA-treated (20min) wt cells **(I, J)**.

MW, molecular weights; CE, combined elution; XL, crosslinked; 2W1, transformed cells; WT, wild-type; SA, salicylic acid

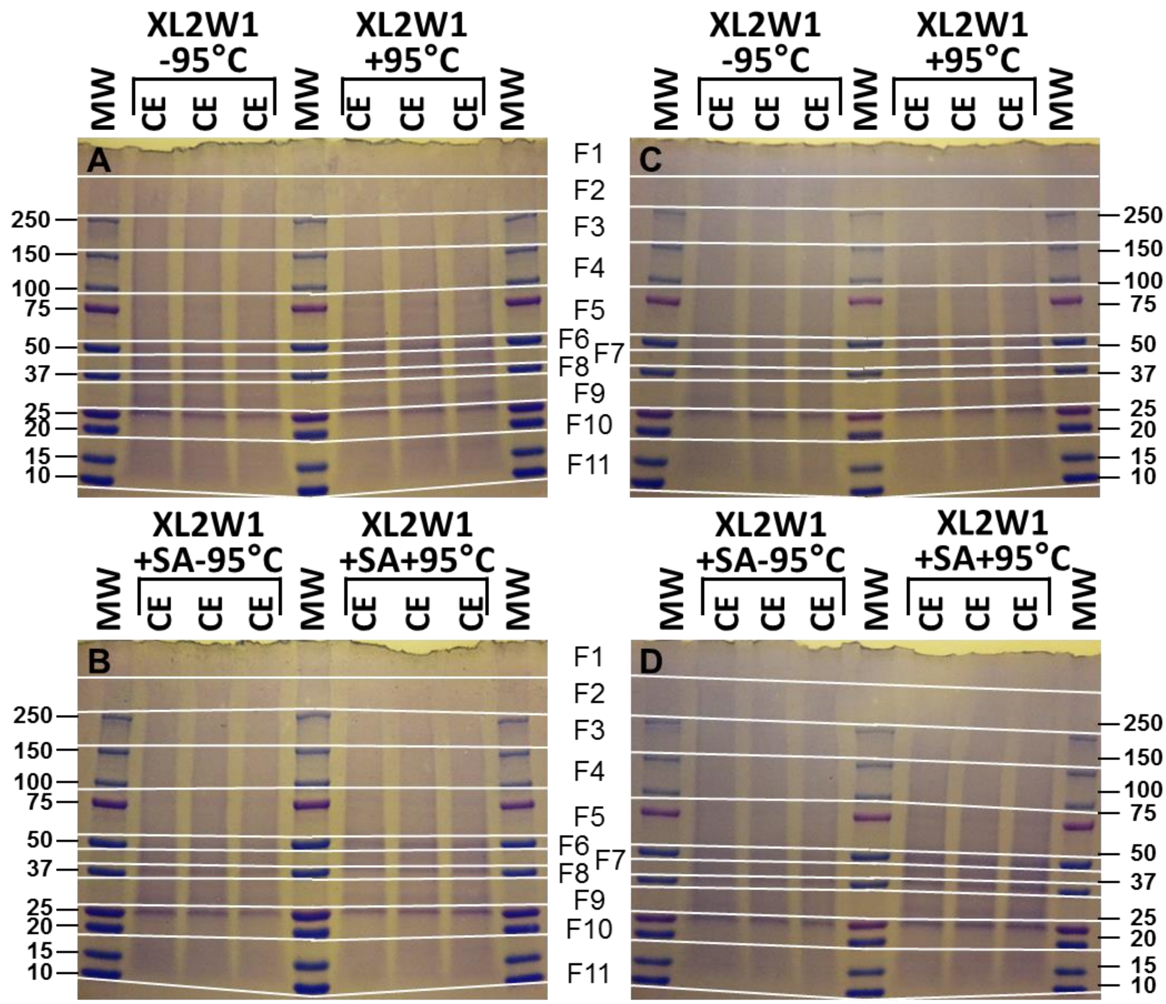

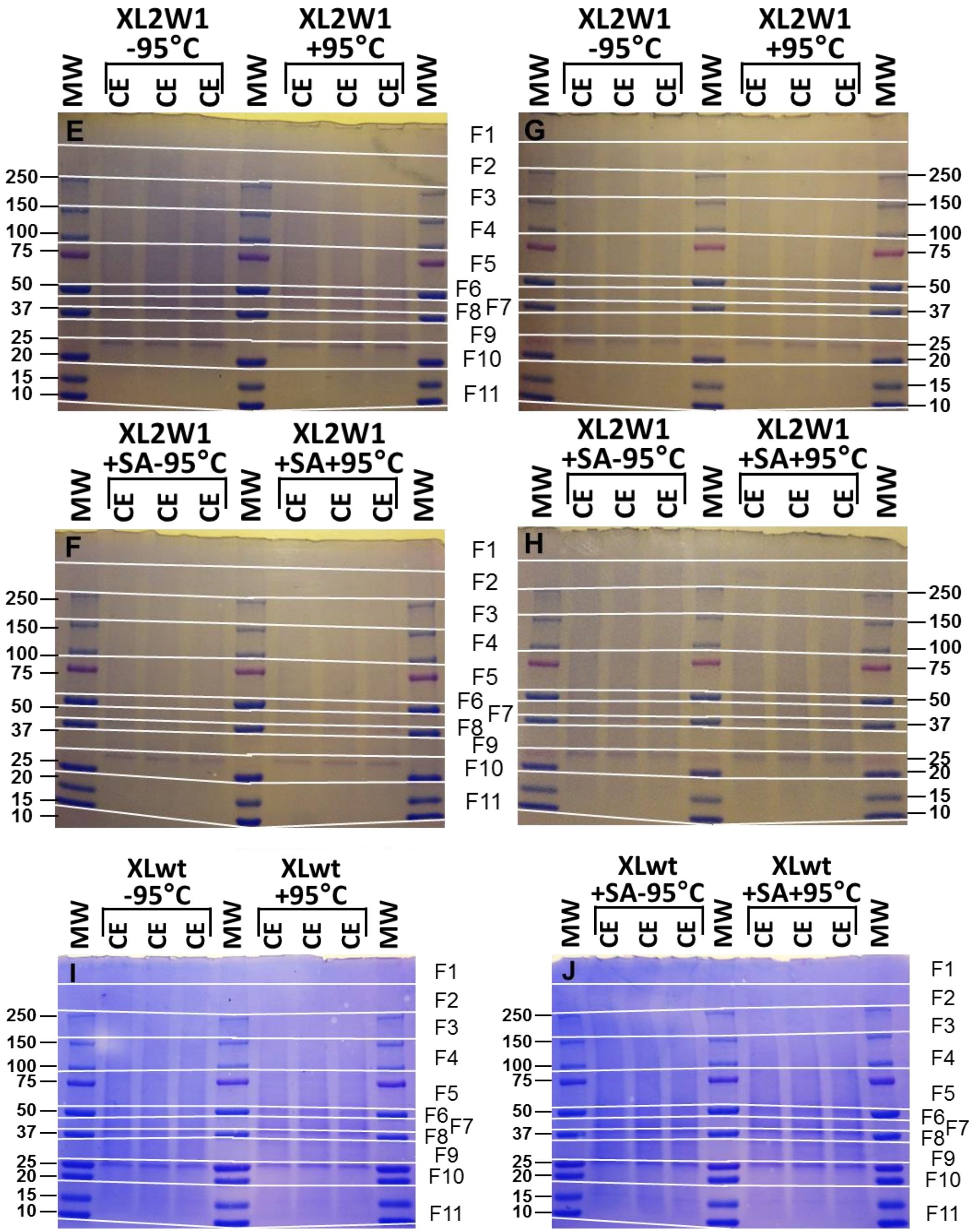

XL2W1 -95°C
XL2W1 +95°C
MW
CE
E
G
F
H
XL2W1 +SA-95°C
XL2W1 +SA+95°C
XLwt -95°C
XLwt +95°C
XLwt +SA-95°C
XLwt +SA+95°C
I
J
250
150
100
75
50
37
25
20
15
10
F1
F2
F3
F4
F5
F6
F7
F8
F9
F10
F11

APPENDIX C

Data Normalization and Optimization of Comparative Analysis

Figure C.1. Selection of Normalization and Comparison Method
PCA plots created without normalization, with minimum normalization, or with Scaffold normalization of total precursor intensity values of XL2W1 cells. Untreated and SA-treated (20min) cells are differentiated by color, blue and red, respectively; replicates are differentiated by shape, circle (Rep1), diamond (Rep2), or square (Rep3). **A)** Whole Sample Comparisons. Protein identifications from the whole sample set (F2-F8 combined) using different normalization methods. Replicates are more different than treatments, thus they are unable to be grouped. **B)** Sliding Duplicate Comparisons. Sliding duplicates include too many proteins and eliminates the difference between treated and untreated samples. Similar to whole sample comparisons, the difference between replicates is greater than the difference between treatment groups. **C)** Individual Band Comparisons. Overall, Scaffold normalization seems to provide the most consistent separation between treatment groups. In F2, the difference between replicates is greater than the difference between treatments in all normalization techniques. In F7, both no normalization and Scaffold normalization provide grouping. In F6, however, no normalization and minimum normalization exhibit more similarity between replicates, as opposed to treatments, but Scaffold normalization is the only on that provides more separation between treatment groups.

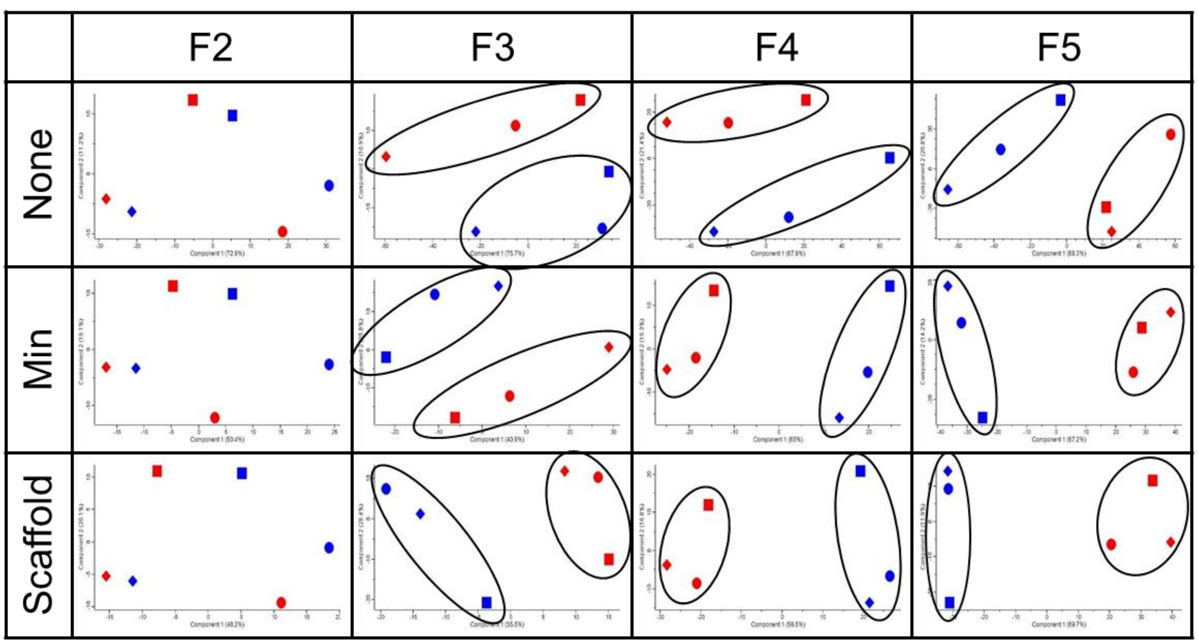

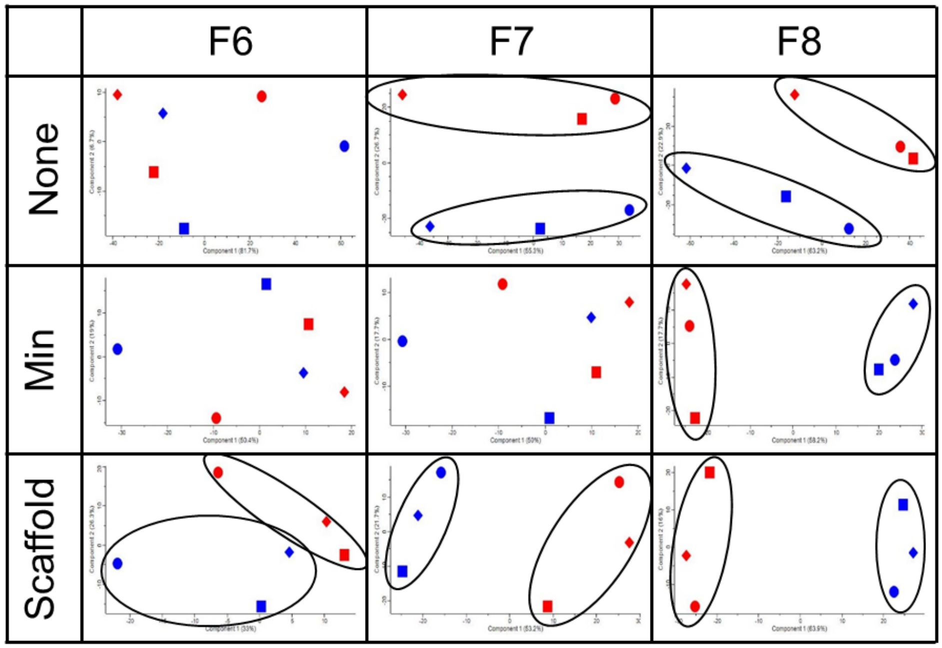
F6
F7
F8
None
Min
Scaffold

APPENDIX D

Complete List of Proteins Unique to XL2W1 Cells

Table D.1 Proteins Unique to SA10. Proteins unique to XL2W1 cells after data filtration of untreated/treated (10-minute SA) analysis.

Accession Number	Identified Proteins
AT3G12915	| Symbols: | Ribosomal protein S5/Elongation factor G/III/V family protein | chr3:4112999-4115708 FORWARD LENGTH=820
AT1G72330	| Symbols: ALAAT2 | alanine aminotransferase 2 | chr1:27233637-27236571 FORWARD LENGTH=540
AT2G42600	| Symbols: ATPPC2, PPC2 | phosphoenolpyruvate carboxylase 2 | chr2:17734541-17738679 REVERSE LENGTH=963
AT1G71380	| Symbols: ATGH9B3, ATCEL3, CEL3 | cellulase 3 | chr1:26899989-26901749 REVERSE LENGTH=484
AT3G16410	| Symbols: NSP4 | nitrile specifier protein 4 | chr3:5572145-5574359 FORWARD LENGTH=619
AT4G02290	| Symbols: AtGH9B13, GH9B13 | glycosyl hydrolase 9B13 | chr4:1002654-1005125 REVERSE LENGTH=516
AT1G24280	| Symbols: G6PD3 | glucose-6-phosphate dehydrogenase 3 | chr1:8609495-8612383 FORWARD LENGTH=599
AT5G43010	| Symbols: RPT4A | regulatory particle triple-A ATPase 4A | chr5:17248563-17251014 REVERSE LENGTH=399
AT3G53870	| Symbols: | Ribosomal protein S3 family protein | chr3:19951547-19952782 FORWARD LENGTH=249
AT5G16570	| Symbols: GLN1;4 | glutamine synthetase 1;4 | chr5:5421898-5424523 REVERSE LENGTH=356
AT3G48870	| Symbols: ATCLPC, ATHSP93-III, HSP93-III | Clp ATPase | chr3:18122363-18126008 REVERSE LENGTH=952
AT1G17745	| Symbols: PGDH | D-3-phosphoglycerate dehydrogenase | chr1:6101157-6104979 FORWARD LENGTH=624
AT5G54510	| Symbols: GH3.6, DFL1 | Auxin-responsive GH3 family protein | chr5:22131321-22133564 REVERSE LENGTH=612
AT1G70830	| Symbols: MLP28 | MLP-like protein 28 | chr1:26710203-26711395 REVERSE LENGTH=335
AT5G53460	| Symbols: GLT1 | NADH-dependent glutamate synthase 1 | chr5:21700518-21709629 FORWARD LENGTH=2208
AT3G46440	| Symbols: UXS5 | UDP-XYL synthase 5 | chr3:17089268-17091611 REVERSE LENGTH=341
AT1G80240	| Symbols: | Protein of unknown function, DUF642 | chr1:30171520-30172799 REVERSE LENGTH=370
AT4G18440	| Symbols: | L-Aspartase-like family protein | chr4:10186385-10188832 REVERSE LENGTH=536

Table D.1 Continued

AT4G09320	| Symbols: NDPK1 | Nucleoside diphosphate kinase family protein | chr4:5923424-5924366 FORWARD LENGTH=169
AT2G40010	| Symbols: | Ribosomal protein L10 family protein | chr2:16708578-16710448 REVERSE LENGTH=317
AT1G36180	| Symbols: ACC2 | acetyl-CoA carboxylase 2 | chr1:13546047-13558339 FORWARD LENGTH=2355
AT4G29720	| Symbols: ATPAO5, PAO5 | polyamine oxidase 5 | chr4:14553456-14555057 REVERSE LENGTH=533
AT1G01090	| Symbols: PDH-E1 ALPHA | pyruvate dehydrogenase E1 alpha | chr1:47705-49166 REVERSE LENGTH=428
AT3G18860	| Symbols: | transducin family protein / WD-40 repeat family protein | chr3:6501774-6508352 FORWARD LENGTH=760
AT4G01370	| Symbols: ATMPK4, MPK4 | MAP kinase 4 | chr4:567219-568889 FORWARD LENGTH=376
AT4G02230	| Symbols: | Ribosomal protein L19e family protein | chr4:979391-980640 REVERSE LENGTH=208
AT1G07660	| Symbols: | Histone superfamily protein | chr1:2369212-2369523 FORWARD LENGTH=103
AT1G20220	| Symbols: | Alba DNA/RNA-binding protein | chr1:7005090-7007285 REVERSE LENGTH=315
AT4G15390	| Symbols: | HXXXD-type acyl-transferase family protein | chr4:8792941-8794281 REVERSE LENGTH=446
AT5G28850	| Symbols: | Calcium-binding EF-hand family protein | chr5:10877360-10881278 REVERSE LENGTH=536
AT1G14000	| Symbols: VIK | VH1-interacting kinase | chr1:4797606-4800043 FORWARD LENGTH=438
AT1G30510	| Symbols: ATRFNR2, RFNR2 | root FNR 2 | chr1:10807150-10808984 REVERSE LENGTH=381
AT4G05390	| Symbols: ATRFNR1, RFNR1 | root FNR 1 | chr4:2738839-2740483 REVERSE LENGTH=378
AT3G01120	| Symbols: MTO1, CGS, ATCYS1, CGS1 | Pyridoxal phosphate (PLP)-dependent transferases superfamily protein | chr3:39234-41865 REVERSE LENGTH=563
AT3G04520	| Symbols: THA2 | threonine aldolase 2 | chr3:1217397-1219571 REVERSE LENGTH=355
AT1G01300	| Symbols: | Eukaryotic aspartyl protease family protein | chr1:117065-118522 FORWARD LENGTH=485
AT5G21060	| Symbols: | Glyceraldehyde-3-phosphate dehydrogenase-like family protein | chr5:7149153-7152745 REVERSE LENGTH=376
AT4G11010	| Symbols: NDPK3 | nucleoside diphosphate kinase 3 | chr4:6732780-6734298 REVERSE LENGTH=238
AT5G26570	| Symbols: PWD, OK1, ATGWD3 | catalytics;carbohydrate kinases;phosphoglucan, water dikinases | chr5:9261580-9267526 FORWARD LENGTH=1196

Table D.1 Continued

AT1G07790	| Symbols: HTB1 | Histone superfamily protein | chr1:2413049-2413495 FORWARD LENGTH=148
AT1G18270	| Symbols: | ketose-bisphosphate aldolase class-II family protein | chr1:6283634-6293772 REVERSE LENGTH=1373
AT1G32500	| Symbols: ATNAP6, NAP6 | non-intrinsic ABC protein 6 | chr1:11750091-11751994 REVERSE LENGTH=475
AT1G52730	| Symbols: | Transducin/WD40 repeat-like superfamily protein | chr1:19642866-19644978 FORWARD LENGTH=343
AT4G04910	| Symbols: NSF | AAA-type ATPase family protein | chr4:2489696-2495666 REVERSE LENGTH=742

Table D.2 Ratios of SA10 Unique Proteins. Ratios of protein abundance in **Table D.1** when comparing untreated cells to 20-minute SA-treated cells.

Accession Number	MW	F2	F3	F4	F5	F6	F7	F8
AT3G12915	91 kDa			5.2				
AT1G72330	60 kDa				0.1	0.5		
AT2G42600	110 kDa	0.1						
AT1G71380	53 kDa					0.8	1.8	
AT3G16410	68 kDa				7.9	1.2	5.9	
AT4G02290	57 kDa					9.0	1.6	
AT1G24280	67 kDa				0.8	1.3		
AT5G43010	45 kDa						1.5	
AT3G53870	27 kDa					0.4	0.2	0.1
AT5G16570	39 kDa				0.7		0.6	1.0
AT3G48870	106 kDa	0.5			0.6			
AT1G17745	66 kDa				1.2	4.7		0.1
AT5G54510	69 kDa				1.0			
AT1G70830	38 kDa							0.3
AT5G53460	242 kDa	3.7	0.9					
AT3G46440	38 kDa							2.1
AT1G80240	40 kDa							0.9
AT4G18440	60 kDa					0.6		
AT4G09320	19 kDa	1.4						
AT2G40010	34 kDa							15.9
AT1G36180	263 kDa		0.5					
AT4G29720	59 kDa				0.5			
AT1G01090	47 kDa						0.8	
AT3G18860	84 kDa				1.4			
AT4G01370	43 kDa							2.2

Table D.2 Continued

AT4G11010	26 kDa						0.6	
AT5G26570	131 kDa			0.9				
AT1G07790	16 kDa	0.3						
AT1G18270	147 kDa	0.8						
AT1G32500	53 kDa						0.3	
AT1G52730	38 kDa							2.2
AT4G04910	81 kDa				0.5			
AT4G02230	24 kDa						0.3	
AT1G07660	11 kDa	0.2						
AT1G20220	34 kDa						3.1	
AT4G15390	49 kDa					2.4		
AT5G28850	62 kDa				1.1			
AT1G14000	49 kDa						3.9	
AT1G30510	43 kDa							0.1
AT4G05390	42 kDa							0.1
AT3G01120	60 kDa					2.5		
AT3G04520	38 kDa						2.3	
AT1G01300	52 kDa							4.3
AT5G21060	40 kDa						1.5	

Table D.3 Proteins Unique to SA20. Proteins unique to XL2W1 cells after data filtration of untreated/treated (20-minute SA) triplicate analysis.

Accession Number	Identified Proteins
AT5G20400	| Symbols: | 2-oxoglutarate (2OG) and Fe(II)-dependent oxygenase superfamily protein | chr5:6894871-6896185 FORWARD LENGTH=348
AT2G31810	| Symbols: | ACT domain-containing small subunit of acetolactate synthase protein | chr2:13524271-13528246 FORWARD LENGTH=491
AT4G00620	| Symbols: | Amino acid dehydrogenase family protein | chr4:259265-260788 REVERSE LENGTH=360
AT1G66530	| Symbols: | Arginyl-tRNA synthetase, class Ic | chr1:24819064-24822277 REVERSE LENGTH=590
AT5G06120	| Symbols: | ARM repeat superfamily protein | chr5:1844797-1852601 FORWARD LENGTH=1066
AT5G28850	| Symbols: | Calcium-binding EF-hand family protein | chr5:10877360-10881278 REVERSE LENGTH=536
AT5G38830	| Symbols: | Cysteinyl-tRNA synthetase, class Ia family protein | chr5:15545764-15548094 REVERSE LENGTH=511

Table D.3 Continued

AT3G53580	| Symbols: | diaminopimelate epimerase family protein | chr3:19864784-19866907 FORWARD LENGTH=362
AT1G01300	| Symbols: | Eukaryotic aspartyl protease family protein | chr1:117065-118522 FORWARD LENGTH=485
AT3G18490	| Symbols: | Eukaryotic aspartyl protease family protein | chr3:6349090-6350592 REVERSE LENGTH=500
AT2G32240	| Symbols: | FUNCTIONS IN: molecular_function unknown; INVOLVED IN: response to cadmium ion; LOCATED IN: plasma membrane; EXPRESSED IN: 25 plant structures; EXPRESSED DURING: 13 growth stages; CONTAINS InterPro DOMAIN/s: Prefoldin (InterPro:IPR009053); BEST Arabidopsis thaliana protein match is: unknown protein (TAIR:AT1G05320.3); Has 470429 Blast hits to 168274 proteins in 4282 species: Archae – 6896; Bacteria – 131956; Metazoa – 175525; Fungi – 33166; Plants – 25441; Viruses – 2243; Other Eukaryotes – 95202 (source: NCBI Blink). | chr2:13684614-13689330 REVERSE LENGTH=1333
AT3G15090	| Symbols: | GroES-like zinc-binding alcohol dehydrogenase family protein | chr3:5076847-5078870 FORWARD LENGTH=366
AT5G48960	| Symbols: | HAD-superfamily hydrolase, subfamily IG, 5'-nucleotidase | chr5:19849645-19853382 FORWARD LENGTH=642
AT4G18440	| Symbols: | L-Aspartase-like family protein | chr4:10186385-10188832 REVERSE LENGTH=536
AT2G46140	| Symbols: | Late embryogenesis abundant protein | chr2:18959163-18960362 FORWARD LENGTH=166
AT5G12940	| Symbols: | Leucine-rich repeat (LRR) family protein | chr5:4087782-4088897 FORWARD LENGTH=371
AT1G24360	| Symbols: | NAD(P)-binding Rossmann-fold superfamily protein | chr1:8640820-8643283 FORWARD LENGTH=319
AT3G05900	| Symbols: | neurofilament protein-related | chr3:1761408-1763854 REVERSE LENGTH=673
AT3G10350	| Symbols: | P-loop containing nucleoside triphosphate hydrolases superfamily protein | chr3:3208310-3210678 FORWARD LENGTH=411
AT1G70770	| Symbols: | Protein of unknown function DUF2359, transmembrane | chr1:26688622-26691185 REVERSE LENGTH=610
AT1G29980	| Symbols: | Protein of unknown function, DUF642 | chr1:10503411-10505994 REVERSE LENGTH=407
AT1G80240	| Symbols: | Protein of unknown function, DUF642 | chr1:30171520-30172799 REVERSE LENGTH=370
AT4G32460	| Symbols: | Protein of unknown function, DUF642 | chr4:15663036-15664859 REVERSE LENGTH=365
AT4G15000	| Symbols: | Ribosomal L27e protein family | chr4:8571896-8572303 FORWARD LENGTH=135

Table D.3 Continued

AT2G20450	| Symbols: | Ribosomal protein L14 | chr2:8813923-8815071 FORWARD LENGTH=134
AT5G27850	| Symbols: | Ribosomal protein L18e/L15 superfamily protein | chr5:9873169-9874297 FORWARD LENGTH=187
AT2G44120	| Symbols: | Ribosomal protein L30/L7 family protein | chr2:18249227-18250402 REVERSE LENGTH=242
AT3G53870	| Symbols: | Ribosomal protein S3 family protein | chr3:19951547-19952782 FORWARD LENGTH=249
AT5G39410	| Symbols: | Saccharopine dehydrogenase | chr5:15768415-15770274 REVERSE LENGTH=454
AT4G04950	| Symbols: | thioredoxin family protein | chr4:2517882-2519924 REVERSE LENGTH=488
AT3G18860	| Symbols: | transducin family protein / WD-40 repeat family protein | chr3:6501774-6508352 FORWARD LENGTH=760
AT3G49910	| Symbols: | Translation protein SH3-like family protein | chr3:18504311-18504751 FORWARD LENGTH=146
AT5G05890	| Symbols: | UDP-Glycosyltransferase superfamily protein | chr5:1772567-1774012 FORWARD LENGTH=455
AT1G53345	| Symbols: | unknown protein; INVOLVED IN: biological_process unknown; LOCATED IN: endomembrane system; EXPRESSED IN: 8 plant structures; EXPRESSED DURING: 4 anthesis, F mature embryo stage, petal differentiation and expansion stage, E expanded cotyledon stage, D bilateral stage; BEST Arabidopsis thaliana protein match is: unknown protein (TAIR:AT5G09580.1); Has 201 Blast hits to 201 proteins in 75 species: Archae - 6; Bacteria - 102; Metazoa - 2; Fungi - 0; Plants - 47; Viruses - 7; Other Eukaryotes - 37 (source: NCBI BLink). | chr1:19902561-19903538 FORWARD LENGTH=325
AT2G20280	| Symbols: | Zinc finger C-x8-C-x5-C-x3-H type family protein | chr2:8740054-8742349 REVERSE LENGTH=371
AT1G36180	| Symbols: ACC2 | acetyl-CoA carboxylase 2 | chr1:13546047-13558339 FORWARD LENGTH=2355
AT5G19530	| Symbols: ACL5 | S-adenosyl-L-methionine-dependent methyltransferases superfamily protein | chr5:6589176-6591091 REVERSE LENGTH=339
AT5G22630	| Symbols: ADT5 | arogenate dehydratase 5 | chr5:7524645-7525922 FORWARD LENGTH=425
AT1G48410	| Symbols: AGO1 | Stabilizer of iron transporter SufD / Polynucleotidyl transferase | chr1:17886285-17891892 REVERSE LENGTH=1048
AT1G72330	| Symbols: ALAAT2 | alanine aminotransferase 2 | chr1:27233637-27236571 FORWARD LENGTH=540
AT5G15450	| Symbols: APG6, CLPB3, CLPB-P | casein lytic proteinase B3 | chr5:5014399-5018255 REVERSE LENGTH=968

Table D.3 Continued

AT5G08590	| Symbols: ASK2, SNRK2-1, SNRK2.1, SRK2G | SNF1-related protein kinase 2.1 | chr5:2783537-2785869 FORWARD LENGTH=353
AT3G48870	| Symbols: ATCLPC, ATHSP93-III, HSP93-III | Clp ATPase | chr3:18122363-18126008 REVERSE LENGTH=952
AT5G05980	| Symbols: ATDFB, DFB, FPGS1 | DHFS-FPGS homolog B | chr5:1799738-1804441 REVERSE LENGTH=571
AT5G64300	| Symbols: ATGCH, GCH, ATRIBA1, RFD1 | GTP cyclohydrolase II | chr5:25718459-25720790 FORWARD LENGTH=543
AT1G70710	| Symbols: ATGH9B1, CEL1, GH9B1 | glycosyl hydrolase 9B1 | chr1:26659356-26662962 REVERSE LENGTH=492
AT4G02290	| Symbols: AtGH9B13, GH9B13 | glycosyl hydrolase 9B13 | chr4:1002654-1005125 REVERSE LENGTH=516
AT1G71380	| Symbols: ATGH9B3, ATCEL3, CEL3 | cellulase 3 | chr1:26899989-26901749 REVERSE LENGTH=484
AT5G22060	| Symbols: ATJ2, J2 | DNAJ homologue 2 | chr5:7303798-7305668 REVERSE LENGTH=419
AT4G01370	| Symbols: ATMPK4, MPK4 | MAP kinase 4 | chr4:567219-568889 FORWARD LENGTH=376
AT1G32500	| Symbols: ATNAP6, NAP6 | non-intrinsic ABC protein 6 | chr1:11750091-11751994 REVERSE LENGTH=475
AT2G42600	| Symbols: ATPPC2, PPC2 | phosphoenolpyruvate carboxylase 2 | chr2:17734541-17738679 REVERSE LENGTH=963
AT4G05390	| Symbols: ATRFNR1, RFNR1 | root FNR 1 | chr4:2738839-2740483 REVERSE LENGTH=378
AT2G37270	| Symbols: ATRPS5B, RPS5B | ribosomal protein 5B | chr2:15647883-15649042 REVERSE LENGTH=207
AT4G17770	| Symbols: ATTPS5, TPS5 | trehalose phosphatase/synthase 5 | chr4:9877055-9880084 FORWARD LENGTH=862
AT5G42980	| Symbols: ATTRX3, ATH3, ATTRXH3, TRXH3, TRX3 | thioredoxin 3 | chr5:17242772-17243718 FORWARD LENGTH=118
AT5G40870	| Symbols: ATUK/UPRT1, UKL1, UK/UPRT1 | uridine kinase/uracil phosphoribosyltransferase 1 | chr5:16375021-16378384 FORWARD LENGTH=486
AT3G02260	| Symbols: BIG, DOC1, TIR3, UMB1, ASA1, LPR1, CRM1 | auxin transport protein (BIG) | chr3:431152-448489 REVERSE LENGTH=5098
AT5G50920	| Symbols: CLPC, ATHSP93-V, HSP93-V, DCA1, CLPC1 | CLPC homologue 1 | chr5:20715710-20719800 REVERSE LENGTH=929
AT5G42970	| Symbols: COP8, FUS4, EMB134, COP14, CSN4, FUS8, ATS4 | Proteasome component (PCI) domain protein | chr5:17237470-17240649 REVERSE LENGTH=397
AT5G20720	| Symbols: CPN20, CPN10, CHCPN10, ATCPN21, CPN21 | chaperonin 20 | chr5:7015015-7016354 FORWARD LENGTH=253

Table D.3 Continued

AT4G22690	| Symbols: CYP706A1 | cytochrome P450, family 706, subfamily A, polypeptide 1 | chr4:11929847-11931520 FORWARD LENGTH=557
AT2G14120	| Symbols: DRP3B | dynamin related protein | chr2:5954253-5960015 REVERSE LENGTH=780
AT3G12670	| Symbols: emb2742 | CTP synthase family protein | chr3:4020351-4024086 REVERSE LENGTH=591
AT5G47880	| Symbols: ERF1-1 | eukaryotic release factor 1-1 | chr5:19386555-19387865 REVERSE LENGTH=436
AT3G26618	| Symbols: ERF1-3 | eukaryotic release factor 1-3 | chr3:9788854-9790161 FORWARD LENGTH=435
AT5G26030	| Symbols: FC1, FC-I, ATFC-I | ferrochelatase 1 | chr5:9096675-9098752 FORWARD LENGTH=466
AT5G13110	| Symbols: G6PD2 | glucose-6-phosphate dehydrogenase 2 | chr5:4158952-4161640 FORWARD LENGTH=596
AT1G24280	| Symbols: G6PD3 | glucose-6-phosphate dehydrogenase 3 | chr1:8609495-8612383 FORWARD LENGTH=599
AT5G60600	| Symbols: GCPE, ISPG, CSB3, CLB4, HDS | 4-hydroxy-3-methylbut-2-enyl diphosphate synthase | chr5:24359447-24363274 FORWARD LENGTH=741
AT5G54510	| Symbols: GH3.6, DFL1 | Auxin-responsive GH3 family protein | chr5:22131321-22133564 REVERSE LENGTH=612
AT5G53460	| Symbols: GLT1 | NADH-dependent glutamate synthase 1 | chr5:21700518-21709629 FORWARD LENGTH=2208
AT1G22300	| Symbols: GRF10, 14-3-3EPSILON, GF14 EPSILON | general regulatory factor 10 | chr1:7879146-7881103 REVERSE LENGTH=254
AT4G03190	| Symbols: GRH1, ATGRH1, AFB1 | GRR1-like protein 1 | chr4:1405108-1407057 REVERSE LENGTH=585
AT5G26040	| Symbols: HDA2 | histone deacetylase 2 | chr5:9099321-9101598 REVERSE LENGTH=359
AT5G56000	| Symbols: Hsp81.4, AtHsp90.4 | HEAT SHOCK PROTEIN 81.4 | chr5:22677602-22680067 REVERSE LENGTH=699
AT4G15550	| Symbols: IAGLU | indole-3-acetate beta-D-glucosyltransferase | chr4:8877877-8879301 REVERSE LENGTH=474
AT5G26860	| Symbols: LON_ARA_ARA, LON1 | lon protease 1 | chr5:9451183-9456631 FORWARD LENGTH=940
AT3G53110	| Symbols: LOS4 | P-loop containing nucleoside triphosphate hydrolases superfamily protein | chr3:19687968-19690423 FORWARD LENGTH=496
AT3G16950	| Symbols: LPD1, ptlpd1 | lipoamide dehydrogenase 1 | chr3:5786761-5790383 REVERSE LENGTH=570
AT5G50850	| Symbols: MAB1 | Transketolase family protein | chr5:20689671-20692976 FORWARD LENGTH=363

Table D.3 Continued

AT1G70830	| Symbols: MLP28 | MLP-like protein 28 | chr1:26710203-26711395 REVERSE LENGTH=335
AT3G01120	| Symbols: MTO1, CGS, ATCYS1, CGS1 | Pyridoxal phosphate (PLP)-dependent transferases superfamily protein | chr3:39234-41865 REVERSE LENGTH=563
AT5G27450	| Symbols: MVK, MK | mevalonate kinase | chr5:9691051-9692975 FORWARD LENGTH=378
AT5G56950	| Symbols: NFA03, NFA3, NAP1;3 | nucleosome assembly protein 1;3 | chr5:23032618-23035299 FORWARD LENGTH=374
AT4G04910	| Symbols: NSF | AAA-type ATPase family protein | chr4:2489696-2495666 REVERSE LENGTH=742
AT3G16410	| Symbols: NSP4 | nitrile specifier protein 4 | chr3:5572145-5574359 FORWARD LENGTH=619
AT3G10050	| Symbols: OMR1 | L-O-methylthreonine resistant 1 | chr3:3099164-3101741 REVERSE LENGTH=592
AT1G22530	| Symbols: PATL2 | PATELLIN 2 | chr1:7955773-7958326 REVERSE LENGTH=683
AT1G01090	| Symbols: PDH-E1 ALPHA | pyruvate dehydrogenase E1 alpha | chr1:47705-49166 REVERSE LENGTH=428
AT5G56630	| Symbols: PFK7 | phosphofructokinase 7 | chr5:22924311-22926728 FORWARD LENGTH=485
AT1G17745	| Symbols: PGDH | D-3-phosphoglycerate dehydrogenase | chr1:6101157-6104979 FORWARD LENGTH=624
AT5G26570	| Symbols: PWD, OK1, ATGWD3 | catalytics;carbohydrate kinases;phosphoglucan, water dikinases | chr5:9261580-9267526 FORWARD LENGTH=1196
AT5G26667	| Symbols: PYR6 | P-loop containing nucleoside triphosphate hydrolases superfamily protein | chr5:9276659-9278091 FORWARD LENGTH=202
AT5G58590	| Symbols: RANBP1 | RAN binding protein 1 | chr5:23680319-23681714 REVERSE LENGTH=219
AT2G36620	| Symbols: RPL24A | ribosomal protein L24 | chr2:15350548-15351819 REVERSE LENGTH=164
AT5G43010	| Symbols: RPT4A | regulatory particle triple-A ATPase 4A | chr5:17248563-17251014 REVERSE LENGTH=399
AT1G14320	| Symbols: SAC52, RPL10, RPL10A | Ribosomal protein L16p/L10e family protein | chr1:4888270-4889408 FORWARD LENGTH=220
AT5G26780	| Symbols: SHM2 | serine hydroxymethyltransferase 2 | chr5:9418299-9421725 FORWARD LENGTH=517
AT5G06140	| Symbols: SNX1, ATSNX1 | sorting nexin 1 | chr5:1856212-1858752 REVERSE LENGTH=402
AT5G27640	| Symbols: TIF3B1, EIF3B, ATEIF3B-1, EIF3B-1, ATTIF3B1 | translation initiation factor 3B1 | chr5:9781207-9784759 REVERSE LENGTH=712

Table D.3 Continued

AT5G06600	| Symbols: UBP12 | ubiquitin-specific protease 12 | chr5:2019545-2027834 REVERSE LENGTH=1116
AT2G15480	| Symbols: UGT73B5 | UDP-glucosyl transferase 73B5 | chr2:6758817-6763398 FORWARD LENGTH=494
AT3G27440	| Symbols: UKL5 | uridine kinase-like 5 | chr3:10155555-10157931 FORWARD LENGTH=465
AT1G14000	| Symbols: VIK | VH1-interacting kinase | chr1:4797606-4800043 FORWARD LENGTH=438

Table D.4 Ratios of Unique SA20 Proteins. Ratios of protein abundance in **Table D.2** when comparing untreated cells to 20-minute SA-treated cells.

Accession Number	MW	F2	F3	F4	F5	F6	F7	F8
AT5G20400	40 kDa							1.6
AT2G31810	54 kDa	0.2	1.3					
AT4G00620	39 kDa							1.0
AT1G66530	66 kDa				1.2			
AT5G06120	121 kDa			1.1				
AT5G28850	62 kDa					0.5	2.0	
AT5G38830	58 kDa				0.6			
AT3G53580	39 kDa				1.9			0.2
AT1G01300	52 kDa							0.4
AT3G18490	53 kDa							1.2
AT2G32240	?	0.7						
AT3G15090	39 kDa							1.3
AT5G48960	73 kDa				1.6			
AT4G18440	60 kDa					0.7		
AT2G46140	18 kDa	1.1						
AT5G12940	40 kDa							0.3
AT1G24360	34 kDa							2.2
AT3G05900	73 kDa		1.3					
AT3G10350	45 kDa							0.7
AT1G70770	67 kDa				1.7			
AT1G29980	44 kDa					0.2		
AT1G80240	40 kDa							1.2
AT4G32460	40 kDa						0.6	
AT4G15000	16 kDa						0.5	
AT2G20450	16 kDa							2.0
AT5G27850	21 kDa				0.5			4.0
AT2G44120	28 kDa						0.5	0.6

Table D.4 Continued

AT3G53870	27 kDa				0.1	0.6	0.4	0.7
AT5G39410	50 kDa					0.7		
AT4G04950	53 kDa			1.6	0.4	0.6		0.4
AT3G18860	84 kDa				1.5			
AT3G49910	17 kDa				1.1			
AT5G05890	52 kDa					1.0		
AT1G53345	?							1.3
AT2G20280	42 kDa					1.6		
AT1G36180	263 kDa	0.5	0.6					
AT5G19530	39 kDa							2.0
AT5G22630	46 kDa							2.3
AT1G48410	116 kDa		0.3	0.8				
AT1G72330	60 kDa					1.6		
AT5G15450	109 kDa	0.7						
AT5G08590	40 kDa							4.5
AT3G48870	106 kDa	1.0	0.2	2.1	1.3			
AT5G05980	63 kDa					0.3		
AT5G64300	59 kDa				1.3	1.0		
AT1G70710	55 kDa						0.9	
AT4G02290	57 kDa					0.7	0.6	
AT1G71380	53 kDa					1.1	0.7	1.7
AT5G22060	46 kDa	0.4				0.8		
AT4G01370	43 kDa						2.0	0.8
AT1G32500	53 kDa					0.5	0.7	
AT2G42600	110 kDa	0.2						
AT4G05390	42 kDa							0.4
AT2G37270	23 kDa			1.1	0.5		0.5	1.9
AT4G17770	97 kDa	0.9						
AT5G42980	13 kDa						2.4	
AT5G40870	54 kDa			0.7		0.9	2.1	
AT3G02260	568 kDa	0.6						
AT5G50920	?	0.2	0.1	1.5	1.1			
AT5G42970	45 kDa						2.0	
AT5G20720	27 kDa			0.7				
AT4G22690	63 kDa					0.7		
AT2G14120	87 kDa	1.4						
AT3G12670	64 kDa				2.4			
AT5G47880	49 kDa					1.0		
AT3G26618	49 kDa					0.6		

Table D.4 Continued

AT5G26030	52 kDa						0.9	1.0
AT5G13110	67 kDa			0.6		0.9		
AT1G24280	67 kDa	0.3	0.3	0.8	0.1	0.5	1.3	
AT5G60600	82 kDa				1.5			
AT5G54510	69 kDa			1.2	0.6			
AT5G53460	242 kDa	0.3	0.6	2.5				
AT1G22300	29 kDa			1.0				
AT4G03190	66 kDa				1.3			
AT5G26040	41 kDa							1.1
AT5G56000	80 kDa	0.0		0.0				
AT4G15550	54 kDa					0.3		
AT5G26860	?	1.0	0.8	0.6				
AT3G53110	55 kDa			2.0		1.0		
AT3G16950	61 kDa				1.0	1.5		
AT5G50850	39 kDa			0.4				
AT1G70830	38 kDa							0.5
AT3G01120	60 kDa						0.9	
AT5G27450	41 kDa							1.2
AT5G56950	43 kDa				1.2			
AT4G04910	81 kDa		1.1		10.2			
AT3G16410	68 kDa				0.8			
AT3G10050	65 kDa				0.6			
AT1G22530	76 kDa				2.4			
AT1G01090	47 kDa						1.2	0.9
AT5G56630	53 kDa	0.3	1.0	0.6	2.6	1.1		
AT1G17745	66 kDa		3.7	0.2	1.0	2.4		
AT5G26570	131 kDa	0.3	0.4	0.9	1.1			1.9
AT5G26667	22 kDa				3.3			
AT5G58590	25 kDa							3.0
AT2G36620	19 kDa				0.3		0.6	2.7
AT5G43010	45 kDa						18.3	
AT1G14320	25 kDa				1.5		1.3	2.7
AT5G26780	57 kDa					0.3		
AT5G06140	47 kDa						0.7	
AT5G27640	82 kDa	0.5			1.2			
AT5G06600	131 kDa		0.4	0.7				
AT2G15480	55 kDa					2.5		
AT3G27440	52 kDa						0.6	
AT1G14000	49 kDa						2.4	